12-2016

Influence of pH and Acidic Side Chain Charges on the Behavior of Designed Model Peptides in Lipid Bilayer Membranes

Venkatesan Rajagopalan
University of Arkansas, Fayetteville

Influence of pH and Acidic Side Chain Charges on the Behavior of Designed Model Peptides in Lipid Bilayer Membranes

A dissertation submitted in partial fulfillment
of the requirements for the degree of
Doctor of Philosophy in Cell and Molecular Biology

by

Venkatesan Rajagopalan
University of Mumbai
Bachelor of Science in Microbiology, 2006
Padmashree Dr. D.Y. Patil University
Master of Technology in Biotechnology, 2009

December 2016
University of Arkansas

This dissertation is approved for recommendation to the Graduate Council.

_____
Dr. Roger E. Koeppe II
Dissertation Director

_____
Dr. Suresh Kumar Thallapuranam
Committee Member

_____
Dr. Ralph L. Henry
Committee Member

_____
Dr. David S. McNabb
Committee Member

_____
Dr. Dan Davis
Committee Member

Abstract

The molecular properties of transmembrane proteins and their interactions with lipids regulate biological function. Of particular interest are interfacial aromatic residues and charged residues in the core helix whose functions range from stabilizing the native structure to regulating ion channels. This dissertation addresses the pH dependence and influence of potentially negatively charged tyrosine, glutamic acid or aspartic acid side chains. We have employed GWALP23 (acetyl-GGALW^{5}LALALALALALALW^{19}LAGA-amide) as favorable host peptide framework. We have substituted W5 with Tyr (Y^{5}GWALP23) and Leu residues with Glu (L12E, L14E or L16E) or Asp (L14D or L16D), and have incorporated specific ^{2}H-labeled alanine residues within the core helix or near the ends of the sequence. Solid-state ^{2}H-NMR spectra reveal a pK_a of about 10.5 for bilayer incorporated Y^{5}GWALP23.

Solid-state ^{2}H-NMR spectra of GWALP23-E12, –E14 and –E16 with core labels reveal little change to the orientation of the transmembrane helix over a pH range of 4 to 12.5 but modest changes in quadrupolar splitting magnitudes above pH 12.5 in DLPC bilayer membranes, with E12 peptides showing no change even at pH 13. The E12, E14 and E16 peptides display broad ^{2}H NMR spectra in aligned DOPC bilayers, with individual resonances not being observed for the core labels. Labeling the ends of the helix at A3 and A21 provided insights into the pH-dependent unwinding of the E14 and E16 peptide helices in both lipid systems.

An aspartic acid residue at position 14 shows contrasting behavior to that of its Glu counterpart. The ^{2}H-NMR spectra for core ^{2}H-alanines of GWALP23-D14 show a preference for a well oriented conformation in DOPC bilayers in comparison to DLPC lipids. While the core helix does not respond to pH, the helix terminals show changes in unwinding between pH 6 and 13 suggesting a possible pK_a around 13. The polar but uncharged Gln residue at position 14 behaves

similarly to Glu in DLPC and DOPC lipid bilayers. The Q14 peptide, however, does not titrate in either lipid and displays well-resolved sharper ^{2}H-NMR resonances in DLPC bilayers. The combined results illustrate complex behavior for carboxyl and carboxamide side chains in bilayer membranes.

Acknowledgements

I would first and foremost like to thank my research advisor Dr. Roger E. Koeppe II for giving me the chance to work in his lab for the past 5 years and be part of the research team. I sincerely thank him for his tremendous patience, guidance, encouragement and belief through all the projects I have worked on. I appreciate his kind support in both my personal and professional life. He imparted his wisdom and insights to me for getting a clearer understanding of protein-lipid interactions and I want to thank him for that.

My sincere thanks to Dr. Denise V. Greathouse for her invaluable assistance in the lab as a source of knowledge, help and guidance. You have been the glue holding the lab together. I cherish our discussions on cooking Indian food recipes (as well as making and eating them).

I would also like to thank Ashley Martfeld-Henderson for being the best lab mate one could ask for. Your presence and work ethic greatly influenced me and motivated me to do my best. Your helpfulness and suggestions are genuinely appreciated. I wish you the best in both your personal and professional life.

I am also sincerely thankful to my best friend Gail Joseph, whose constant motivation and kind words got me through the toughest of situations during my career. You have always been there by my side and I really appreciate every moment.

Dedication

I dedicate this dissertation to my parents Rajagopalan Soundararajan and Hema Rajagopalan who have been the reason for my success and passion for science. Their unconditional love and support have been the pillar of my existence. I also dedicate this work to my sister Poonam who has been the best sister one could ask for. I also want to dedicate my work to my cousin Devanathan Raghunathan who has been an inspiration to me and served as a constant reminder to keep chasing my goals.

Table of Contents

Chapter 3: Venkatesan Rajagopalan, Denise V. Greathouse, Roger E. Koeppe II, 2016. "Influence of Glutamic Acid Residues and pH on the Properties of Transmembrane Helices." (Submitted for publication and currently in review)

CHAPTER 1: Introduction

The biological membrane is heterogeneous, crowded by a variety of lipids of different lengths and by a variety of proteins. This brings in a lot of complexity for experiments to examine and understand the membrane proteins in detail. The lipid bilayer has been shown to alter protein shape and function in a various fashion. For example, rhodopsin's photochemical functions as well as the enzymatic activity of cytochrome oxidase c are affected by bilayer curvature, thickness and elasticity (1,2), and glucose transport activity in red blood cells has been shown to have a dependence on lipid composition (3). Conversely, membrane proteins too have significant effects on the lipid bilayer itself (4,5).

Dynamic transmembrane helix motions are crucial for the functions of the membrane proteins and subtle molecular interactions can govern the stability of the native states and biological activation of membrane proteins. An example of this is the helix motions in voltage-gated channel proteins. Voltage gated Na^{+}, K^{+} and Ca^{+2} channels play crucial roles in excitable cells. Each of these channels contains voltage sensors and a selective ion-conduction pore, with the general structure comprised either of four independent protein subunits or one long polypeptide containing four homologous domains. Each domain contains six transmembrane segments (S1-S6) and a pore loop between segments S5 and S6. Segments S1-S4 form the voltage sensor. Of key importance is the S4 helix segment which was recognized as a voltage sensing unit owing to the presence of basic residues (Arg or Lys) at every third position (6). This segment along with the S2 helix, rich in intracellular acidic residue are involved in gating. Despite the energetic cost for inserting positive charges into a hydrophobic environment could be significant as shown by the surface bound configuration of the synthetic S4 analog in model membranes (7,8). In some

instances, (eg. KvAP channels) (9) the surrounding lipid matrix is known to strongly influence channel activation by rearrangement of the head groups when the membrane potential is shifted.

The seven transmembrane helix polypeptide of visual rhodopsin form a tightly packed cylindrical conformation with TM1 and TM3 forming the stable core. Activation of the protein results in large conformational changes in TM5, TM6 and TM7 helix. The retinal chromophore sits in a tight binding site at the core of the protein and is attached via a protonated Schiff base linkage with Lys296 on TM7. The counter-ion, Glu113 onTM3, stabilizes the inactive form of the protein (10). Upon light activated isomerization of the retinal from 11-cis to all-trans configuration there is a concerted local conformational change in the TM5 and TM6 helices which are mainly governed by the aromatic residues Phe261, Trp265 and Tyr268 on the extracellular end of TM6 (11). These collective motions serve towards the functional activation.

Charged residues have also been implicated in aiding fold-switching of metamorphic transmembrane proteins like the chloride ion channel CLIC1 (12). The CLIC1 intracellular chloride channels exists in both a soluble conformation in the cytoplasm as well as a membrane bound conformation. The conformation is dictated by the pH sensitivity that is governed by specific residues functioning as pH sensors. The monomeric soluble protein has an N-domain comprising of helices α1 and α3 and a beta strand β2. The α1 helix and β2 strand form the transmembrane domain. The conformational switch results when the N-domain detaches itself from the C-domain and restructures itself for insertion into the membrane (13). In the cytoplasm at a pH around 7, Glu81 on α3 is charged and forms a salt-bridge with Arg29 on α1 which stabilizes the native conformation. As CLIC1 nears the low pH membrane surface, Glu81 loses its charge causing a break in the salt bridge. This allows the detachment and insertion of the N-domain into the membrane.

Peptides which initially associate with lipid-bilayer membrane surfaces may undergo dynamic transitions from surface bound to tilted-transmembrane orientations, sometimes accompanied by changes in the molecularity, formation of a pore or, more generally, the activation of biological function (14,15). The large number of parameters governing the protein-lipid interaction therefore necessitates the use of less complex model systems to systematically evaluate the various interactions involved. To observe the lipid bilayer contributions more accurately, studies using synthetic lipids with unique head groups, chain length and degree of unsaturation can be employed to examine the effect of varying the lipid environment. Membrane proteins typically consists of multiple spans through the bilayer that lead to protein-protein interactions and forces that create more factors complicating pure protein-lipid interaction studies. To simplify this problem, small α-helical peptides with a single membrane span may be used.

The WALP model peptides of the form acetyl- GWWA$(LA)_n$LWWA-amide were an early model peptide system used for studying the peptide-lipid interactions and the general rules that govern them, such as hydrophobic mismatch (16,17). The WALP framework consists of a hydrophobic core helix composed of leucines and alanines flanked by two amphipathic Trp residues on each end. Further development of this system yielded GWALP23, acetyl- GGALW $(LA)_6$LWLAGA-amide, that features only one single Trp residue on each end, with glycine replacing the other Trp residues (18). The new model has the same benefits of the WALP model but with two less anchoring residues it shows greater sensitivity to changes in the lipid environment. GWALP23 also shows less dynamic averaging of NMR observables including the ^{2}H quadrupolar splitting and the ^{15}N-^{1}H dipolar coupling (19). This peptide allows for the examination of the Trp side-chain radial position as compared to an inserted polar residue side-chain since the Trp residues

can be moved throughout the helix sequence. Further modification to the GWALP23 peptide may include substitution of the W5 with a tyrosine residue (Y^5GWALP23).

The presence of a single Trp residue improves the sensitivity to fluorescence spectroscopy. Throughout the entirety of this dissertation, the model peptide GWALP23 serves as the framework for which further peptide-lipid interactions have been studied. WALP peptide systems have relied heavily on the excellent anchoring capabilities of the amphipathic aromatic tryptophan residues. While there is a known enrichment of tryptophan at the lipid interfacial regions of single-span transmembrane proteins (20), it is also true for tyrosine, though to a smaller extent on the N-terminal of transmembrane helices. Side chain dihedral angles in an alpha-helix do not project perpendicularly from the peptide backbone or the helix axis. Instead the C_α-C_β bonds project toward the N-terminus (17). This feature leads to asymmetric positioning of the anchoring indole rings in GWALP23 and it has been shown that they adopt differing arrangements, in which the C-terminal Trp indole ring rotates to point its polar nitrogen moiety toward the aqueous phase (21).

Indeed, while it has also been observed that Trp is heavily populated at both interfaces of single-span alpha-helices, tyrosine is to some extent less populated at the C-terminus (20). The tyrosine phenol group can get hydrated by hydrogen bonding with the waters and lipid head groups. We will show results for the titration of Tyr residues at position 5 in the GWALP23 peptide helix and discuss how the Tyr titration affects the study of Y^5GWALP23 peptides incorporated with Glu residues.

Solid state ^{2}H NMR spectroscopy with deuterium labeled alanines on a transmembrane peptide helix in macroscopically aligned lipid bilayers is a useful technique to analyze the extent of helix formation, helix tilt, and azimuthal rotation about the helix axis. Oriented glass plate samples

provide a common method for bilayer alignment that can be achieved by means of macroscopic insertion of a sealed, hydrated sample of parallel plates into the NMR probe. The technique utilizes hydrated and sealed oriented plate samples that mechanically align the lipid bilayer with the magnetic field. These samples can be placed in a probe with the lipid bilayer normal either parallel ($\beta = 0°$) or perpendicular ($\beta = 90°$) to the external magnetic field. For a peptide with fast averaging around the lipid bilayer normal (but not the peptide axis), the ^2H quadrupolar splittings ($\Delta\nu_q$) observed at $\beta = 90°$ have absolute magnitude of one-half those at $\beta = 0°$. The peptide tilt is sensitive to the thickness of the bilayer and the length of the peptide. Solid state NMR is very sensitive to changes in the peptide tilt and rotation and hence is a useful tool in the analysis of peptide-lipid interactions.

While GWALP-like peptides have allowed for valuable insight into the properties of helix-anchoring residues, the peptide family was then used for the study of polar, charged residues within the non-polar bilayer interior. Ionizable residues found incorporated within the transmembrane segments of membrane proteins have gained recent interest, particularly in terms of quantifying the energetic cost of potentially burying them (22,23). Crystal structure data from an array of membrane proteins reveal the side chains of polar residues in the lipid bilayers to be directed away from the membrane core, extending toward the head-group region (24,25), a result also found in experiments (17). Simulation studies also show charged amino acids form hydrogen bonds with the lipid head groups and bind water molecules (26,27), and additionally found the hydrogen-bonding abilities of these polar residues to be crucial for membrane helix di- and trimerization (28). The energetic penalty of burying charged residue in bilayer membranes are evident in case of voltage sensor domain of voltage-gated potassium channels which possesses several arginine residue and reorients with a change in membrane potential to mediate

channel gating. One can observe discrepancy between theoretical and experimental estimates of the cost of forcing Arg into the center of the bilayer (which is estimated to range from 5-25 kcal/mol) (29,30). Similarly, a highly conserved buried lysine critical for integrin proteins is thought to snorkel towards the interfacial region and impart a helix tilt that is needed for binding subunit proteins (31).

The GWALP23 system is a constructive model for investigating the effects of placing polar residues in the bilayer. Previous work using the GWALP23 and Y^5GWALP23 host peptides entailed studying the effects of inserting Arg, Lys or His into DLPC or DOPC bilayers (32-34). Positioning the Arg slightly off center (GWALP23-R14, ~ 3 Å from helix midpoint) changed the helix tilt by 10° but had a larger effect on azimuthal rotation. When positioned at the center of the helix (GWALP23-R12), the peptide produced multiple low-intensity ^{2}H NMR signals indicative of multi-state behavior, including a surface-bound population. Much like R12 peptide, K12 appears unoriented in the thicker DOPC bilayers. But in contrast to -R12, -K12 titrates at higher pH to adopt a defined orientation similar to the host GWALP23. Lysine at position 14 also titrates at high pH and adopts a tilt of 9° while maintaining its rotation of 244°. The titration revealed a two-state equilibrium in fast-exchange on NMR time scale with a pK_a of 6.2 under experimental conditions. GWALP23 peptides incorporated with His at position 12 in DOPC bilayers have comparable results to both –K12 and –R12 peptides. The neutral H12 peptide remains in a tilted orientation identical to the parent GWALP23 but the charged H^+12 peptide, at pH 2.3, abandons the transmembrane orientation, exiting the membrane surface very similar to the orientations observed for the charged –R12 peptide. GWALP23-$H^0$14 peptide adopts a tilted membrane orientation distinct from GWALP23, just like Y^5GWALP23-$K^0$14.

In comparison to the positively charged polar amino acids, Glu residues show distinct behavior with respect to their titration and peptide dynamics in the lipid bilayer. Both GWALP23-E14 and –E16 peptide consistently titrate at a high pK_a over 12 in DLPC bilayers. The neutral $–E^0$14 peptide has a distinct orientation from GWALP23 and shows a consistent change in azimuthal rotation of about 50°, very similar to $–K^0$14 and $–H^0$14 peptides. The charged $–E^-$14 peptide does not alter its orientation by much from the neutral state but shows a change in the unwinding of the helix terminal. The neutral $–E^0$16 peptide also displays a slightly straight orientation in comparison to GWALP23, with the charged $–E^-$16 straightening further to a helix tilt of 10.7°. The charged –E16 peptide displays significant helix fraying, possibly to allow access for Glu to hydrogen bond with the waters. In the DOPC bilayers however, the Glu incorporated peptides display low intensity poorly resolved spectra independent of its position at 12, 14 or 16.

We have also incorporated Asp residues at positions 14 and 16. GWALP23-D14 surprisingly behaves in contrast to –E14 peptide in both DLPC and DOPC ether linked bilayers. The incorporation of aspartic acid at position 14 revealed quite unique characteristics. Solid-state ^2H NMR spectra of GWALP23-D14 alanine methyl group show moderately resolved low intensity peaks in DLPC ether-linked bilayers indicative of possible multiple conformations in slow exchange. In contrast, we observe well-defined spectra for –D14 alanine methyl groups in DOPC ether bilayers with sharp resonances which improved for deuterated alanine near the C-terminal. The results in DOPC ether bilayers is indicative of a possible single conformation. However, we observe no pH dependent change in the alanine methyl quadrupolar splittings for –D14 peptide in either DLPC or DOPC ether bilayers. Tilt analysis for –D14 peptide in DOPC ether bilayers indeed suggests a much tilted conformation compared to parent GWALP23.

Membrane proteins are complex due to the heterogeneous lipid bilayer in which they reside and this often presents a challenge in their examination. Throughout this dissertation we attempt to demonstrate the unique ability of synthetic membrane peptides, biophysical measurements and quantitative analysis to illuminate some of the important fundamental interactions that arise between membrane proteins and the lipid bilayer. While some of the forces can be masked by the entirety of a larger membrane protein system, when isolated from other factors, the individual contributions to the collective whole can be investigated.

1.1 References

1. Brown, M. F. (1994) Modulation of Rhodopsin Function by Properties of the Membrane Bilayer. *Chem. Phys. Lipids* **73**, 159-180

2. Montecucco, C., Smith, G. A., Dabbenisala, F., Johannsson, A., Galante, Y. M., and Bisson, R. (1982) Bilayer Thickness and Enzymatic-Activity in the Mitochondrial Cytochrome C-oxidase and ATPase Complex. *FEBS Lett.* **144**, 145-148

3. Carruthers, A., and Melchior, D. L. (1984) Human- Erythrocyte Hexose Transporter Activity is Governed by Lipid-Composition in Reconstituted Vesicles. *Biochemistry* **23**, 6901-6911

4. Killian, J. A., Taylor, M. J., and Koeppe, R. E. (1992) Orientation of the Valine-1 Side-chain of the Gramicidin Transmembrane Channel and Implications for Channel Functioning a ^{2}H-NMR study. *Biochemistry* **31**, 11283-11290

5. Yang, F. Y., and Hwang, F. (1996) Effect of non-bilayer lipids on the activity of membrane enzymes. *Chem. Phys. Lipids* **81**, 197-202

6. Noda, M., Shimizu, S., Tanabe, T., Takai, T., Kayano, T., Ikeda, T., Takahashi, H., Nakayama, H., Kanaoka, Y., Minamino, N., Kangawa, K., Matsuo, H., Raftery, M. A., Hirose, T., Inayama, S., Hayashida, H., Miyata, T., and Numa, S. (1984) Primary Structure of electrophorus-Electricus Sodium-Channel Deduced from cDNA Sequence. *Nature* **312**, 121-127

7. Halsall, A., and Dempsey, C. E. (1999) Intrinsic helical propensities and stable secondary structure in a membrane-bound fragment (S4) of the Shaker potassium channel. *J. Mol. Biol.* **293**, 901-915

8. Mattila, K., Kinder, R., and Bechinger, B. (1999) The alignment of a voltage-sensing peptide in dodecylphosphocholine micelles and in oriented lipid bilayers by nuclear magnetic resonance and molecular modeling. *Biophys. J.* **77**, 2102-2113

9. Zheng, H., Liu, W. R., Anderson, L. Y., and Jiang, Q. X. (2011) Lipid-dependent gating of a voltage-gated potassium channel. *Nat. Commun.* **2**, 9

10. Hofmann, K. P., Scheerer, P., Hildebrand, P. W., Choe, H. W., Park, J. H., Heck, M., and Ernst, O. P. (2009) A G protein-coupled receptor at work: the rhodopsin model. *Trends Biochem.Sci.* **34**, 540-552

11. Ahuja, S., Hornak, V., Yan, E. C. Y., Syrett, N., Goncalves, J. A., Hirshfeld, A., Ziliox, M., Sakmar, T. P., Sheves, M., Reeves, P. J., Smith, S. O., and Eilers, M. (2009) Helix movement is coupled to displacement of the second extracellular loop in rhodopsin activation. *Nat. Struct. Mol. Biol.* **16**, 168-175

12. Legg-E'Silva, D., Achilonu, I., Fanucchi, S., Stoychev, S., Fernandes, M., and Dirr, H. W. (2012) Role of Arginine 29 and Glutamic Acid 81 Interactions in the Conformational Stability of Human Chloride Intracellular Channel 1. *Biochemistry* **51**, 7854-7862

13. Ashley, R. H. (2003) Challenging accepted ion channel biology: p64 and the CLIC family of putative intracellular anion channel proteins (Review). *Molecular Membrane Biology* **20**, 1-11

14. Barrera, F. N., Weerakkody, D., Anderson, M., Andreev, O. A., Reshetnyak, Y. K., and Engelman, D. M. (2011) Roles of Carboxyl Groups in the Transmembrane Insertion of Peptides. *J. Mol. Biol.* **413**, 359-371

15. Su, Y. C., Li, S. H., and Hong, M. (2013) Cationic membrane peptides: atomic-level insight of structure-activity relationships from solid-state NMR. *Amino Acids* **44**, 821-833

16. Killian, J. A., Salemink, I., dePlanque, M. R. R., Lindblom, G., Koeppe, R. E., and Greathouse, D. V. (1996) Induction of nonbilayer structures in diacylphosphatidylcholine model membranes by transmembrane alpha-helical peptides: Importance of hydrophobic mismatch and proposed role of tryptophans. *Biochemistry* **35**, 1037-1045

17. van der Wel, P. C. A., Strandberg, E., Killian, J. A., and Koeppe, R. E. (2002) Geometry and intrinsic tilt of a tryptophan-anchored transmembrane alpha-helix determined by H-2 NMR. *Biophys. J.* **83**, 1479-1488

18. Vostrikov, V. V., Grant, C. V., Daily, A. E., Opella, S. J., and Koeppe, R. E., II. (2008) Comparison of "Polarization Inversion with Spin Exchange at Magic Angle" and

"Geometric Analysis of Labeled Alanines" methods for transmembrane helix alignment. *Journal of the American Chemical Society* **130**, 12584-+

19. Vostrikov, V. V., Grant, C. V., Opella, S. J., and Koeppe, R. E., 2nd. (2011) On the combined analysis of ^{2}H and $^{15}N/^{1}H$ solid-state NMR data for determination of transmembrane peptide orientation and dynamics. *Biophys. J.* **101**, 2939-2947

20. Landolt-Marticorena, C., Williams, K. A., Deber, C. M., and Reithmeier, R. A. F. (1993) Non-Random Distribution of Amino Acids in the Transmembrane Segments of Human Type-I Single Span Membrane-Proteins. *J. Mol. Biol.* **229**, 602-608

21. Vostrikov, V. V., and Koeppe, R. E. (2011) Response of GWALP Transmembrane Peptides to Changes in the Tryptophan Anchor Positions. *Biochemistry* **50**, 7522-7535

22. Hessa, T., Kim, H., Bihlmaier, K., Lundin, C., Boekel, J., Andersson, H., Nilsson, I., White, S. H., and von Heijne, G. (2005) Recognition of transmembrane helices by the endoplasmic reticulum translocon. *Nature* **433**, 377-381

23. Dorairaj, S., and Allen, T. W. (2007) On the thermodynamic stability of a charged arginine side chain in a transmembrane helix. *Proc. Natl. Acad. Sci. U. S. A.* **104**, 4943-4948

24. Chamberlain, A. K., Lee, Y., Kim, S., and Bowie, J. U. (2004) Snorkeling preferences foster an amino acid composition bias in transmembrane helices. *J. Mol. Biol.* **339**, 471-479

25. Granseth, E., von Heijne, G., and Elofsson, A. (2005) A study of the membrane-water interface region of membrane proteins. *J. Mol. Biol.* **346**, 377-385

26. Freites, J. A., Tobias, D. J., von Heijne, G., and White, S. H. (2005) Interface connections of a transmembrane voltage sensor. *Proc. Natl. Acad. Sci. U. S. A.* **102**, 15059-15064

27. Kandasamy, S. K., and Larson, R. G. (2005) Molecular dynamics study of the lung surfactant peptide SP-B1-25 with DPPC monolayers: Insights into interactions and peptide position and orientation. *Biophys. J.* **88**, 1577-1592

28. Stockner, T., Ash, W. L., MacCallum, J. L., and Tieleman, D. P. (2004) Direct simulation of transmembrane helix association: Role of asparagines. *Biophys. J.* **87**, 1650-1656

29. MacCallum, J. L., Bennet, W. F. D., and Tieleman, D. P. (2007) Distribution of amino acid side chains in a lipid bilayer from atomistic computer simulations. *Biophys. J.*, 248A-248A

30. Moon, C. P., and Fleming, K. G. (2011) Side-chain hydrophobicity scale derived from transmembrane protein folding into lipid bilayers. *Proc. Natl. Acad. Sci. U. S. A.* **108**, 10174-10177

31. Kim, C., Ye, F., and Ginsberg, M. H. (2011) Regulation of Integrin Activation. in *Annual Review of Cell and Developmental Biology, Vol **27*** (Schekman, R., Goldstein, L., and Lehmann, R. eds.), Annual Reviews, Palo Alto. pp 321-345

32. Vostrikov, V. V., Daily, A. E., Greathouse, D. V., and Koeppe, R. E. (2010) Charged or Aromatic Anchor Residue Dependence of Transmembrane Peptide Tilt. *J. Biol. Chem.* **285**, 31723-31730

33. Gleason, N. J., Vostrikov, V. V., Greathouse, D. V., and Koeppe, R. E. (2013) Buried lysine, but not arginine, titrates and alters transmembrane helix tilt. *Proc. Natl. Acad. Sci. U. S. A.* **110**, 1692-1695

34. Martfeld, A. N., Greathouse, D. V., and Koeppe, R. E. (2016) Ionization Properties of Histidine Residues in the Lipid-Bilayer Membrane Environment. *J. Biol. Chem.*

CHAPTER 2: Ionization of Interfacial Tyr Residues

2.1 Abstract

Model peptides have proven useful for examining fundamental peptide-lipid interactions. A frequently employed peptide design consists of a hydrophobic core of Leu-Ala residues with polar or aromatic amino acids flanking each side at the interfacial positions, which serve to "anchor" a specific transmembrane orientation. We have recently modified the design of WALP peptides (acetyl-GWW$(LA)_n$LWWA-[ethanol]amide) by reducing the number of Trp anchors to only one near each end of the peptide or further modifying the sequence to incorporate a single tyrosine (Y^5) at one end. The resulting GWALP23 (acetyl-GGALW^5$(LA)_6$LW^{19}LAGA-[ethanol]amide) and its sister peptide Y^5GWALP23 display reduced dynamics and greater sensitivity to lipid-peptide hydrophobic mismatch than the traditional WALP peptides. The Y^5GWALP23, with a single Trp residue is more informative when subjected to fluorescence experiments. By incorporating specific ^{2}H labels in the core of the Y^5GWALP23 we were able to use solid-state NMR spectroscopy to examine the titration of the Tyr residue at the membrane water interface. We observe the bilayer incorporated Y^5GWALP23 to titrate at a pH of about 10.5. Control experiments with GWALP23 show no titration throughout the pH range due to a lack of titrable group. This work corroborates the more recent calculations on anionic Tyr residues along the membrane normal and sheds importance on properly modeling the protonation equilibrium in peptides interacting with membranes using MD simulations.

2.2 Introduction

Membrane proteins are complex, creating difficulties for implementing experimental techniques for characterization of their structural and functional properties. Synthetic model peptides have proved to be invaluable tools for examining the fundamental principles that modulate protein-lipid interactions. The peptide model systems allow for examining direct lipid interactions by placing limits upon external factors such as multiple transmembrane helices or large steric hindrances in oligomers.

A study of type I single-span membrane proteins revealed a conserved distribution of the aromatic Trp, Tyr and Phe residues (1). The aromatic residues are typically located near the membrane-water interface where they may act as anchors to help position the transmembrane helix within the bilayer (2). In some cases a short tryptophan-rich peptide may promote lipid H_{II} phase formation (3). WALP peptides (acetyl-GWWA$(LA)_n$LWWA-[ethanol]amide) with multiple Trp anchors and a helical core of Leu-Ala repeats also may induce lipid phase changes much like gramicidin A (4). The four Trp residues were further mutated to incorporate various other aromatic or charged residues (Tyr, Phe, Lys, Arg, or His) to monitor the importance of the anchor's physiochemical properties (5,6). A modification of the WALP peptides by reducing the number of Trp to one on each side in GWALP23 (acetyl-GGALW^5$(LA)_6$LW^{19}LAGA-[ethanol]amide) has made the transmembrane helix more responsive to the lipid bilayer thickness. A further modification to GWALP23 was replacing a tryptophan with a different anchoring residue which opens up avenues for fluorescence experiments involving a single Trp residue. To this end, we modified the GWALP23 by replacing Trp at position 5 with a Tyr (7). The Y^{5}GWALP23 confers a stable transmembrane orientation with low dynamic averaging of the NMR resonances similar to the GWALP23 peptide. These model systems have proven to be

good hosts for studying incorporation of potentially charged polar residues at the core of the helix (8-10). In particular, the Y^5GWALP23 peptide served as the host for introducing lysine residues at position 12 or 14 to study its titration and ionization properties in DOPC lipid bilayer membranes. Both Y^5GWALP23-K12 and Y^5GWALP23-K14 peptides are observed to titrate at a low pK_a close to 6 when examined by experiments over a pH range of 4.0-9.0. On the same note we have also studied bilayer incorporated Y^5GWALP23-E14 in DLPC and DOPC bilayers where we find the Glu to be charged up to a pH of 12.5. We however observe a titration of the Tyr residue at pH 10.5. Here we show and confirm the titration of the Tyr residue in Y^5GWALP23.

2.3 Materials and Methods

Solid Phase Synthesis of ^{2}H-Labeled Peptides

Commercial L-alanine-d4 from Cambridge Isotope Laboratories (Andover, MA) was modified with an Fmoc group, as described previously (11), and recrystallized from ethyl acetate:hexane, 80:20. NMR spectra (^{1}H) were used to confirm successful Fmoc-Ala-d_4 synthesis. Other protected amino acids and acid-labile "Rink" amide resin were purchased from NovaBiochem (San Diego, CA). All peptides were synthesized on a 0.1 mmol scale using "FastMoc™" methods and a model 433A synthesizer from Applied Biosystems by Life Technologies (Foster City, CA). Typically, two deuterated alanines of differing isotope abundances were incorporated into each synthesized peptide. Selected precursors for deuterated residues therefore contained either 100% Fmoc-L-Ala-d_4 or 50% Fmoc-L-Ala-d_4 with 50% non-deuterated Fmoc-L-Ala. The final residue on each peptide was acetyl-Gly to yield a blocked, neutral N-terminal.

A peptide cleavage solution was prepared containing 85% trifluoroacetic acid (TFA) and 5% each (v/v or w/v) of triisopropylsilane, water, and phenol. TFA cleavage from "Rink" resin in 2 mL volume (2-3 hrs at 22 °C) leads to a neutral, amidated C-terminal. Peptides were precipitated

by adding the TFA solution to 25 volumes of cold 50/50 MtBE/hexane. Peptides were collected by centrifugation, washed multiple times with MtBE/hexane and lyophilized from (1:1) acetonitrile/water. After lyophilization, crude peptide dissolved in TFE was purified via HPLC on a Zorbax Rx-C8 9.4 mm x 25 cm column packed with 5 μm octyl-silica (Agilent Technologies, Santa Clara, CA) with a typical gradient of 92-96% methanol/water (0.1% TFA) and a 1.7 mL/min. flow rate. Collected product is lyophilized multiple times to remove residual TFA. MALDI-TOF mass spectrometry was used to confirm peptide identity by molecular mass (Figure S1). Peptide purity was examined by reversed-phase HPLC (Figure S2) with 280 nm detection, using a 4.6 x 50 mm Zorbax SB-C8 column packed with 3.5 μm octyl-silica (Agilent Technologies, Santa Clara, CA), operated at 1 mL/min using a methanol/water gradient from 85% to 99% methanol (with 0.1% TFA) over five min. Peptide quantity was calculated by means of UV absorbance at 280 nm, using molar extinction coefficients of 5,600 M^{-1} cm^{-1} for each Trp and 1,490 M^{-1} cm^{-1} for each Tyr residue in the peptide (12).

^{2}H NMR Spectroscopy using Oriented Bilayer samples

Mechanically aligned samples for solid-state NMR spectroscopy (1/40, peptide/lipid) were prepared using DOPC or DLPC lipids from Avanti Polar Lipids (Alabaster, AL), and deuterium-depleted water (Cambridge; 45% w/w hydration), as described previously (17). Bilayer alignment within each sample was confirmed using ^{31}P NMR at 50 ˚C on a Bruker Avance 300 spectrometer (Billerica, MA) at both $\beta = 0^{\circ}$ (bilayer normal parallel to magnetic field) and $\beta = 90^{\circ}$ macroscopic sample orientations (Figure S3). Deuterium NMR spectra were recorded at both sample orientations on a Bruker Avance 300 spectrometer, utilizing a quadrupolar echo pulse sequence (18) with 90 ms recycle delay, 3.2 μs pulse length and 115 μs echo delay. Between 0.5 and 1.5 million scans were accumulated during each ^{2}H NMR experiment. An

exponential weighting function with 100 Hz line broadening was applied prior to Fourier transformation.

Buffers for oriented samples were prepared at room temperature using vacuum-dried reagents and prepared in deuterium-depleted water. Buffers include: pH 4 Acetate buffer 50 mM (sodium acetate and acetic acid, Sigma, St. Louis, MO); pH 6 Citrate buffers 10 mM (EMD, Gibbstown, NJ); pH 8.5, and 9 Tris buffers 50 mM (Trizma® hydrochloride and Trizma® base, St. Louis, MO), pH 11.5 and 12 CABS buffer (Sigma Aldrich, St. Louis, MO), and pH 13 Phosphate buffers (Sigma Aldrich, St. Louis, MO).

CD Spectroscopy

Small lipid vesicles incorporating 125 nM peptide and 7.5 μM lipid (1/60) were prepared by sonication in unbuffered water. An average of ten scans was recorded on a JASCO (Easton, MD) J710 CD spectropolarimeter, using a 1 mm cell path length, 1.0 nm bandwidth, 0.1 nm slit and a scan speed of 20 nm/min.

2.4 Results

To investigate the titration of a Tyr phenol side chain positioned on a transmembrane helix near the membrane/water interface, we used the model Y^5GWALP23 peptide in DLPC bilayers. Circular dichroism (CD) spectra indicate that the peptides retain their alpha-helical secondary structure even upon introduction of glutamic acid within the central core helix (Figure S4). Characteristic CD spectra for alpha-helices were observed for E14-containing samples of Y^5GWALP23 and GWALP23 peptides in lipid vesicles of DLPC.

Titration of Tyrosine

We prepared oriented samples of Y^5GWALP23-E14 in DLPC bilayers and experimented under pH conditions ranging from pH 6 to 13. The alanine methyl quadrupolar splittings remained universally unchanged for the –E14 peptide up to pH 9.5 (Figure 1). However, we do observe changes in the quadrupolar splittings at pH 11.5 followed by more change in quadrupolar splittings at pH 13.

To verify the titration of both Glu and Tyr residues we then used oriented samples of Y^5GWALP23 and GWALP23 peptides as control experiments in DLPC bilayers under neutral to basic conditions. The alanine ^{2}H quadrupolar splittings for GWALP23 remain largely unchanged between pH 6 to 13 due to the lack of any possible titrable side-chain (Figure 2A). Y^5GWALP23 peptide, conversely, does not show any change in its methyl ^{2}H quadrupolar splittings between pH 6 to 9.5 but shows a change at pH 11.5 (Figure 2B) suggesting that the phenolic hydroxyl group of the tyrosine at the membrane water interface has a pKa of 10.5. The combined results of alanine quadrupolar splittings for the neutral Y^5GWALP23 (Figure 3, Table 1) reveal a single well defined state which upon titration at high pH produces a minimal change in tilt ($\Delta\tau$) of about 3.6° and a change in rotation ($\Delta\rho$) of 6° (Figure 4, Table 2). The results indicate that the Y^5GWALP23 helix orientation shows a minimal but measurable change upon titration of the Tyr residue.

2.5 Discussion

To determine the titration behavior of a polar aromatic tyrosine residue at the membrane/water interface, α-helical Y^5GWALP23 was used as the transmembrane host model system. We observe the tyrosine side chain to titrate and deprotonate between pH 10 and 11.5 suggesting a pK_a of ~10.5. We used the GWALP23 parent peptide as a pH-independent control

to confirm the titration of tyrosine in Y^5GWALP23. GWALP23 is has its core helix flanked by a Trp residue at each end thus rendering the peptide devoid of any titrable group. The Y^5GWALP23 peptide was previously used as a host for studying the titration behavior and dynamics of lysine residues (13). Experiments with introduction of lysine in Y^5GWALP23 were carried out below pH 9 and hence did not involve the deprotonation of tyrosine.

The dynamics and average orientation of Y^5GWALP23 and GWALP23 in DLPC are found to be very similar (7) with the Gaussian and semi-static fits for dynamics based on the six ^{2}H quadrupolar splittings yielding similar tilt (τ_0) values of about 21°. Our results with titration of Tyr indicates that the helix orientation of Y^5GWALP23 is not much affected by the charge status of the Tyr residue. A possible explanation for the minimal response at high pH change could be the location of the Tyr residue near the membrane-water interface where the hydroxyl side chain remains fully hydrated. The observed pK_a value of 10.5 also is reasonable for a phenolic group in aqueous solution. We conclude that the Y5 side chain is not buried in DLPC bilayers but rather is exposed to the aqueous buffer.

Aromatic residues such as Tyr and Trp are found in the interfacial layer of transmembrane proteins. They may function as anchoring residues by “locking” the protein into its correct orientation within the membrane by forming interactions with the lipid head groups and water molecules in the interfacial region (14). Simulation studies with OmpA and KcsA proteins along with experimental literature on interactions of aromatic residue containing transmembrane proteins with lipid bilayers (14,15) are in agreement with the concept. The aromatic residues are positioned in the interfacial region with their polar moieties (ring nitrogen of Trp; hydroxyl group of Tyr) facing the aqueous solution. This arrangement makes the amphipathic rings perfect for the role of anchoring membrane proteins.

2.6 Acknowledgement

I thank Vitaly Vostrikov for software for semi-static GALA and modified Gaussian methods for analysis of helix integrity and dynamics. I would also like to thank Nick Gleason for the initial work with Y^5GWALP23 peptides.

2.7 References

1. Landolt-Marticorena, C., Williams, K. A., Deber, C. M., and Reithmeier, R. A. F. (1993) Non-Random Distribution of Amino Acids in the Transmembrane Segments of Human Type-I Single Span Membrane-Proteins. *J. Mol. Biol.* **229**, 602-608

2. Schiffer, M., Chang, C. H., and Stevens, F. J. (1992) The Functions of Tryptophan Residues in Membrane Proteins. *Protein Engineering* **5**, 213-214

3. Killian, J. A., Prasad, K. U., Urry, D. W., and Dekruijff, B. (1989) A Mismatch Between the Length of Gramicidin and the Lipid Acyl Chains is a Pre-requisite for H_{II} Phase Formation in Phosphatidyl Choline Model Membranes. *Biochimica Et Biophysica Acta* **978**, 341-345

4. Killian, J. A., Salemink, I., dePlanque, M. R. R., Lindblom, G., Koeppe, R. E., and Greathouse, D. V. (1996) Induction of nonbilayer structures in diacylphosphatidylcholine model membranes by transmembrane alpha-helical peptides: Importance of hydrophobic mismatch and proposed role of tryptophans. *Biochemistry* **35**, 1037-1045

5. de Planque, M. R. R., Boots, J. W. P., Rijkers, D. T. S., Liskamp, R. M. J., Greathouse, D. V., and Killian, J. A. (2002) The effects of hydrophobic mismatch between phosphatidylcholine bilayers and transmembrane alpha-helical peptides depend on the nature of interfacially exposed aromatic and charged residues. *Biochemistry* **41**, 8396-8404

6. de Planque, M. R. R., Kruijtzer, J. A. W., Liskamp, R. M. J., Marsh, D., Greathouse, D. V., Koeppe, R. E., de Kruijff, B., and Killian, J. A. (1999) Different membrane anchoring positions of tryptophan and lysine in synthetic transmembrane alpha-helical peptides. *J. Biol. Chem.* **274**, 20839-20846

7. Gleason, N. J., Vostrikov, V. V., Greathouse, D. V., Grant, C. V., Opella, S. J., and Koeppe, R. E., II. (2012) Tyrosine Replacing Tryptophan as an Anchor in GWALP Peptides. *Biochemistry* **51**, 2044-2053

8. Vostrikov, V. V., Hall, B. A., Greathouse, D. V., Koeppe, R. E., and Sansom, M. S. P. (2010) Changes in Transmembrane Helix Alignment by Arginine Residues Revealed by Solid-State NMR Experiments and Coarse-Grained MD Simulations. *J. Am. Chem. Soc.* **132**, 5803-5811

9. Gleason, N. J., Vostrikov, V. V., Greathouse, D. V., and Koeppe, R. E. (2013) Buried lysine, but not arginine, titrates and alters transmembrane helix tilt. *Proceedings of the National Academy of Sciences of the United States of America* **110**, 1692-1695

10. Martfeld, A. N., Greathouse, D. V., and Koeppe, R. E. (2016) Ionization Properties of Histidine Residues in the Lipid-Bilayer Membrane Environment. *J. Biol. Chem.*

11. Thomas, R., Vostrikov, V. V., Greathouse, D. V., and Koeppe, R. E. (2009) Influence of Proline upon the Folding and Geometry of the WALP19 Transmembrane Peptide. *Biochemistry* **48**, 11883-11891

12. Pace, C. N., Vajdos, F., Fee, L., Grimsley, G., and Gray, T. (1995) How to Measure and Predict the Molar Absorption Coefficient of a Protein. *Protein Sci.* **4**, 2411-2423

13. Gleason, N. J., Greathouse, D. V., Grant, C. V., Opella, S. J., and Koeppe, R. E. (2013) Single Tryptophan and Tyrosine Comparisons in the N-Terminal and C-Terminal Interface Regions of Transmembrane GWALP Peptides. *Journal of Physical Chemistry B* **117**, 13786-13794

14. de Planque, M. R. R., Bonev, B. B., Demmers, J. A. A., Greathouse, D. V., Koeppe, R. E., Separovic, F., Watts, A., and Killian, J. A. (2003) Interfacial anchor properties of tryptophan residues in transmembrane peptides can dominate over hydrophobic matching effects in peptide-lipid interactions. *Biochemistry* **42**, 5341-5348

15. de Planque, M. R. R., and Killian, J. A. (2003) Protein-lipid interactions studied with designed transmembrane peptides: role of hydrophobic matching and interfacial anchoring (Review). *Mol. Membr. Biol.* **20**, 271-284

16. Sparks, K. A., Gleason, N. J., Gist, R., Langston, R., Greathouse, D. V., and Koeppe, R. E. (2014) Comparisons of Interfacial Phe, Tyr, and Trp Residues as Determinants of Orientation and Dynamics for GWALP Transmembrane Peptides. *Biochemistry* **53**, 3637-3645

17. Thomas, R., Vostrikov, V. V., Greathouse, D. V., and Koeppe, R. E. (2009) Influence of Proline upon the Folding and Geometry of the WALP19 Transmembrane Peptide. *Biochemistry* **48**, 11883-11891

18. Davis, J. H., Jeffrey, K. R., Bloom, M., Valic, M. I., and Higgs, T. P. (1976) Quadrupolar echo deuteron magnetic resonance spectroscopy in ordered hydrocarbon chains. *Chemical Physics Letters* **42**, 390-394

2.8 Tables

Table 1. Observed Ala-methyl ^2H quadrupolar splitting magnitudes ($|\Delta\nu_q|$)[a] for GWALP23 and Y^5GWALP23 in DLPC ether lipid bilayers.

	Quadrupolar Splittings (kHz)		
	GWALP23[b]	Y^5GWALP23	
Ala-d_4 position	Neutral	pH 6[b]	pH 11.5
7	26.4	29.3	28.4
9	25.5	24.0	27.4
11	26.9	26.4	26.6
13	14.6	10.5	15.6
15	20.7	19.5	20.6
17	3.4	8.1	5.2

[a] Quadrupolar splittings are reported in kHz for the $\beta = 0°$ sample orientation for GWALP23 and Y^5GWALP23 at pH 6 and 13. Each value is an average of (the magnitude observed when $\beta = 0°$) and (twice the magnitude observed when $\beta = 90°$).
[b] Values have been reported from Ref 7.

Table 2. Calculated Orientation and Dynamics of GWALP23 and Y[5]GWALP23 peptide in DLPC Lipid [a].

Peptide	pH	GALA Fit Results				Reference
		τ_0	ρ_0	S_{zz}	RMSD (kHz)	
GWALP23	-	21°	305°	0.71	0.7	(7) and (16)
Y^5GWALP23	6	18.7°	296°	0.79	0.74	(7)
Y^5GWALP23	11.5	22.3°	302°	0.71	0.57	This work

[a] The parent GWALP23 sequence is acetyl-GGALWLALALAL^{12}AL^{14}AL^{16}ALWLAGA-amide.

2.9 Figures

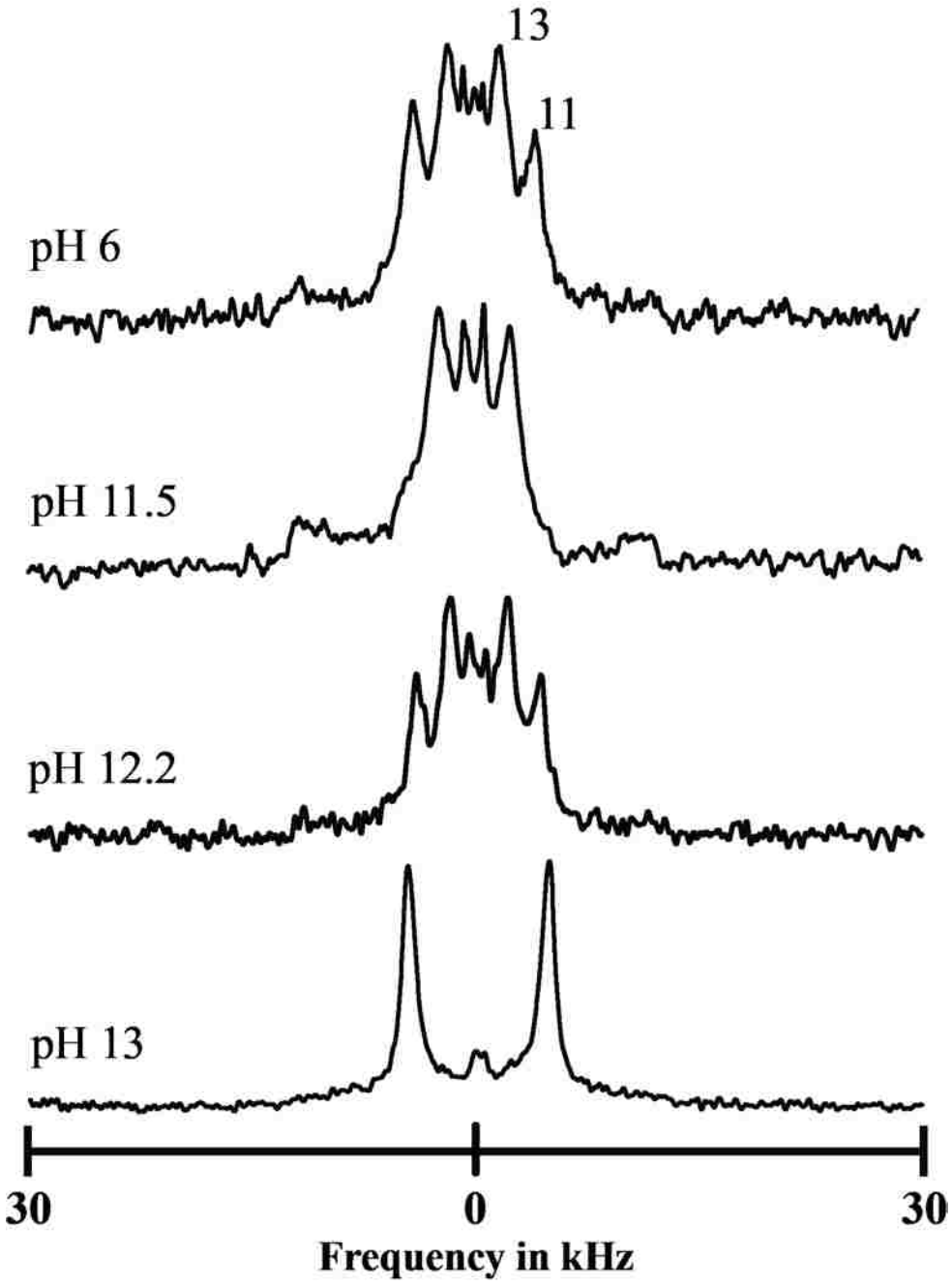

Figure 1: ^{2}H-NMR spectra of Y^{5}GWALP23-E14 peptide with deuterium labeled alanines at position 11 and 13 incorporated in DLPC ether bilayers hydrated with 10 mM buffer at indicated pH. The difference in spectra in DLPC ether bilayers between pH 6 to 13 indicates possible titration of both Tyr and Glu residues at pH 11.5 and 13. Spectra was recorded at $\beta = 90°$ sample orientation at 50°C.

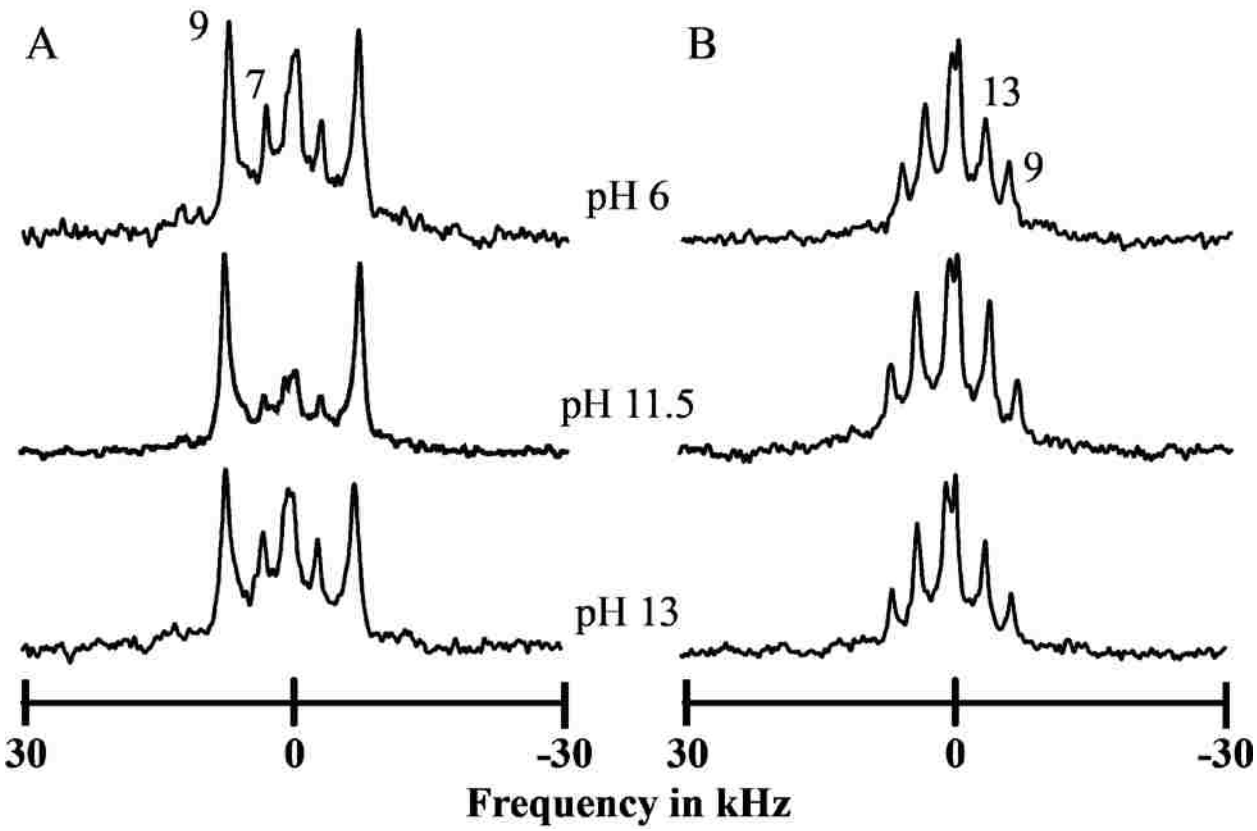

Figure 2: ^{2}H-NMR spectra of GWALP23 (A) and Y^{5}GWALP23 (B) peptides with deuterium labeled alanines at position 7, 9 (GWALP23) and 11, 13 (Y^{5}GWALP23) incorporated in DLPC ether bilayers hydrated with 10 mM buffer at indicated pH. ^{2}H NMR spectra of GWALP23 shows no response to pH change. The difference in spectra for Y^{5}GWALP23 between pH 6 and 11.5 indicates titration of Tyr. Spectra was recorded at $\beta = 90°$ sample orientation at 50°C.

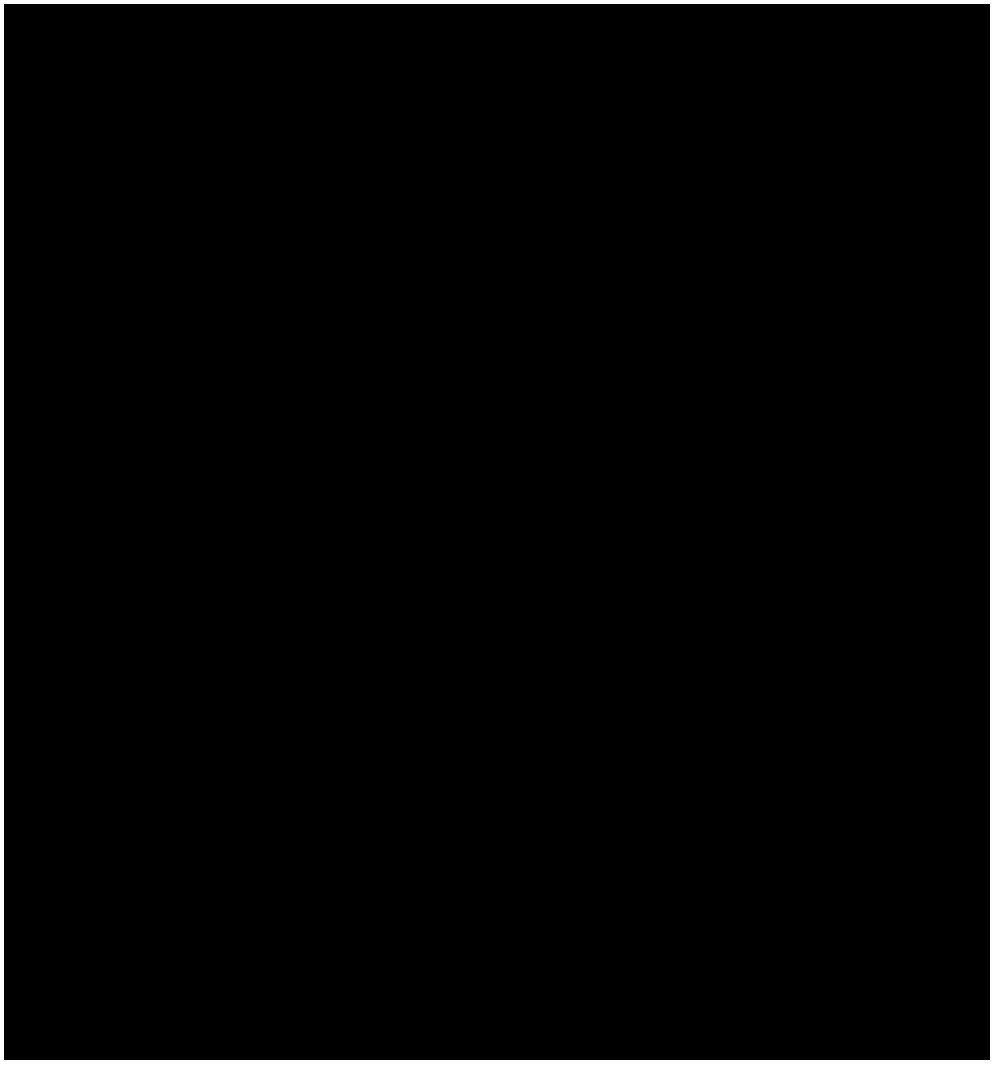

Figure 3: Selected deuterium NMR spectra of Y^5GWALP23 peptide with deuterium labeled alanines at position 7, 9,11,13,15 and 17 incorporated in DLPC ether bilayers hydrated with 10 mM buffer at pH 11.5. The well-resolved signals in DLPC ether for all six ^{2}H-labeled alanines indicate a well-defined tilted transmembrane orientation in the lipid bilayer at high pH. Spectra was recorded at $\beta = 90°$ sample orientation at 50°C.

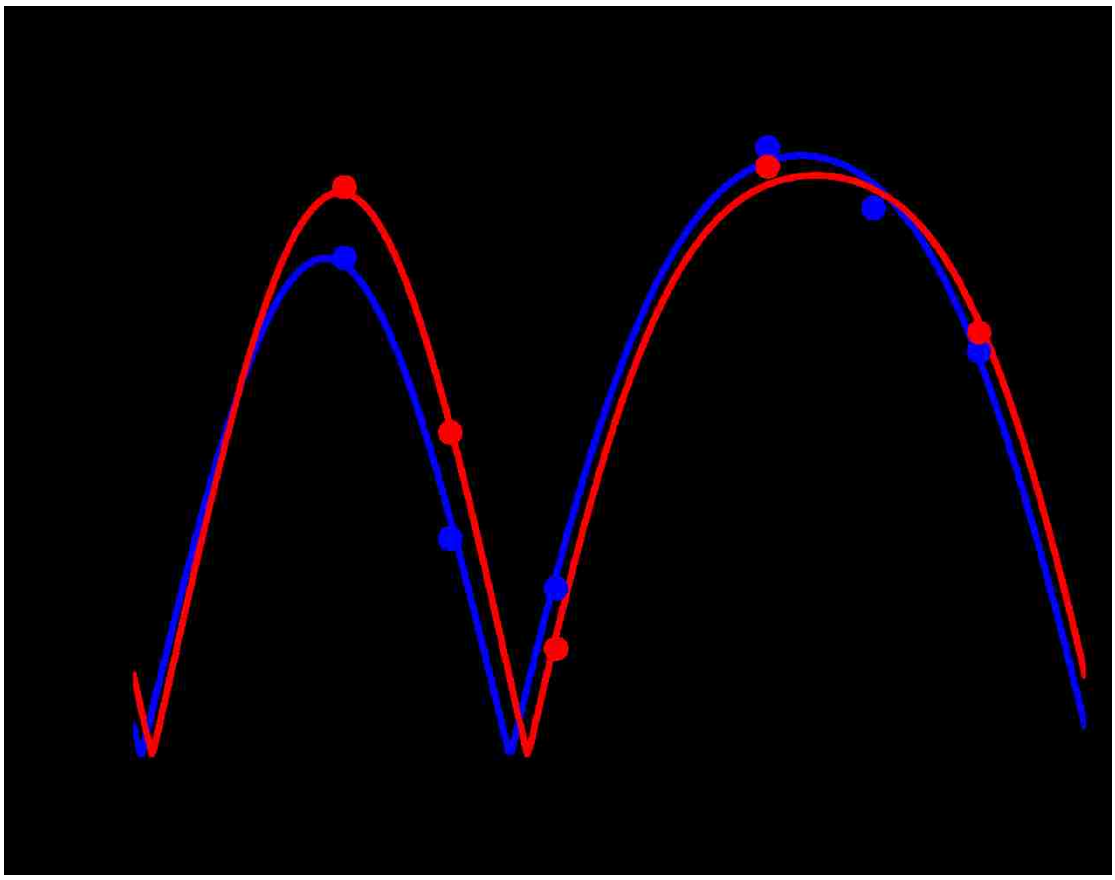

Figure 4: GALA quadrupolar wave plots of tilted membrane peptides in DLPC ether bilayers. Y^5GWALP23 (blue; tilt $\tau = 18.7°$, rotation $\rho = 296°$, pH 6) has a distinct tilt and rotation which shows no significant change from the charged Y^5GWALP23 (red; tilt $\tau = 22.3°$, rotation $\rho = 302°$, pH 11.5).

2.10 Supporting Information

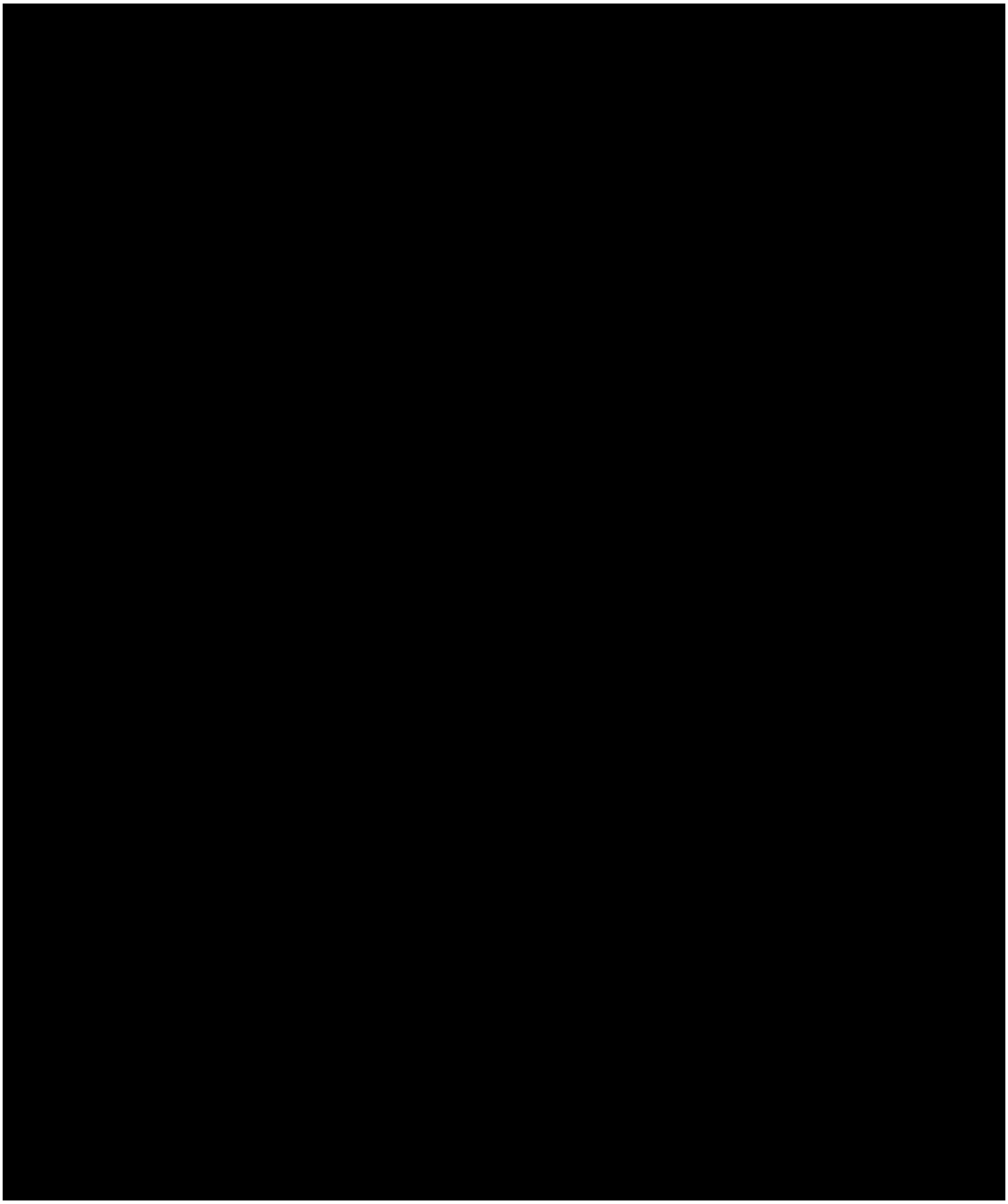

Figure S1: MALDI mass spectrum of synthesized peptides GWALP23 (top) and Y^5GWALP23 (bottom) with labeled ^{2}H-Ala residues. The expected monoisotopic mass for GWALP23 is 2288.83 Daltons; adding 39 for K^+ and one ^{13}C atom is 2332 with 4 deuterons or 2336 with 8 deuterons present. The expected monoisotopic mass for Y^5GWALP23 is 2237.73 Daltons; adding 23 for Na^+ and one ^{13}C atom is 2264 with 4 deuterons or 2268 with 8 deuterons present. Successive m/z peaks differ by ± one ^{13}C atom (present at ~1.1% abundance).

Figure S2: Analytical HPLC chromatogram of purified Y^5GWALP23 (left) and GWALP23 (right).

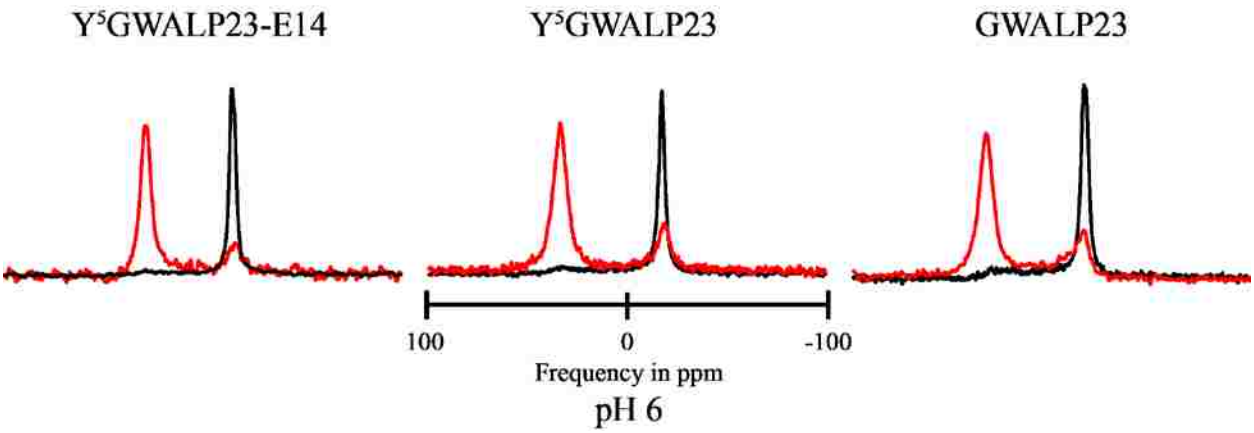

Figure S3: Examples of ^{31}P NMR spectra for oriented bilayers of DLPC ether containing Y^{5}GWALP23-E14, Y^{5}GWALP23, and GWALP23. Samples were hydrated with 10 mM buffer at pH 6 and recorded with orientations parallel ($\beta = 0°$, red) or perpendicular ($\beta = 90°$, black) to the magnetic field.

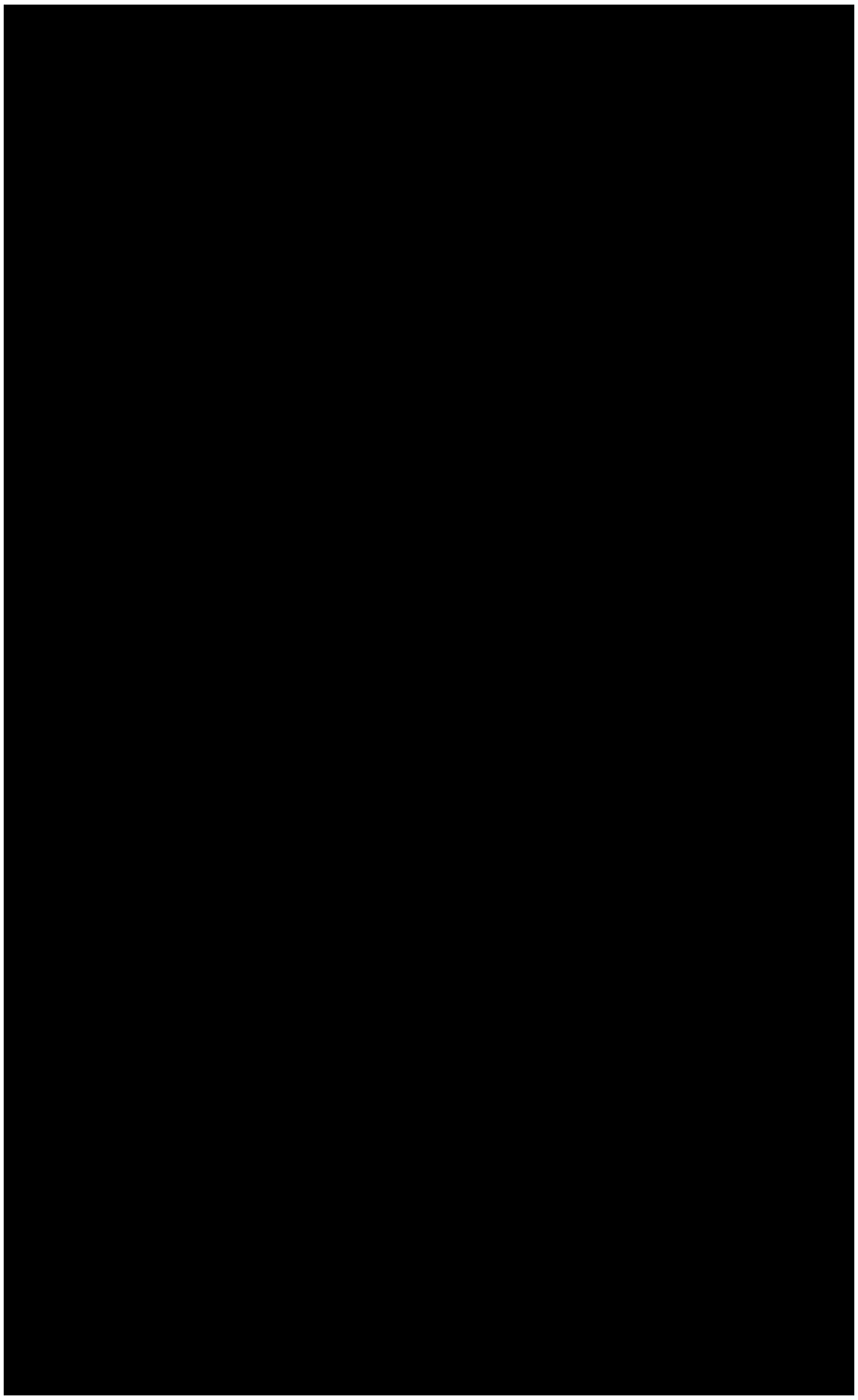

Figure S4: Circular Dichroism of GWALP23 (top) and Y^5GWALP23 (bottom) in DLPC vesicles. Peptide to lipid ratio is 1:60.

CHAPTER 3: Influence of Glutamic Acid Residues and pH on the Properties of Transmembrane Helices

3.1 Abstract

Negatively charged side chains are important for the function of particular ion channels and certain other membrane proteins. To investigate the influence of single glutamic acid side chains on helices that span lipid-bilayer membranes, we have employed GWALP23 (acetyl-GGALW$_5$LALALALALALALW$_{19}$LAGA-amide) as a favorable host peptide framework. We substituted individual Leu residues with Glu residues (L12E or L14E or L16E) and incorporated specific ^{2}H-labeled alanine residues within the core helical region or near the ends of the sequence. Solid-state ^{2}H-NMR spectra reveal little change for the core labels in GWALP23-E12, –E14 and –E16 over a pH range of 4 to 12.5, with the spectra being broader for samples in DOPC compared to DLPC bilayers. The spectra for samples with deuterium labels near the helix ends on alanines 3 and 21 show pH-dependent changes in the unwinding of the helix terminals in both DLPC and DOPC bilayers. The combined results suggest that Glu residues E14 and E16 titrate with pK_a values near 12.5 in DLPC and DOPC lipid bilayer membranes, with the central and most buried residue E12 showing no pH dependence. Interestingly, the titration of E16 causes significant local unwinding of the core helix. Our results are consistent with the expectation that buried carboxyl groups aggressively hold their protons and/or waters of hydration.

3.2 Introduction

Membrane proteins are involved in multitudinous biological processes and form about 30% of the proteins in the cell (1,2). The cell membrane acts as a barrier, prohibiting the unchecked transfer of ions or other polar molecules between the cell and the environment using a low dielectric inner hydrophobic core sandwiched on both sides by the high dielectric media of the inside and outside of the cell (3). The transmembrane protein segments are typically composed of a hydrophobic core with their sequences determining their function (4,5). Despite the predominantly hydrophobic core, potentially charged residues are also observed somewhat often within the core segments of a transmembrane protein and are believed to be important in the functioning of many proteins. These titratable protein side chains, notably those of Asp, Glu, His, Lys and Arg, encounter an environment-dependent energy barrier that governs their ability to pick up or lose a proton in transitioning between charged and neutral states. Changes in the microenvironments of these buried residues, such as the bilayer thickness (6), lipid phosphate head group identity, or presence of water molecules, therefore, have significant influence on the charge status.

The charge status in turn will influence the helix orientations and geometry in lipid bilayer membranes (7-9). Key glutamic acid and arginine residues in the core of a membrane protein, therefore, may be critical for stabilizing the native structure and function (10-12). Ionizable residues moreover may engage in proton transfer reactions at the active sites of transmembrane enzymes (13) and in voltage sensing functions (14).

An avenue for measuring side-chain pK_a in an actual membrane lipid bilayer environment is offered by designed model peptide helices that have well defined properties. One such example is the helix of GWALP23 (acetyl-GGALW$(LA)_6$LWLAGA-[ethanol]amide) (15,16). The

particular GWALP23 transmembrane model helix features two interfacial Trp residues that contribute to a preferred and well-defined tilted transmembrane helix orientation with low dynamic averaging (17-19). The framework of GWALP23 (and its closely related cousin having Y5 instead of W5) has been employed to determine a pK_a value of 6.5 at 37 °C for a lipid-facing lysine side chain located close to the center of the DOPC bilayer membrane (20). Notably, this pK_a value is about four pH units lower than the standard value for lysine in aqueous solution. Further titration experiments with GWALP23-R14 reveal that bilayer-incorporated arginine does not titrate below pH 9, with Arg essentially preferring to exit the lipid bilayer rather than to lose a proton. (8,20) It is interesting to note that the bilayer environment, in comparison to a bulk water environment, influences the pK_a of lysine more than that of arginine.

In this paper we focus on examining the pK_a values for the neutral to negative charge transitions of Glu side chains at three specific positions in bilayer membranes with varying lipid thickness, namely DLPC and DOPC. We find that the lipid-bilayer environment tends to favor a neutral protonated state of Glu even more strongly than for His and Lys side chains. We further report that Glu appears not to titrate below pH 12.5, suggesting a shift in pK_a of about eight pH units from the aqueous value. Molecular dynamics simulations (21) indicate increased water penetration near buried negative carboxylates in fold proteins than near buried positive Lys side chains (21). Our results, with similar trends for Glu 12, 14 and 16 in the GWALP23 helix, in each case disfavoring negative glutamate in the bilayer, are in agreement with the relative hydration tendencies. We also will examine the possibilities for helix fraying and for the onset of multistate behavior as a single Glu residue on a transmembrane helix becomes more buried in a lipid bilayer.

3.3 Materials and Methods

Solid Phase Synthesis of ^{2}H-Labeled Peptides

Solid-phase peptide synthesis was carried out on a 0.1 mmol scale using an Applied Biosystems 433A synthesizer from Life Technologies (Foster City, CA). N-Fmoc amino acids with additional side chain protections were purchased from NovaBiochem (San Diego, CA). Glutamic acid with *t*-butyl ester and tryptophan with *t*-butoxycarbonyl protecting groups were used. Cleavage of peptides from the Rink amide resin (NovaBiochem) was achieved using trifluoroacetic acid to yield an amidated C-terminal. Two deuterated alanine residues from Cambridge Isotope Labs (Tewksbury, MA) with differing isotopic abundances were incorporated in each peptide, according to previous methods (22). The peptides were purified using reversed-phase HPLC on an octyl-silica column (Zorbax Rx-C8, 9.4 x 250 mm, 5 μm particle size; Agilent Technologies, Santa Clara, CA) using a gradient of 94-98% methanol, with 0.1% trifluroacetic acid over 22 min. Analytical HPLC and MALDI-TOF analysis to confirm peptide identity and purity are provided in Figure S1 of the Supporting Information.

CD Spectroscopy

Samples for circular dichroism (CD) spectroscopy were prepared by using a mixture of 62.5 nM peptide and 3.75 μM lipid (1/60), sonicated in unbuffered water to create small lipid vesicles incorporating the peptides. An average of 10 scans was recorded with a Jasco (Easton, MD) J-1500 CD/fluorescence spectropolarimeter, using a 1 mm cell path length, 1.0 nm bandwidth, 0.1 nm slit, and a scan speed of 20 nm/min.

^{2}H NMR Spectroscopy using Oriented Bilayer samples

Aligned samples with a 1:60 peptide:lipid ratio, for solid-state ^{2}H NMR experiments, were prepared using DOPC or DLPC bilayer membranes. For experiments at high pH or low pH,

DLPC ether (1,2-di-0-dodecyl-*sn*-glycero-3-phosphocholine) or DOPC ether (1,2-di-O-(9Z-octadecenyl)-*sn*-glycero-3-phosphocholine) lipids from Avanti Polar Lipids (Alabaster, AL) were used. Peptide:lipid films were deposited from 95% methanol, dried under vacuum (10^{-4} Torr for 48 h) and hydrated (45% w/w) with 10 mM acetate, glycine, citrate, 4-(cyclohexylamino)-1-butanesulfonate or phosphate buffer in deuterium-depleted water at pH values between 4 and 13. The bilayer alignment of a sample was assessed by means of ^{31}P NMR spectra recorded using a Bruker (Billerica, MA) Avance 300 MHz spectrometer (see Figure S2 of the Supporting Information). Deuterium NMR spectra were recorded on a Bruker Avance 300 MHz spectrometer at 50 °C with $\beta = 90°$ and $\beta = 0°$ macroscopic sample orientations using a quadrupolar echo pulse sequence (23) with a 90 ms recycle delay, 3.2 μs pulse length, and 115 μs echo delay. About 0.6 to 1 million free induction decays were recorded for each ^{2}H experiment. Fourier transformation was accomplished using an exponential weighting function with 150 Hz line broadening. Helix orientations were analyzed using semi-static "GALA" method, taking the average tilt τ of the helix axis, the azimuthal rotation ρ about the helix axis, and the principal order parameter S_{zz} as variables (24). Helix dynamics were further analyzed using a three-parameter modified Gaussian method (18,25), with the mean helix tilt τ_o, mean azimuthal rotation ρ_o and rotational distribution $\sigma\rho$ as variables.

3.4 Results

To investigate the ionization behavior and influence of a Glu carboxyl side chain on a transmembrane helix in lipid bilayers, single Glu residues were introduced into the GWALP23 peptide sequence at position 14, located on the opposite helix face from the Trp residues; position 16, located right below the W19 indole ring and close to the interfacial layer; or at

position 12, located directly between the two anchoring Trp residues spaced evenly on the same helix face **(**Figure 1**)**. The GWALP23 core sequence features a central (Leu-Ala)$_6$ repeat that should favor peptide folding into α-helical secondary structure within the hydrophobic region of a lipid bilayer. Circular dichroism (CD) spectra largely confirm the retention of α-helical secondary structure with the introduction of each single Glu residue, although the ^{2}H NMR results indicated that A15 and especially A17 of the core domain may deviate from helical geometry in some samples under some conditions. Nevertheless, CD spectra for bilayer-incorporated GWALP23-E14, GWALP23-E16 and GWALP23-E12 (Figure S3 of the Supporting Information) all show pronounced double minima near 208 nm and 222 nm, indicative of principally α-helical secondary structure.

Helix integrity and helical orientations were assessed by means of ^{2}H-NMR spectra of deuterated alanine residues in GWALP23-E14, -E16 and -E12 peptides in aligned bilayers of DLPC, DOPC or their ether-linked alternatives. The samples were hydrated with 10 mM buffer at a variety of pH conditions. We will present results in turn for each particular location of the Glu substitution in the GWALP23 sequence.

GWALP23-E14.

The ^{2}H NMR spectra for the aligned samples reveal well-defined signals for the ^{2}H-Ala methyl groups of GWALP23-E14 in DLPC and its ether-linked lipid bilayers. The spectra from samples hydrated with pH 6 buffer exhibit distinct resonances for the CD_3 methyl side chains of each of the six core Ala residues, although the peaks are notably broader than observed with GWALP23-R14 (7). In spite of the broader peaks, the varying quadrupolar splittings for the alanine CD_3 groups suggest a relatively well-defined tilted transmembrane orientation in DLPC and ether-linked DLPC bilayer membranes **(**Figure 2A**)**. When comparing the spectra for GWALP23-E14

at pH 6 in the ether- versus ester-linked DLPC, we observed small yet measurable changes in the quadrupolar splittings for alanine CD_3 groups (Figure S4 of the Supporting Information). As a consequence, we decided to persist with only the ether-linked DLPC lipid bilayers at all of the experimental pH values, to avoid the possibility of ambiguity while investigating spectral changes due to Glu titration when the pH is changed.

The ^{2}H NMR spectra for aligned samples of GWALP23-E14 in DOPC bilayers exhibit multiple weak resonances and low signal-to-noise for each labeled alanine residue, suggesting multiple slowly exchanging states for the peptide population in the bilayers (Figure 2B). Because of the spectral difficulties exhibited by the DOPC samples (Figure S5 of the Supporting Information), we persevered mainly with the study of Glu residues in DLPC bilayers.

Focusing on the DLPC-ether bilayers, the GWALP23–E14 helix indicates remarkably little change in the NMR observables between pH 6.0-12.5, but shows changes between pH 12.5-13 (Figure 3A**)**. Based on the pH dependence of the quadrupolar splittings, one can deduce the pK_a of E14 substituted in GWALP23 to be around 12.5 in DLPC-ether bilayers. The spectra in DOPC-ether bilayers indicate that a broad distribution of closely related states persists for GWALP23-E14 over the pH range of 6-13 (Figure 3B**)**.

The rather small changes in the ^{2}H NMR signals from the core helix, even at pH 13 (Figure 3A), suggested that perhaps the ends of the GWALP23-E14 helix might respond to pH in DLPC bilayers. To examine the possibility of changes in the helix fraying (19), we labeled alanines 3 and 21 of GWALP23-E14 with deuterium. Indeed, the ^{2}H spectra for A3 and A21 suggest a change in the unwinding of the C-terminal of GWALP23-E14 between pH 6 and 13 (Figure 3C**)**. The ^{2}H quadrupolar splitting for the A3 methyl group remains fixed in place between pH 6 and 13 in DLPC, while that for A21 shows significant change (Figure 3C). The end labels

furthermore show somewhat better resolved spectra in DOPC as compared to the core labels, and suggest small changes with pH (Figure 3D).

The combined results for the observed quadrupolar splittings (Table 1) from core and juxta-terminal Ala ^{2}H-methyl groups in DLPC-ether bilayers serve to define the helix orientation and integrity at pH 6 and pH 13. Both the semi-static GALA (24,26) and modified Gaussian dynamic (18,25) methods of analysis reveal an intact core helix between residues 7-15 at pH 6 that is nevertheless, surprisingly, interrupted or "unwound" at A17 (Figure 4). Indeed, the ^{2}H quadrupolar splitting magnitudes $|\Delta\nu_q|$ of not only the outer alanines 3 and 21 but also A17 (considered within the "core" domain) deviate and fail to fit the helix backbone geometry (Figure 4). This situation is unique for glutamic acid, as deviations from the core helix geometry have not been observed for R14 (7) or K14 (20) or H14 (27). The observed deviations from the quadrupolar wave that corresponds to the backbone of the core helix (Figure 4) are 2 kHz for A3, 5 kHz for A17 and 10 kHz for A21 (in the context of an experimental uncertainty of 1 kHz). We note that the helix is interrupted at residue A17 even though residue E14 is neutral and polar, but not charged, as E14 titrates only at much higher pH (see below).

The slightly truncated core helix of GWALP23-E14 exhibits a single major transmembrane orientation at pH 6. The transition from pH 6 to pH 13 involves deprotonation of E14 to produce the carboxylate side chain. The titration of E14 changes the observed quadrupolar wave (Figure 4) yet involves mainly an alteration of the helix dynamics with only minor effects on the mean helix tilt, unwinding or azimuthal rotation. One notes that the spectral resonances become sharper at high pH (Figure 3), suggesting altered dynamics. Furthermore, both methods of analysis (Table 2) suggest a smaller spread, or perhaps a faster averaging, about sharper mean values. In the GALA method S_{zz} is seen to increase at high pH, while in the modified Gaussian

method, σρ is seen to decrease at high pH (Table 2), both indicating a lower extent of motional averaging of the ^{2}H quadrupolar splittings. Interestingly, the amplitude of the quadrupolar wave increases somewhat at high pH (Figure 4), due to the reduced dynamic averaging, even though the mean helix tilt becomes smaller at high pH. The modified Gaussian analysis shows a small reduction in tilt from 22° to 20° at pH 13. The GALA method, which underestimates the influence of the dynamics (25), returns for the helix tilt estimates of 25° at pH 6 and 17° at pH 13 (Table 2) again, notably in spite of the larger amplitude of the quadrupolar wave at high pH. At pH 13, the ^{2}H resonances from the methyl groups of A3, A17 and A21 remain off of the quadrupolar wave defined by the core helix (Figure 4), but the large deviation for A21 is somewhat reduced, being about 7 kHz at pH 13 instead of 10 kHz at pH 6. The (unchanging) $|\Delta\nu_q|$ magnitude for the A3 methyl is seen to be above the curve at pH 6 but below the curve at pH 13 (Figure 4).

Because the ^{2}H NMR spectral changes when E14 titrates can be attributed largely to changes in helix dynamics, the modifications to the orientation of the GWALP23-E14 helix are notably less than when K14 or H14 titrates (see Discussion). The adaptation is a consequence of E14 being deprotonated at high pH (E^-) in contrast to the neutral state for E14 (E^0) observed at lower pH (Figure 4). The tilted transmembrane orientation shows a significant change in helix azimuthal rotation Δρ of about 50° when L14 is replaced with the polar (but neutral) $E14^0$ (Figure 4; Table 2). Upon titration of $E14^0$ to $E14^-$, nevertheless, the further changes to the core helix orientation (Δρ = 5°; Δτ = only 2° when the modified Gaussian dynamics are considered), are small (Table 2). There is nevertheless a change (decrease) in the unwinding of the helix C-terminal, as the quadrupolar splitting for the A21 CD_3 group changes significantly for $E14^-$ in comparison to

$E14^0$ (Figure 4). Interestingly, the quadrupolar splitting for A3 does not change during the titration (Figure 4), but the core helix may move in relation to A3.

GWALP23-E16.

This peptide displays similar properties to its –E14 counterpart, but we observe distinct differences in the extent of helix unwinding near the guest Glu residue between pH 6 and pH 13. The ^{2}H NMR spectra for samples in DLPC bilayers display well-defined resonances for all of the core alanine methyl groups (Figure S6 of the Supporting Information). Again, GWALP23–E16 remains neutral and does show spectral changes over the pH range of 6 to 12.4 (Figure 5A), with the pattern of ^{2}H quadrupolar splittings suggesting an intact core helix and a single orientation throughout the pH range. Only at high pH, between pH 12.4 and pH 13, is a second transmembrane helix orientation observed, albeit with substantial unwinding near residue E16. Provisionally, we assign this orientation for the deprotonated $E16^-$ carboxylate, as indicated by changes in the ^{2}H quadrupolar splittings between pH 12.4 and 13. Again, based on the pH dependent changes in the quadrupolar splittings near pH 13, it appears that the pK_a for E16 is about 12.5, a value which may seem surprisingly high given the side chain location within the moderately thin DLPC bilayer environment (see Discussion).

Notably, although residue A17 is unwound from the core helix of GWALP23-E14 (see above; Figure 4), residue A17 remains part of the core helix in GWALP23-E16 between pH 6 and pH 12. Above pH 12, however, both of the core residues A15 and A17 that surround E16 become unwound at high pH. The amount of sequence that is unwound at high pH is therefore larger for GWALP23-E16 than for GWALP23-E14. In other words, the ^{2}H quadrupolar splitting magnitudes for the methyl groups of A15 and A17 move off of the curve defined by the rest of the core helix when E16 titrates at high pH (Figure 6).

Deuterium labels on A3 and A21 suggest, once again, differences in the extent of unwinding of the helix terminals of GWALP23-E16 at high pH (Figure 5B). A tilt analysis, based on either the semi-static GALA or a modified Gaussian dynamic analysis (Table 2), can serve to clarify both the helix tilt and the extent of unwinding at neutral and high pH (Figure 6). Comparing the results for $E16^0$ with those for the parent L16 helix of GWALP23 in DLPC (Figure 6) reveals changes in helix tilt $\Delta\tau$ and azimuthal rotation $\Delta\rho$ of about 7° and 54°, respectively, when L16 is replaced with the polar (but neutral) $E16^0$ (Figure 6; Table 2). When E16 titrates in DLPC, the major changes are helix unwinding near E16 together with a decreased tilt of the remaining, shortened, core helix. The modified Gaussian analysis (Table 2) shows a general agreement with the semi-static GALA method and furthermore indicates a much lower $\sigma\rho$, consistent also with the spectral sharpening at high pH (Figure 5). The $|\Delta\nu_q|$ value for A3 is found to be off the core helix curve at both low and high pH (Figure 6). The assignments at high pH were confirmed using a peptide with only A3 labeled (Figure S7 of the Supplementary Material). Altogether, the extended C-terminal (residues 15-23) becomes substantially less helical at high pH, perhaps influenced by the proximity of the titrating Glu residue to W19 (see Discussion). Regarding A21, even though the CD_3 $|\Delta\nu_q|$ value happens to fall near the helical wave at high pH, we think that this is a fortuitous coincidence, not reflecting helicity near A21, because of the dramatic unwinding at A17 and A15 (Figure 6). It is possible that an upward movement together with substantial unwinding could enable access of the negatively charged E16 carboxylate to the interfacial layer (see Discussion).

GWALP23-E12.

For the case of GWALP23-E12, the peptide in DLPC shows well defined ^2H NMR spectra albeit with low intensity signals for all of the core alanine methyl groups (Figure S8 of the Supporting

Information). The situation contrasts with that of GWALP23-R12 in DOPC, for which multi-state behavior is observed (8). The key difference could be the identity of residue 12 or the identity of the lipid (DLPC as opposed to DOPC). When the pH is raised from 6 to 13 in DLPC-ether bilayers, there are no observed changes in $|\Delta\nu_q|$ values for the CD_3 groups of the core alanines (Table 1, Figure 7A). This is a distinct contrast to the results for the E14 and E16 peptides, yet indicates striking agreement with results for GWALP23-H12 in DLPC (27). Indeed, when the central residue 12 is modified, the ^2H NMR spectra for both GWALP23-E12 and GWALP23-H12 in DLPC bilayers appear to be independent of pH. To pursue the issue further, the possibility of helix unwinding was again investigated by observing ^2H labels on alanine residues A3 and A21. Actually, GWALP23-E12 in DLPC does exhibit unwinding of the helix ends, but no change is observed in the fraying between pH 6 and pH 12.5 (Figure 7B). The collective $|\Delta\nu_q|$ magnitudes (Table 1) reveal a well-defined transmembrane orientation, with minor fraying near residues 3 and 21, for GWALP23-E12 in DLPC (Figure 8). Comparing the results for $E12^0$ with GWALP23-$H12^0$ (27) reveals only small differences in helix tilt $\Delta\tau$ and azimuthal rotation $\Delta\rho$ (about 0.3° and 3°, respectively), when His at position 12 is replaced with $E12^0$. The substituted helices, with a neutral polar residue at position 12, furthermore have the same helix tilt and rotation as the parent L12 helix of GWALP23 (Table 2). Analysis using the modified Gaussian method (Table 2) showed a general agreement with the semi-static method for the GWALP23-E12 peptide. The transmembrane orientation of GWALP23–$E12^0$ is therefore found to be very similar to those for the neutral GWALP23 (Figure 8) and GWALP23-H12 helices. It is of further interest that the terminal unwinding of the –E12 peptide in DLPC, while present, shows no inclination to change with pH, unlike the changes observed with E14 and E16 that seem to alter the interfacial layer access for the Glu residue. Rather, GWALP23-E12 seems

to exist in the DLPC bilayer in the same single orientation throughout the pH range, similar to observations with GWALP23-H12 (27).

3.5 Discussion

We have investigated the ionization properties of lipid-facing Glu residues incorporated into transmembrane helices at three positions, as well as the influence of these buried Glu residues on the peptide orientation, dynamics and helix integrity. The primary findings include rather broad ^{2}H NMR resonances when even a neutral buried Glu residue is present, very high pK_a values for Glu residues in lipid bilayers, and in some cases local helix unwinding. We will discuss the influence of Glu residue position and protonation state on the orientation of the host GWALP23 transmembrane helix, the titration behavior of E12, E14 and E16 in DLPC and DOPC bilayers, and a potential role of helix-terminal unwinding in stabilizing the transmembrane state upon Glu ionization in GWALP23-E16. We will address the lack of response of the buried central E12 residue in DLPC bilayers and will compare experimental results with predicted differences in titration behavior when Glu is incorporated into a lipid-bilayer membrane.

Major parts of our experiments were conducted using ether-linked DLPC and DOPC lipids, which are more stable than natural ester lipids under alkaline conditions. One notes that small but measurable changes are observed in some of the ^{2}H-Ala methyl quadrupolar splittings when comparing the ether and ester DLPC bilayers (e.g., Figure S4). The ^{2}H NMR quadrupolar splittings are very sensitive. Notably, therefore, for the results discussed here, we used the same ether lipid bilayers over the full range of pH.

With bilayer-incorporated GWALP23-E14, we have consistently observed broad alanine ^{2}H-methyl NMR signals for the E^{0}14 peptide at neutral pH. The signal broadening suggests that the neutral peptide may have intermediate motion. The neutral E14 peptide adopts a tilted

conformation in DLPC distinct from that of the host peptide, attributable to the presence of a polar residue at position 14 and similar to the observations with neutral Y^5GWALP23-$K^0$14 in DOPC bilayers (20) and GWALP23-$H^0$14 in DLPC or DOPC bilayers (27). The incorporation of a neutral polar residue at position 14, be it His, Lys or Glu, interestingly results in a 40°-50° change in rotation about the helix axis (Table 2 and (20,27)). The results confirm that a polar residue at position 14 modulates the orientation of the helix.

At higher pH, the ^{2}H-Ala resonances from labeled GWALP23-E14 in aligned bilayers become sharper, although only above pH 12.5 when there are also changes in the ^{2}H quadrupolar splittings. The GWALP23-E14 helix orientation shows slightly smaller tilt but conspicuously less rotational averaging following the transition from a neutral to a charged state, between pH 12 and 13 (Table 2). Notably, the adjustments are qualitatively different from those observed when K14 or H14 titrates (20,27). The responses to the E14 titration may therefore involve other factors.

The respective peptide terminals respond differently during the E14 titration. While the A3 ^{2}H quadrupolar splitting magnitude remains unchanged with pH (Figure 4), there are changes in the ^{2}H $|\Delta\nu_q|$ magnitudes for the methyl groups of not only A21 but also A17 between pH 6 and 13 (Figure 4 and Table 2). This suggests that the tilt of the N-terminal portion of the core helix and extent of unwinding near A3 do not change even as E14 titrates. A21 and A17, meanwhile, exhibit changes in their local orientations (with respect to the external magnetic field), suggesting changes in not only the orientation but also the extent of unwinding of the C-terminal between pH 6 and 13.

Residue E16 in GWALP23-E16, surprisingly, appears also to have a pK_a near 12.5 in DLPC bilayers, despite being located closer than E14 to the interfacial layer. The neutral GWALP23-

$E^0$16 helix adopts a tilted conformation in DLPC, with a change in azimuthal rotation about the helix axis by about 50° and a change in tilt of about 5° in comparison to GWALP23. These results are similar to observations with the neutral $E^0$14 and $K^0$14 residues. Surprisingly, nevertheless, when charged, residue E^-16 causes significant local unwinding, as the values for both A15 and A17 move away from the helical quadrupolar wave (Figure 6). The remaining, shortened core helix of GWALP23-E^-16 is tilted by ~5.3°. At the same time, A3 also remains off of the core helix. Remarkably, the C-terminal unwinds up to residue 15 in the presence of the charged residue E^-16. The combined results suggest shortening of the core helix to about three helical turns. A possible though not yet proven helix translocation could bury the N-terminal more deeply in the bilayer while exposing the E^-16 side chain at the other interface.

The results for GWALP23-E16 largely agree with solvation structure studies using molecular dynamics (MD) simulations on single transmembrane peptides with Asp or Glu at various offset positions from the helix center (28). The significant unwinding observed for GWALP23-E^-16 could be due to the propensity of Glu residues to form hydrogen bonds with water or choline of the lipid head groups. This can lead to significant distortion of the peptide, either by bending the helix backbone or unwinding the helix secondary structure, to expose peptide bonds to water as is observed in the MD simulations. We do not observe such exaggerated unwinding for the charged –E^-14 helix, possibly because the E14 Glu residue is more buried and may not be able to reach up to the interface. The E14 hydration, nevertheless, could potentially be satisfied by water defects in the bilayer, as observed for GWALP23-R14 (8).

The GWALP23-E12 properties are independent of pH, and the helix adopts a transmembrane orientation very similar to that of the parent GWALP23 in DLPC bilayers. This behavior is comparable to the observations for GWALP23-H12 (27) in DLPC bilayers. Both the E12 and

H12 peptides display helix orientations that are independent of pH in DLPC, with differences in helix tilt and rotation of only about 0.3° and 3°, respectively between the E14 and H14 transmembrane peptides.

We also observed no changes in the unwinding of the terminals of GWALP23-E12 over a pH range of 4-13. We consider two possible explanations for the absence of response from GWALP23-E12: either the pK_a of the central buried Glu residue is possibly higher than 13, or the Glu side chain is possibly charged in some samples but the peptide helix does not respond to the changes in pH. Being present at the center of the peptide, and dependent on water to satisfy its hydration, the E12 side chain might not be able to snorkel up to the interface. On the other hand, the thinner DLPC bilayers may permit Glu to pull in water more easily and satisfy its charge without altering the helix orientation. It nevertheless remains puzzling why the GWALP23-E14 and -E16 helices respond to pH but GWALP23-E12 does not.

The local unwinding of A15 and A17 when E16 titrates is a new finding for the core region (residues 6-18) of any GWALP23 family peptide. The unwinding could be driven in part by the solvation structure of glutamic acid. The carboxylate side chain charge is delocalized over a large volume, which in turn affects the hydration free energy of the charged moiety and its ability to polarize its microenvironment. The Glu side chain also has a higher hydrogen bonding potential and in general is better hydrated than an amino group, even in internal locations secluded from bulk water (29-31). The preference for forming hydrogen bonds with water may lead E16 to snorkel aggressively and cause helix unwinding.

The labeled Glu-containing GWALP23 peptides exhibit broad ^2H NMR spectra which may indicate multiple closely related states in the longer chain DOPC lipid bilayers, where the spectra furthermore remain unchanged throughout the pH range of 4-13. The contrast between Glu and

Arg is striking. Unlike GWALP23-R14 which exhibits a highly defined tilted orientation in DOPC bilayers (8), the –E14 peptide exhibits very low intensity poorly resolved ^{2}H NMR peaks. With the Arg remaining charged throughout the pH range, the long side chain allows the Arg guanidinium group to snorkel up to the interface while maintaining a stable preferred transmembrane orientation for the helix. E14 has a shorter side chain and thus may struggle more than R14 to reach up to the interface, resulting in a less well defined helix orientation. GWALP23-E16 also exhibits a less well defined orientation in DOPC bilayers despite the closer location of E16 to the interface. GWALP23-E12 exhibits multi-state behavior which is comparable to that of GWALP23-R12 in DOPC bilayers (8).

We also compare our results with recent simulations which make use of constant pH molecular dynamics (32). The computational predictions suggest high pK_a values of 9.8 ± 0.1 for E12 and 9.7 ± 0.1 for E14 in DLPC bilayers but are about 3 units shy of the observed experimental values (pK_a ~12.5 for each Glu residue). The simulations account for the improved charge solvation shells for the charged side chain provided by changing the helix tilt, but the juxta-terminal unwinding is likely outside of the timescale of the simulations.

In soluble proteins such as *staphylococcal* nuclease, depending on the position and the depth of burial, the pK_a values of Glu residues have been observed to range from 4.5-9.4 (33). The nuclease appears to be stable at pH 9.5 where the Glu with highest pK_a was recorded. This is consistent with the idea that the relatively hydrophobic and dehydrated interior of the protein behaves as a material with high dielectric constant. There is also a complex interplay among the local polarity of the charged group, Coulomb interactions and structural reorganization, which together determine the pK_a values of internal charges in the protein. The complexity is confirmed by the perturbation of pK_a's for Glu and Asp residues at position 38 in nuclease in

comparison to Lys at the same position which titrates at normal pK_a (34). The K38 pK_a of 10.4 (35) is governed mainly by structural organization and water penetration upon Lys ionization. The carboxyl group of E38 on the other hand has a shifted pK_a of 7.0. The Glu side-chain of E38 experiences Coulomb interactions with multiple neighboring groups, has difficulty reaching the bulk water and hence experiences only weak interactions with bulk water.

In membrane proteins, the pK_a values for Glu are observed over a large range in transmembrane domains. Glu242, at the C_{uB} catalytic site of bovine cytochrome c oxidase (CcO), functions in proton translocation through CcO, as a donor of all 4 pumped protons and 2-3 chemical protons (36). Calculations suggest that in a low uniform dielectric of ε=4, the glutamate has a pK_a of 14.5 and prefers to be protonated, but with dielectric inhomogeneities consistent with CcO, the pK_a drops to 12.0 (37). The calculated pK_a values of Glu242 therefore range between 9.4 and 14.5 depending on the redox state of heme *a*. These calculations are consistent with our measured results for Glu held in the bilayer in our model system.

Glutamic acid residues are highly conserved and critical not only for soluble protein function but also membrane protein function. We have aimed to elucidate further the Glu carboxyl side chain ionization properties in lipid bilayer membranes. The GWALP23 transmembrane helix with a specific Glu residue buried in DLPC bilayer membranes displays position-specific Glu titration behavior, which in turn affects the peptide helix integrity, orientation and dynamics within the membrane. When located at the center of the helix sequence, E12 does not respond to pH (up to pH 13). The slightly off-center E14 and the four-residue offset E16 display pK_a values around 12.5 in DLPC bilayer membranes. These results are consistent with calculations on these model peptides and membrane proteins such a CcO. The transmembrane orientation of each peptide helix is governed in part by changes in the fraying of helix ends upon Glu ionization. Our results,

in agreement with the solvation structure predicted for Glu using MD simulations (28), shed light on the aggressive nature of Glu in holding the waters of hydration. One is beginning also to compare the ionization behavior and respective influence on helix properties of Glu, His, Lys and Arg side chains in DLPC bilayer membranes. These results are of interest and importance for further experimental as well as calculation based studies that address the properties of membrane proteins.

3.6 Acknowledgements

We thank Vitaly Vostrikov for software for semi-static GALA and modified Gaussian methods for analysis of helix integrity and dynamics. We thank Ashley Martfeld for helpful discussions.

3.7 References

1. G. von Heijne, The membrane protein universe: what's out there and why bother?, J. Intern. Med., **261** (2007) 543-557.

2. E. Wallin, G. von Heijne, Genome-wide analysis of integral membrane proteins from eubacterial, archaean, and eukaryotic organisms, Protein science : a publication of the Protein Society, **7** (1998) 1029-1038.

3. B.H. Honig, W.L. Hubbell, R.F. Flewelling, Electrostatic Interactions in Membranes and Proteins, Annu. Rev. Biophys. Biophys. Chem., **15** (1986) 163-193.

4. H. Gratkowski, J.D. Lear, W.F. DeGrado, Polar side chains drive the association of model transmembrane peptides, Proc. Natl. Acad. Sci. U. S. A., **98** (2001) 880-885.

5. G.A. Caputo, E. London, Cumulative effects of amino acid substitutions and hydrophobic mismatch upon the transmembrane stability and conformation of hydrophobic alpha-helices, Biochemistry, **42** (2003) 3275-3285.

6. L.B.B. Li, I. Vorobyov, T.W. Allen, The role of membrane thickness in charged protein-lipid interactions, Biochim. Biophys. Acta. Biomembr., **1818** (2012) 135-145.

7. V.V. Vostrikov, B.A. Hall, M.S.P. Sansom, R.E. Koeppe, Accommodation of a Central Arginine in a Transmembrane Peptide by Changing the Placement of Anchor Residues, J. Phys. Chem. B, **116** (2012) 12980-12990.

8. V.V. Vostrikov, B.A. Hall, D.V. Greathouse, R.E. Koeppe, M.S.P. Sansom, Changes in Transmembrane Helix Alignment by Arginine Residues Revealed by Solid-State NMR Experiments and Coarse-Grained MD Simulations, J. Am. Chem. Soc., **132** (2010) 5803-5811.

9. J. Fendos, F.N. Barrera, D.M. Engelman, Aspartate Embedding Depth Affects pHLIP's Insertion pK(a), Biochemistry, **52** (2013) 4595-4604.

10. D. Legg-E'Silva, I. Achilonu, S. Fanucchi, S. Stoychev, M. Fernandes, H.W. Dirr, Role of Arginine 29 and Glutamic Acid 81 Interactions in the Conformational Stability of Human Chloride Intracellular Channel 1, Biochemistry, **51** (2012) 7854-7862.

11. A.F.X. Goldberg, L.M. Ritter, N. Khattree, N.S. Peachey, R.N. Fariss, L. Dang, M.Z. Yu, A.R. Bottrell, An intramembrane glutamic acid governs peripherin/rds function for photoreceptor disk morphogenesis, Invest. Ophthalmol. Vis. Sci., **48** (2007) 2975-2986.

12. B.M.P. Huyghues-despointes, J.M. Scholtz, R.L. Baldwin, Helical Peptides with 3 Pairs of Asp-Arg and Glu-Arg Residues in Different Orientations and Spacings, Prot. Sci., **2** (1993) 80-85.

13. H. Taguchi, T. Ohta, H. Matsuzawa, Involvement of Glu-264 and Arg-235 in the essential interaction between the catalytic imidazole and substrate for the D-lactate dehydrogenase catalysis, J. Biochem., **122** (1997) 802-809.

14. S.K. Aggarwal, R. MacKinnon, Contribution of the S4 segment to gating charge in the Shaker K^+ channel, Neuron, **16** (1996) 1169-1177.

15. V.V. Vostrikov, C.V. Grant, A.E. Daily, S.J. Opella, R.E. Koeppe, II, Comparison of "Polarization Inversion with Spin Exchange at Magic Angle" and "Geometric Analysis of Labeled Alanines" methods for transmembrane helix alignment, J. Am. Chem. Soc., **130** (2008) 12584-5.

16. V.V. Vostrikov, A.E. Daily, D.V. Greathouse, R.E. Koeppe, Charged or Aromatic Anchor Residue Dependence of Transmembrane Peptide Tilt, J. Biol. Chem., **285** (2010) 31723-31730.

17. S.L. Grage, E. Strandberg, P. Wadhwani, S. Esteban-Martin, J. Salgado, A.S. Ulrich, Comparative analysis of the orientation of transmembrane peptides using solid-state 2H- and 15N-NMR: Mobility matters, Eur. Biophys. J. Biophys. Lett., **41** (2012) 475-482.

18. K.A. Sparks, N.J. Gleason, R. Gist, R. Langston, D.V. Greathouse, R.E. Koeppe, Comparisons of Interfacial Phe, Tyr, and Trp Residues as Determinants of Orientation and Dynamics for GWALP Transmembrane Peptides, Biochemistry, **53** (2014) 3637-3645.

19. A. Mortazavi, V. Rajagopalan, K.A. Sparks, D.V. Greathouse, R.E. Koeppe, 2nd, Juxta-terminal Helix Unwinding as a Stabilizing Factor to Modulate the Dynamics of Transmembrane Helices, Chembiochem: A European Journal Of Chemical Biology, **17** (2016) 462-465.

20. N.J. Gleason, V.V. Vostrikov, D.V. Greathouse, R.E. Koeppe, Buried lysine, but not arginine, titrates and alters transmembrane helix tilt, Proc. Natl. Acad. Sci. U. S. A., **110** (2013) 1692-1695.

21. A. Damjanovic, B. Garcia-Moreno, E.E. Lattman, A.E. Garcia, Molecular dynamics study of water penetration in staphylococcal nuclease, Proteins, **60** (2005) 433-449.

22. N.J. Gleason, V.V. Vostrikov, D.V. Greathouse, C.V. Grant, S.J. Opella, R.E. Koeppe, II, Tyrosine Replacing Tryptophan as an Anchor in GWALP Peptides, Biochemistry, **51** (2012) 2044-2053.

23. J.H. Davis, K.R. Jeffrey, M. Bloom, M.I. Valic, T.P. Higgs, Quadrupolar echo deuteron magnetic resonance spectroscopy in ordered hydrocarbon chains, Chem. Phys. Lett., **42** (1976) 390-394.

24. P.C.A. van der Wel, E. Strandberg, J.A. Killian, R.E. Koeppe, Geometry and intrinsic tilt of a tryptophan-anchored transmembrane alpha-helix determined by ^{2}H NMR, Biophys. J., **83** (2002) 1479-1488.

25. E. Strandberg, S. Esteban-Martin, A.S. Ulrich, J. Salgado, Hydrophobic mismatch of mobile transmembrane helices: Merging theory and experiments, Biochim. Biophys. Acta-Biomembr., **1818** (2012) 1242-1249.

26. E. Strandberg, S. Ozdirekcan, D.T.S. Rijkers, P.C.A. van der Wel, R.E. Koeppe, R.M.J. Liskamp, J.A. Killian, Tilt angles of transmembrane model peptides in oriented and non-oriented lipid bilayers as determined by 2H solid-state NMR, Biophys. J., **86** (2004) 3709-3721.

27. A.N. Martfeld, D.V. Greathouse, R.E. Koeppe, Ionization Properties of Histidine Residues in the Lipid-Bilayer Membrane Environment, J. Biol. Chem., (2016) 19146-19156.

28. A.C.V. Johansson, E. Lindahl, Amino-acid solvation structure in transmembrane helices from molecular dynamics simulations, Biophys. J., **91** (2006) 4450-4463.

29. A. Damjanović, B.R. Brooks, B. García-Moreno E, Conformational Relaxation and Water Penetration Coupled to Ionization of Internal Groups in Proteins, J. Phys. Chem. A, **115** (2011) 4042-4053.

30. A. Damjanović, B. García-Moreno, E.E. Lattman, A.E. García, Molecular dynamics study of water penetration in staphylococcal nuclease, Proteins: Structure, Function, and Bioinformatics, **60** (2005) 433-449.

31. D.G. Isom, C.A. Castañeda, B.R. Cannon, B. García-Moreno E., Large shifts in pKa values of lysine residues buried inside a protein, Proc. Natl. Acad. Sci. U. S. A., **108** (2011) 5260-5265.

32. A. Panahi, C.L. Brooks, Membrane Environment Modulates the pK(a) Values of Transmembrane Helices, J. Phys. Chem. B, **119** (2015) 4601-4607.

33. D.G. Isom, C.A. Castaneda, P.D. Velu, B. Garcia-Moreno, Charges in the hydrophobic interior of proteins, Proc. Natl. Acad. Sci. U. S. A., **107** (2010) 16096-16100.

34. M.J. Harms, C.A. Castaneda, J.L. Schlessman, G.R. Sue, D.G. Isom, B.R. Cannon, B. Garcia-Moreno E, The pK(a) Values of Acidic and Basic Residues Buried at the Same Internal Location in a Protein Are Governed by Different Factors, J. Mol. Biol., **389** (2009) 34-47.

35. M.J. Harms, J.L. Schlessman, M.S. Chimenti, G.R. Sue, A. Damjanovic, B. Garcia-Moreno E, A buried lysine that titrates with a normal pK(a): Role of conformational flexibility at the protein-water interface as a determinant of pK(a)values, Protein Science, **17** (2008) 833-845.

36. M. Wikstrom, A. Jasaitis, C. Backgren, A. Puustinen, M.I. Verkhovsky, The role of the D- and K-pathways of proton transfer in the function of the haem-copper oxidases, Biochim. Biophys. Acta-Bioenerg., **1459** (2000) 514-520.

37. D.M. Popovic, J. Quenneville, A.A. Stuchebrukhov, DFT/electrostatic calculations of pK(a) values in cytochrome c oxidase, J. Phys. Chem. B, **109** (2005) 3616-3626.

38. N.J. Gleason, D.V. Greathouse, C.V. Grant, S.J. Opella, R.E. Koeppe, Single Tryptophan and Tyrosine Comparisons in the N-Terminal and C-Terminal Interface Regions of Transmembrane GWALP Peptides, J. Phys. Chem. B, **117** (2013) 13786-13794.

3.8 Tables

Table 1. Observed Ala-methyl ^2H quadrupolar splitting magnitudes ($|\Delta\nu_q|$)[a] for GWALP23-E12, -E14 and –E16 in DLPC ether lipid bilayers

	Quadrupolar Splittings (kHz)					
	E12		E14		E16	
Ala-d_4 position	pH 6	pH 13	pH 6	pH 13	pH 6	pH 13
7	26.4	26.0	27.2	30.2	13	11.6
9	29.0	28.2	17.4	13.2	5.0	2.8
11	28.2	28.0	22.0	21.6	19.2	14.0
13	16.0	16.2	6.0	10.0	13.4	8.2
15	23.0	23.2	4.2	4.0	21.4	24.2
17	3.4	3.4	17.6	30.4	14.2	16.0
3	9.2	8.2	29.4	29.2	10.8	8.4
21	25.4	26.0	17.2	25.0	10.8	4.6

[a] Quadrupolar splittings are reported in kHz for the β = 0° sample orientation for GWALP23-E12, -E14 and -E16 at pH 6 and 13. Each value is an average of (the magnitude observed when β = 0°) and (twice the magnitude observed when β = 90°).

Table 2. Calculated Orientations and Dynamics of Related GWALP23 Peptides in DLPC Lipid Bilayers[a]

Peptide	pH	GALA Fit Results				Modified Gaussian Results[b]				Reference
		τ0	ρ0	Szz	RMSD (kHz)	τ0	ρ0	σρ	RMSD (kHz)	
$E14^0$	6	25.3°	262°	0.68	0.13	22°	262°	27°	1.3	This work
$E14^-$	13	17.3°	258°	0.91	0.78	20°	257°	6°	0.75	This work
$H14^{+/0}$	2.0-8.2[c]	26.7°	254°	0.79	0.75	29°	253°	24°	0.62	[27]
$R14^+$	--[d]	30°	259°	0.83	1.58	26°	260°	0°	1.65	[7][27]
$E12^0$	6	23.3°	305°	0.7	1.15	19°	305°	3°	1.6	This work
$E12^-$	13	23.0°	305°	0.7	1.09	19°	306°	6°	1.5	This work
$H12^{+/0}$	2.0-8.2[c]	23.3°	308°	0.70	0.66	18°	305°	15°	1.34	[27]
$E16^0$	6	16°	359°	0.63	0.85	23°	360°	60°	1.9	This work
$E16^-$	13	10.7°	343°	0.56	0.85	8°	360°	4°	1.9	This work
L12,14, 16	--	21.0°	305°	0.71	0.7	23°	304°	33°	0.7	[18]

[a]The parent GWALP23 sequence is acetyl-GGALWLALALAL$_{12}$AL$_{14}$AL$_{16}$ALWLAGA-amide. In the noted examples, either residue L12, L14 or L16 (but not all three) was changed to E, H or R, as indicated, and the other residue remained a leucine.

[b]The modified Gaussian analysis followed Sparks et al. [18], with στ assigned a fixed finite value of 10°.

[c]In DLPC, the results with H12 and H14 do not depend on pH.

[d]The results with $R14^+$ do not depend on pH [7, 8].

3.9 Figures

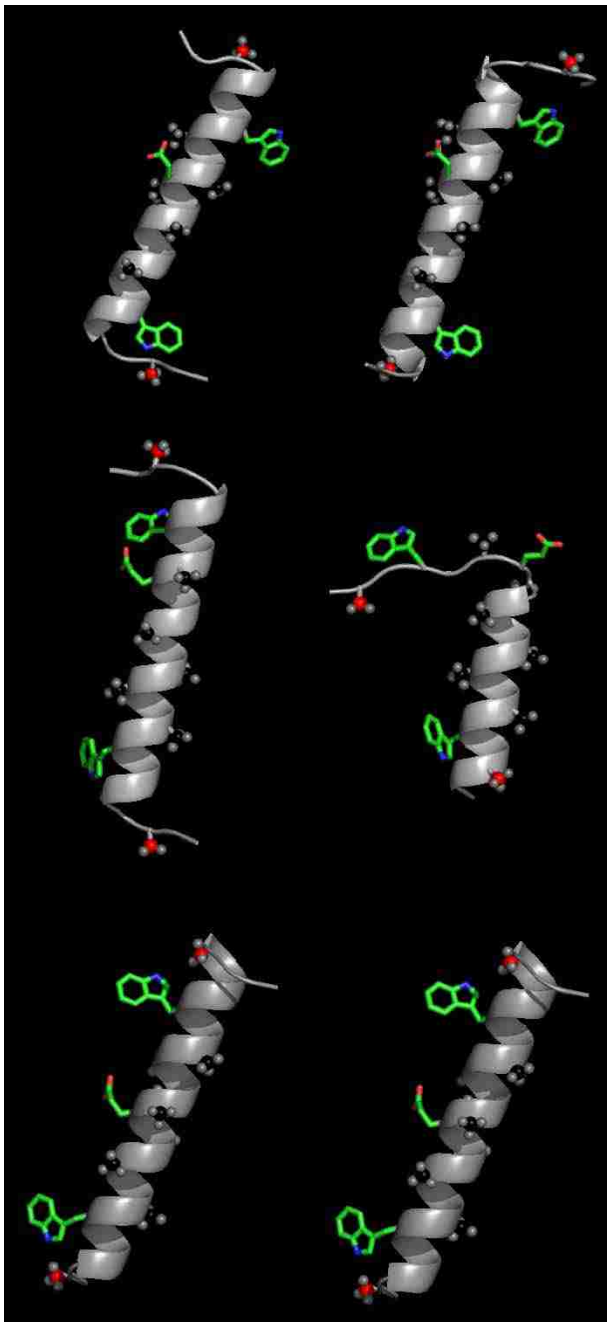

Figure 1: Models for GWALP23-E14 at pH 6 (a), GWALP23-E14 at pH 13 (b), GWALP23-E16 at pH 6 (c), GWALP23-E16 at pH 13 (d), GWALP23-E12 at pH 6 (e) and GWALP23-E12 at pH 13 (f) showing the observed tilted core helix orientations in DLPC ether bilayer, as well as schematic representations of the unwinding of the helix terminals for the peptides. The locations of W5, W19 and residues E14 and E16 are illustrated on a ribbon helix, drawn using PyMOL. The six deuterated alanine methyl groups that underlie the tilt analysis are shown as space filling. The depicted side chain orientations are arbitrary.

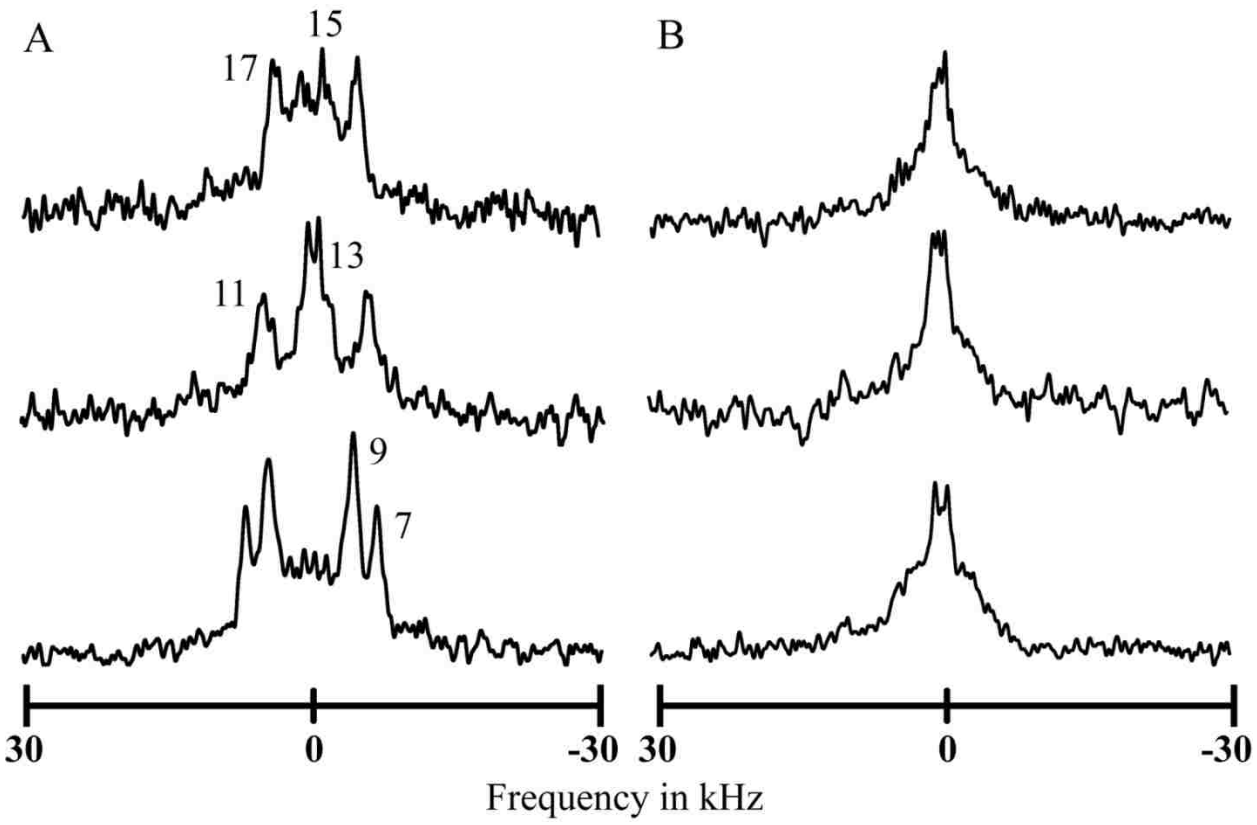

Figure 2: Selected deuterium NMR spectra of GWALP23 E14 peptide with deuterium labeled alanines at position 7,9,11,13,15 and 17 incorporated in DLPC (A) and DOPC (B) ether bilayers hydrated with 10 mM buffer at the pH 6. The well-resolved albeit slightly broad signals in DLPC ether for all six ^{2}H-labeled alanines indicate a well-defined tilted transmembrane orientation in the lipid bilayer. The peptide exhibits multiple weak resonances and low signal-to-noise for each labeled alanine residue in the DOPC ether-linked bilayers indicative of multiple slow exchanging states. Spectra were recorded at $\beta = 90°$ sample orientation, 50°C.

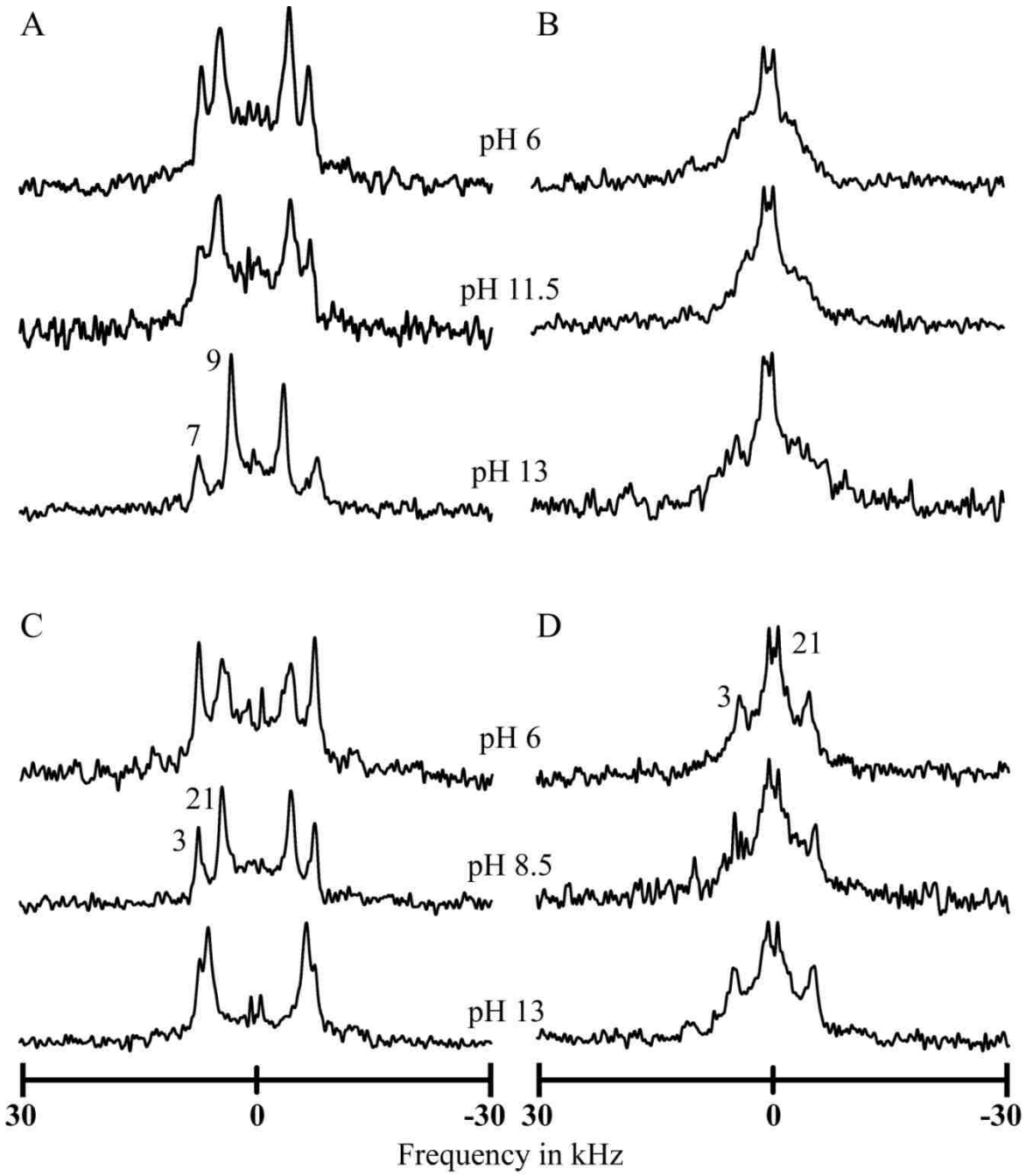

Figure 3: Selected ^{2}H-NMR spectra for two labeled alanines (7 and 9) in GWALP23-E14 in DLPC (A) and DOPC (B). Titration of GWALP23-E14 peptide labeled at Ala-7 and 9 in DLPC ether (A) and DOPC ether (B) bilayers and that for labeled Ala3 and Ala21 in GWALP23-E14 again in DLPC ether (C) and DOPC ether (D) bilayers. The peptide/lipid mixtures were hydrated with 10 mM buffer at the indicated pH. The difference in spectra in DLPC ether bilayers between pH 6 and 13 indicates that E14 residue is charged only at strongly alkaline conditions. No signal change is observed in DOPC bilayers. Spectra were recorded at $\beta = 90°$ sample orientation, 50°C.

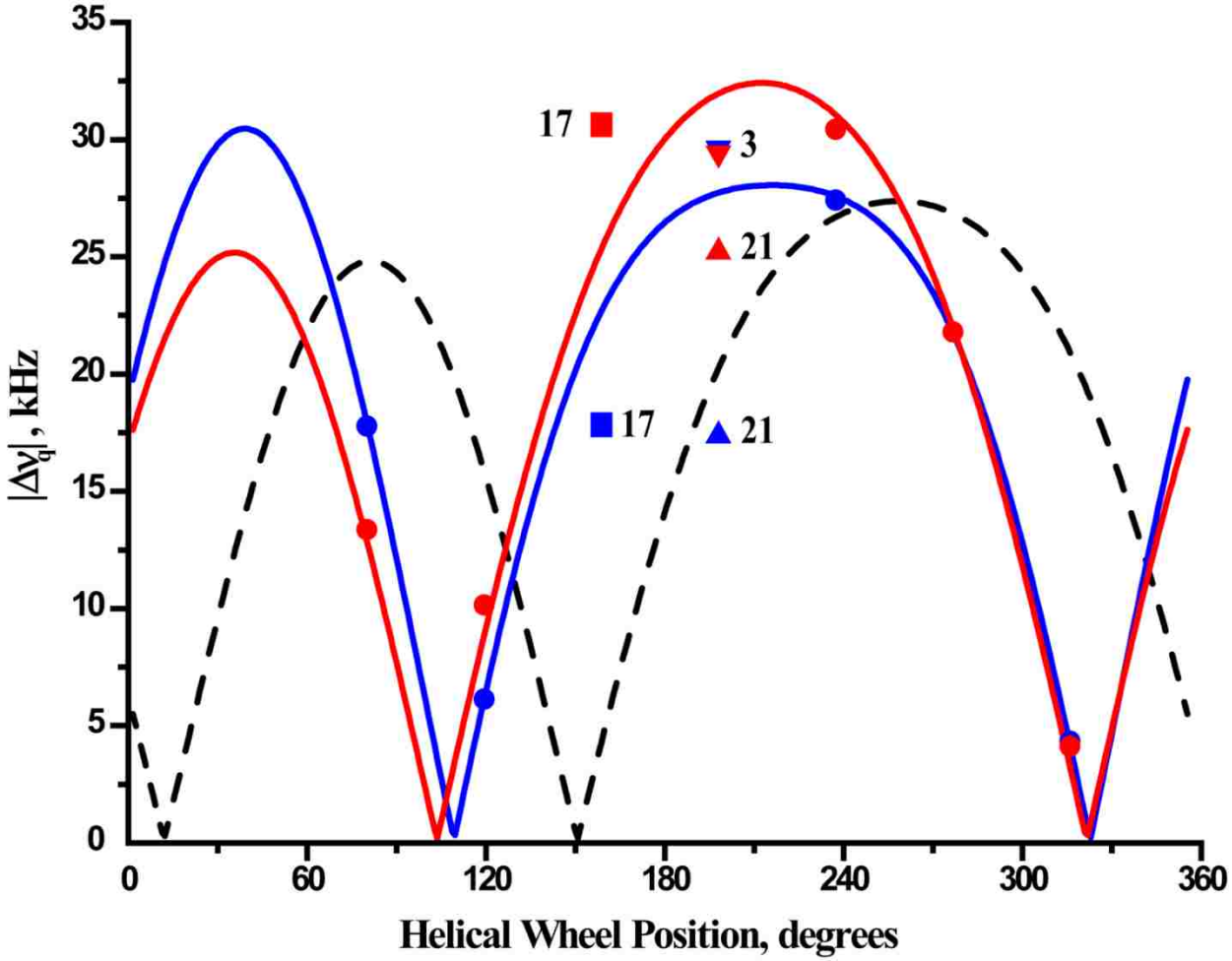

Figure 4: GALA quadrupolar wave plots of tilted membrane peptides in DLPC ether bilayers. GWALP23-E14 (blue; tilt $\tau = 25.3$, rotation $\rho = 262$, pH 6) has a distinct tilt and rotation from GWALP23 (black dash; tilt $\tau = 21$, rotation $\rho = 305$, pH independent) [18]. The charged GWALP23-E^{-}14 (red; tilt $\tau = 17.3$, rotation $\rho = 258$, pH 13) shows a decrease in tilt and rotation from the neutral GWALP23-E14. The labels on A3 and A21 shows the change in unwinding between pH 6 and 13.

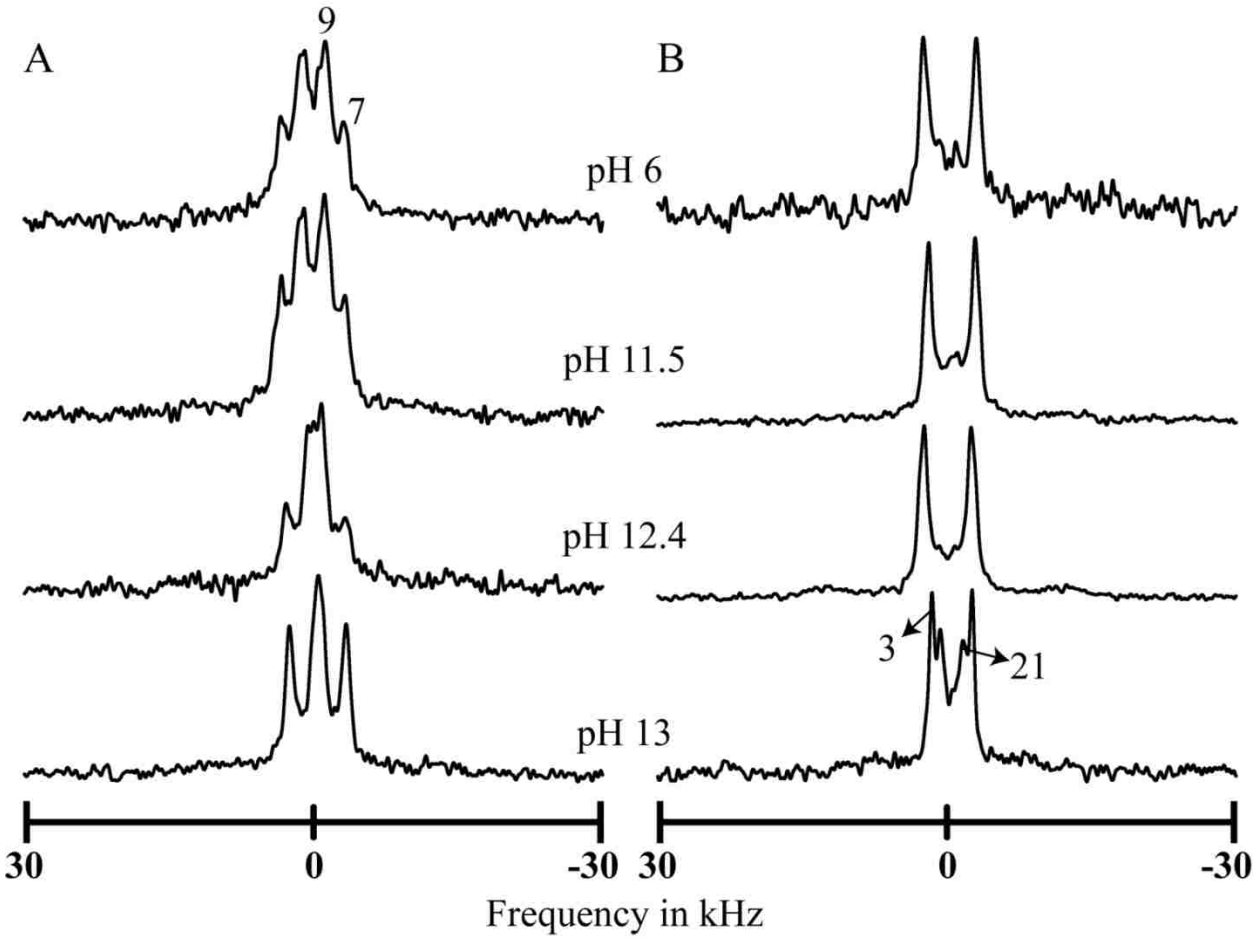

Figure 5: Selected 2H-NMR spectra for two core labeled alanines 7 and 9 (A) and end labeled alanines 3 and 21 (B) in GWALP23-E16 in DLPC ether bilayers and hydrated with 10mM buffers at the indicated pH. Both core and end labeled alanines NMR spectra show a change in quadrupolar splittings between pH 6 and 13 which suggests that E16 residue titrates at higher pH and is accompanied by a change in un-winding. The peaks assignments for A3 and A21 at pH 13 are based on spectra from a sample in which only A3 is deuterated (Figure S7 of the Supporting Information). Spectra were recorded at $\beta = 90°$ sample orientation; 50 °C.

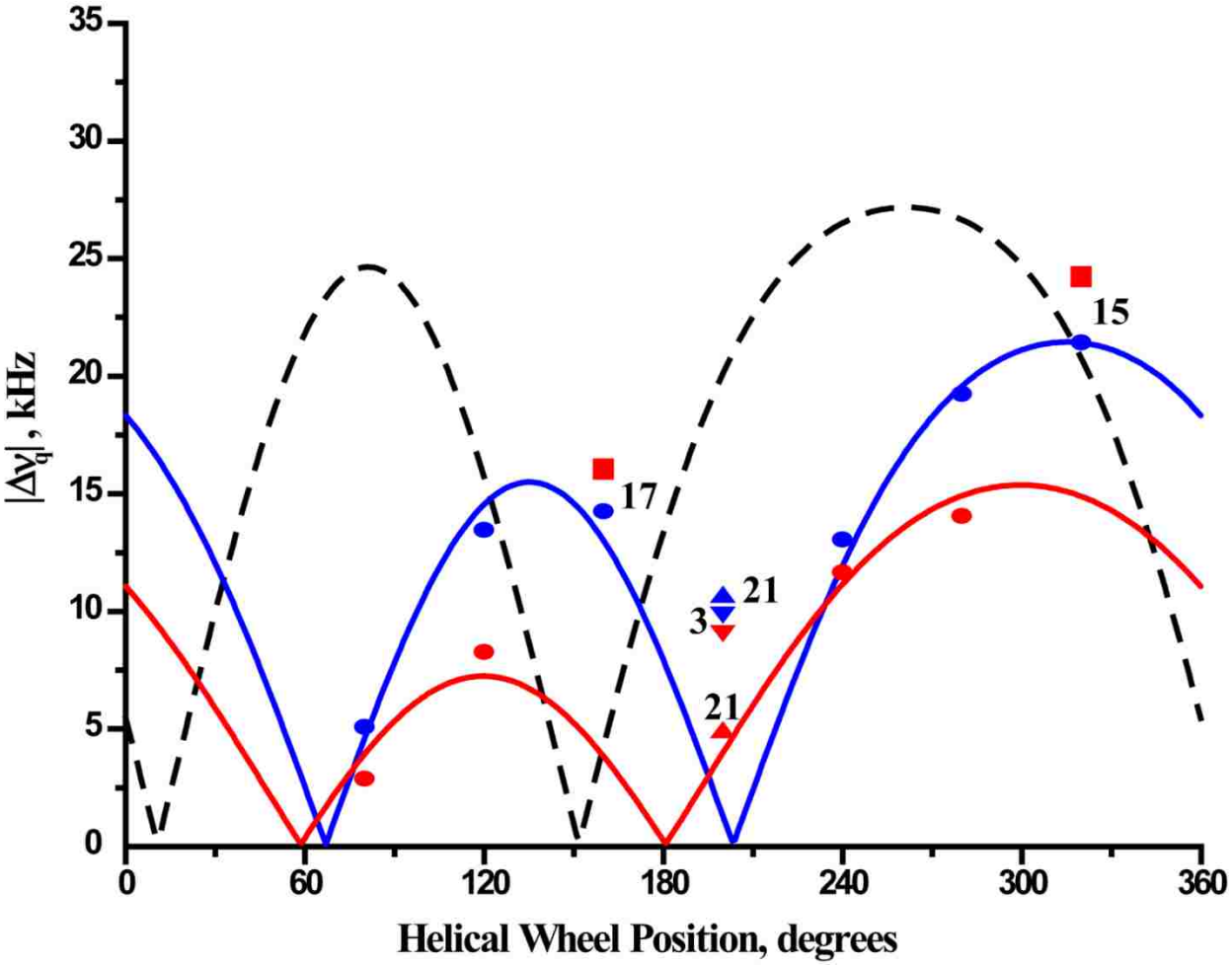

Figure 6: Quadrupolar wave analysis of tilted membrane peptides in DLPC ether bilayers. Neutral GWALP23-E16 (blue; tilt $\tau = 16$, rotation $\rho = 359$, pH 6) show major changes in tilt compared to the parent GWALP23 (black dash; tilt $\tau = 21$, rotation $\rho = 305$, pH independent). The charged GWALP23-E16 (red; tilt $\tau = 10.7$, rotation $\rho = 343$, pH 13) has a decreased tilt and shows major changes in unwinding of the core labeled alanines 15 and 17 compared to the neutral E16. The labels on A3 and A21 shows the change in unwinding between pH 6 and 13.

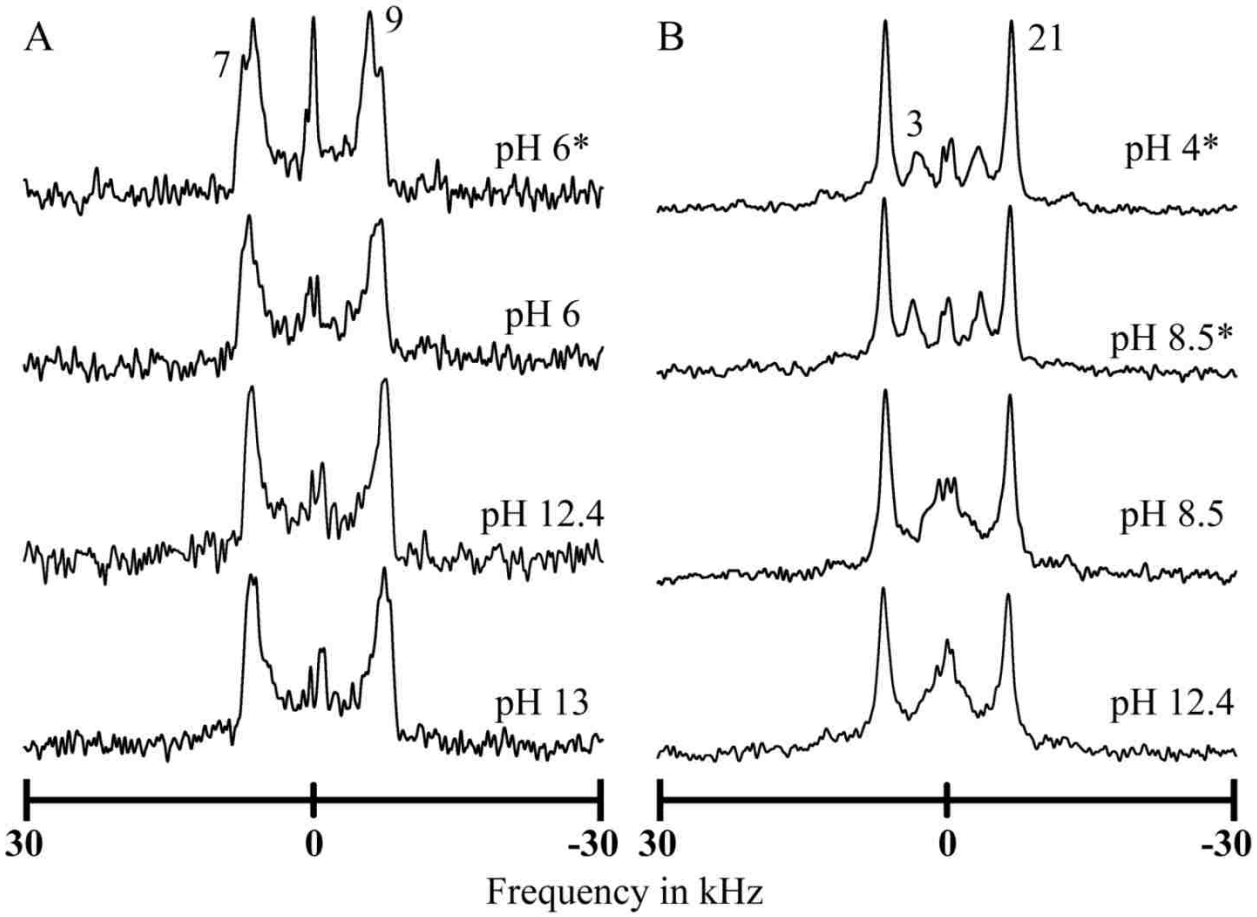

Figure 7: ^{2}H-NMR spectra for core labeled alanines 7 and 9 (A), or end labeled alanines 3 and 21 (B) in GWALP23-E12, in DLPC ether or ester (*) bilayers hydrated with 10 mM buffer at the indicated pH. The spectra indicate a lack of response to pH by GWALP23-E12. Spectra were recorded at $\beta = 90°$ orientation, 50 °C, with the ester bilayers indicated by *.

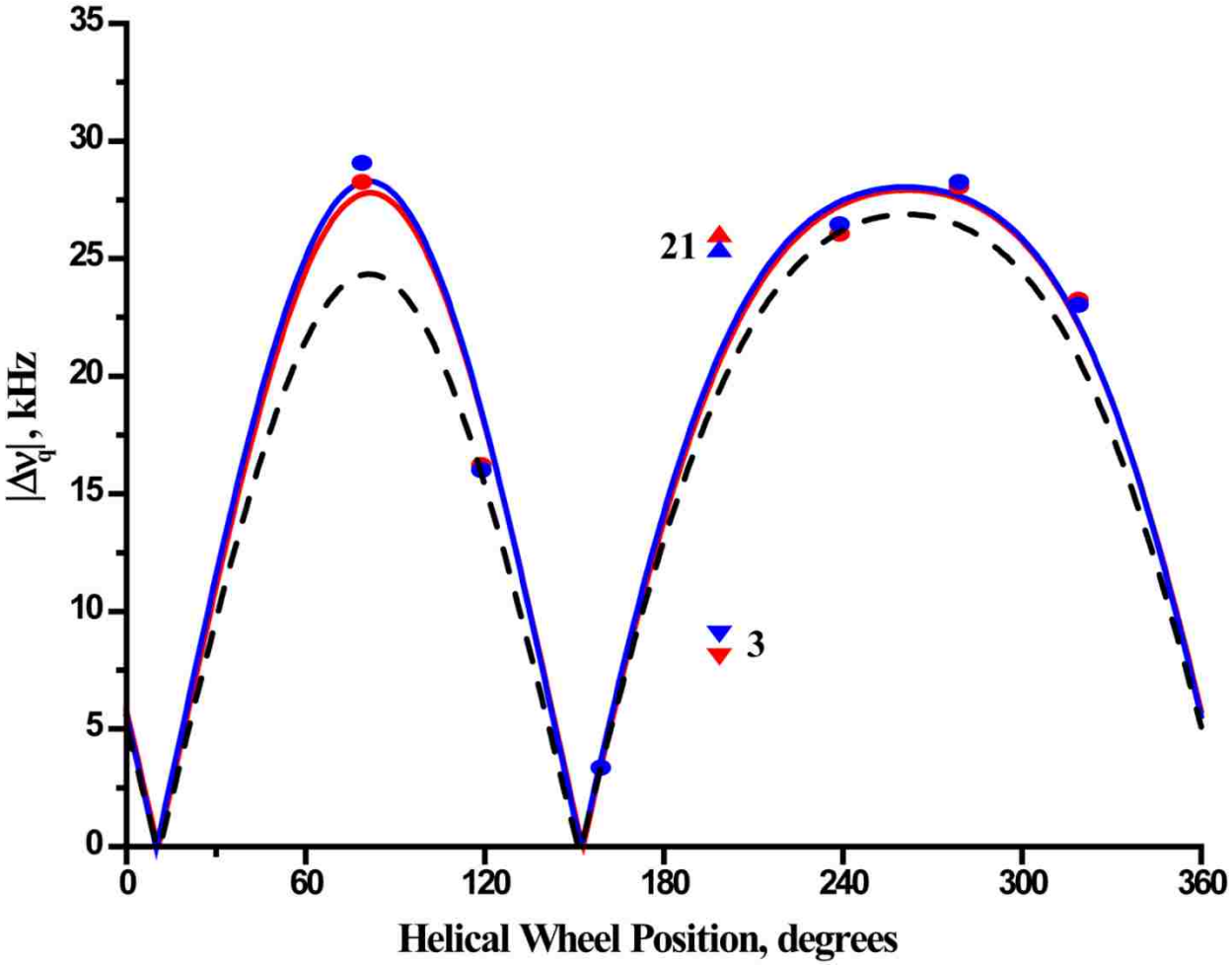

Figure 8: Quadrupolar wave analysis of tilted membrane peptides in DLPC ether bilayers. GWALP23-E12 peptide appears to show no change in orientation or unwinding between pH 6 (blue; tilt $\tau = 23.3$, rotation $\rho = 305$, pH 6) and pH 13 (red; tilt $\tau = 23$, rotation $\rho = 305$, pH 13) and appears to adopt a similar conformation to the neutral GWALP23 (black dash; tilt $\tau = 21$, rotation $\rho = 305$, pH independent). The labels on A3 and A21 shows the change in unwinding between pH 6 and 13.

3.10 Supporting Information

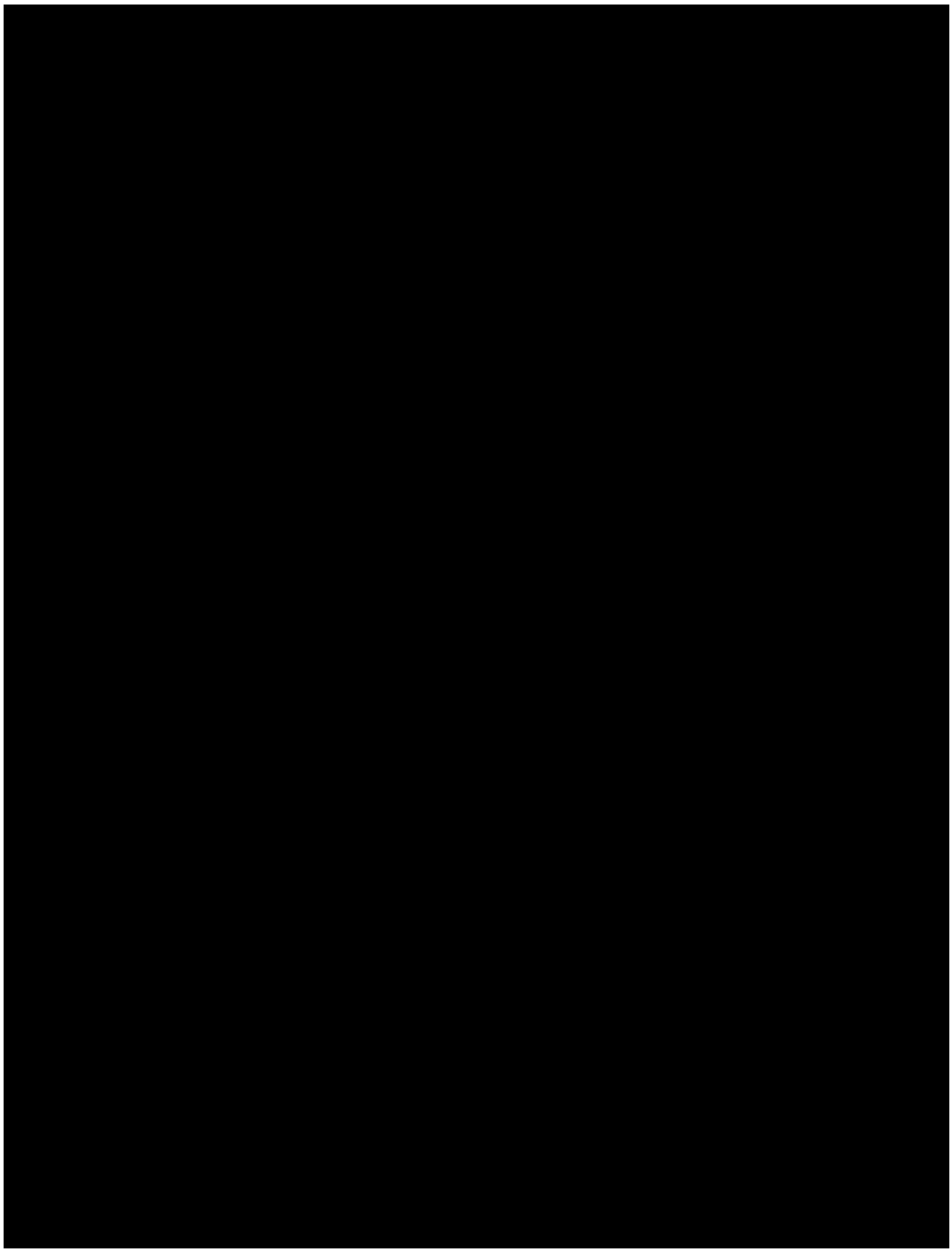

Figure S1. Analytical HPLC chromatogram (left) and MALDI (right) mass spectrum of purified synthesized peptides of GWALP23-E12, GWALP23-E14 and GWALP23-E16. The expected monoisotopic mass for each peptide is 2276.8 Daltons; adding 23 for Na^+ and one ^{13}C atoms is 2305 with four deuterons or 2309 with eight deuterons present. Successive m/z peaks differ by ± one ^{13}C atom (present at ~1.1% natural abundance).

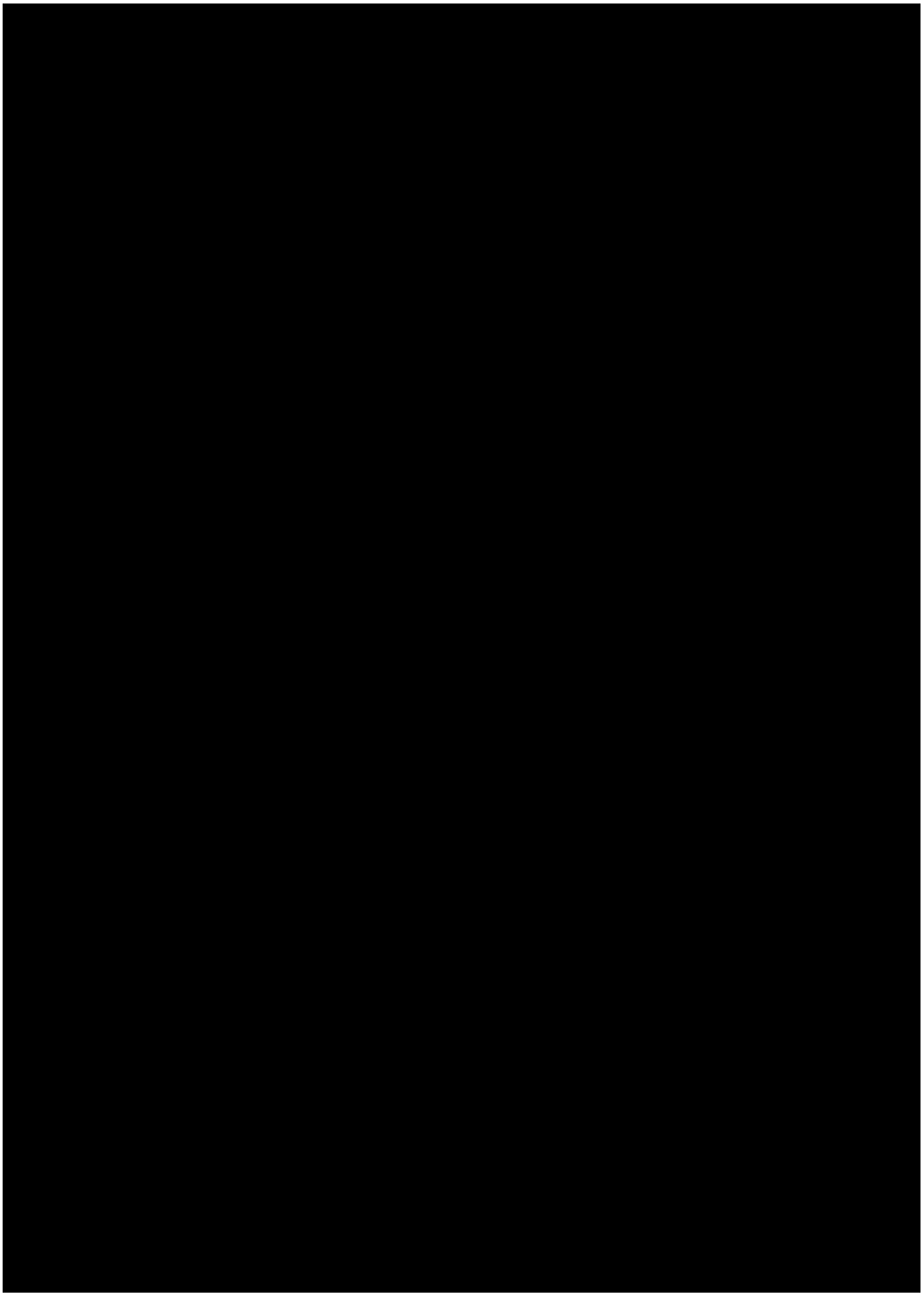

Figure S2. Examples of 31P NMR spectra for oriented bilayers of DLPC and DOPC containing GWALP23, GWALP23-E12, GWALP23-E14 or GWALP23-E16. Samples were hydrated with 10 mM buffer at pH 6 and recorded with orientations parallel ($\beta = 0°$, left) or perpendicular ($\beta = 90°$, right) to the magnetic field.

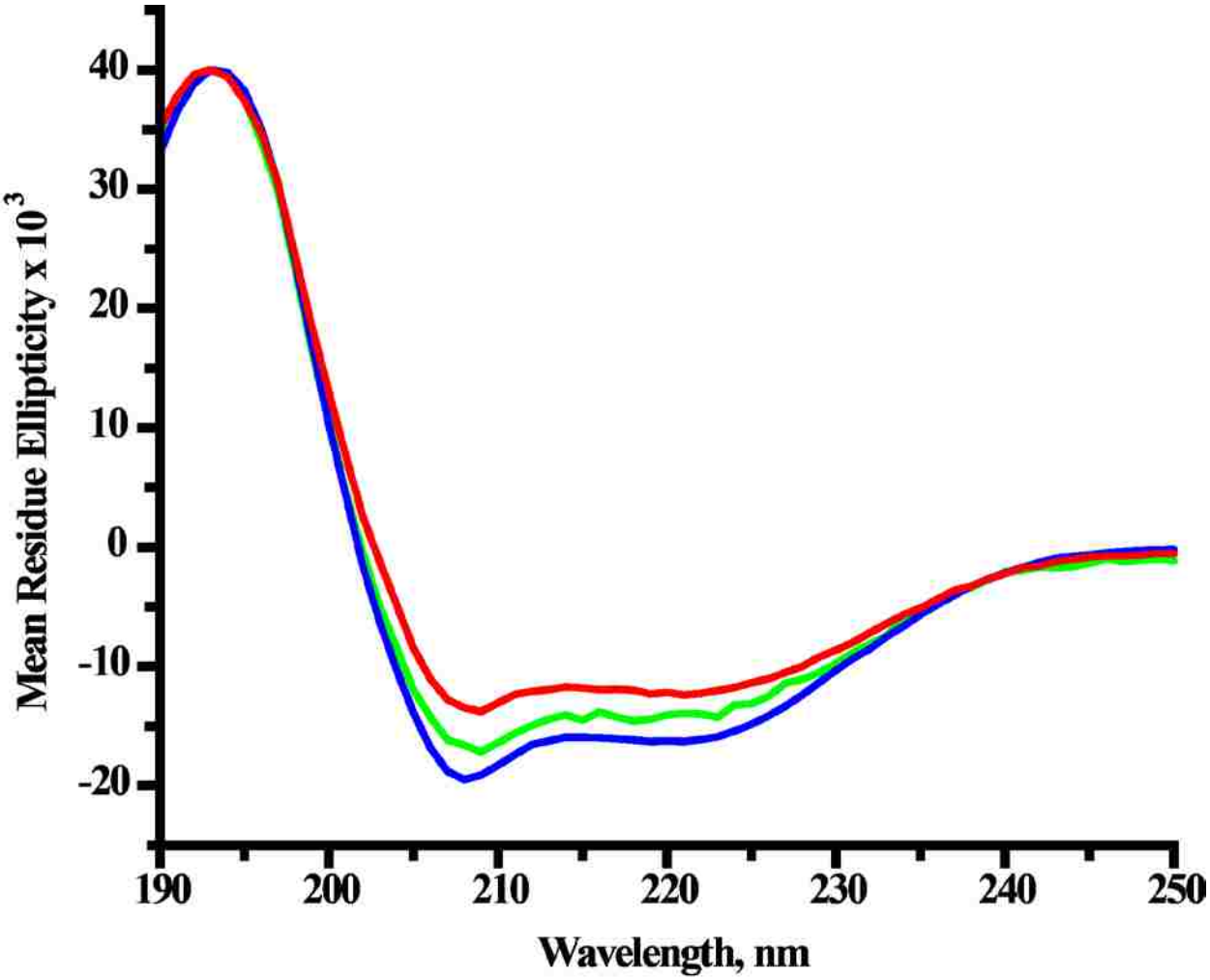

Figure S3. Circular Dichroism of GWALP23-E12 (green), GWALP23-E14 (blue) and GWALP23-E16 (red) in DLPC vesicles. Peptide to lipid ratio is 1:60.

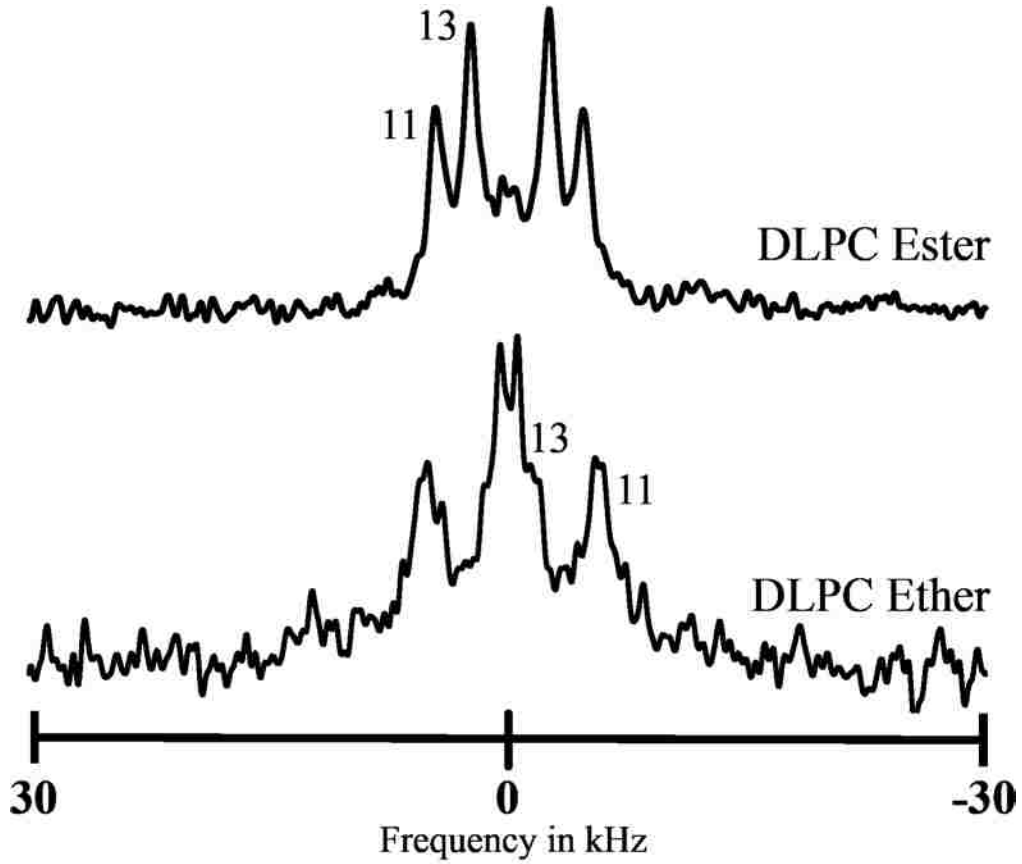

Figure S4. Deuterium NMR spectra for labeled alanines 11 and 13 in GWALP23-E14 in DLPC and DLPC ether bilayers, hydrated with 10 mM buffer at pH 6.0, in $\beta = 90°$ sample orientation. The peptide/lipid ratio is 1:60 at a temperature of 50 °C.

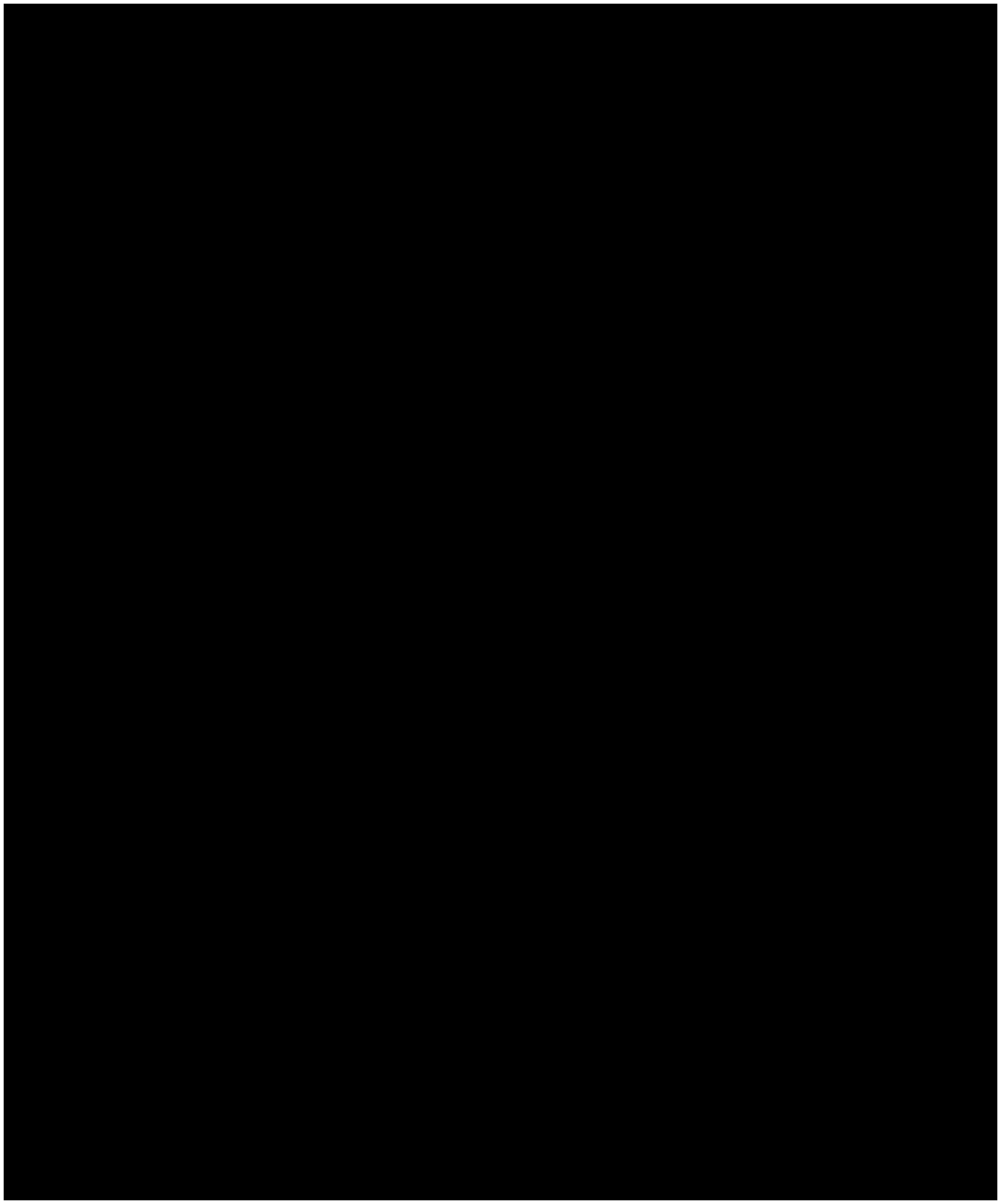

Figure S5. Selected deuterium NMR spectra for labeled alanine residues in GWALP23-E14 in A. DOPC ether bilayers and B. DLPC ether bilayers. Samples are hydrated with 10 mM buffer at indicated pH. The peptide/lipid ratio is 1:60 at a temperature of 50 °C; $\beta = 90°$ sample orientation.

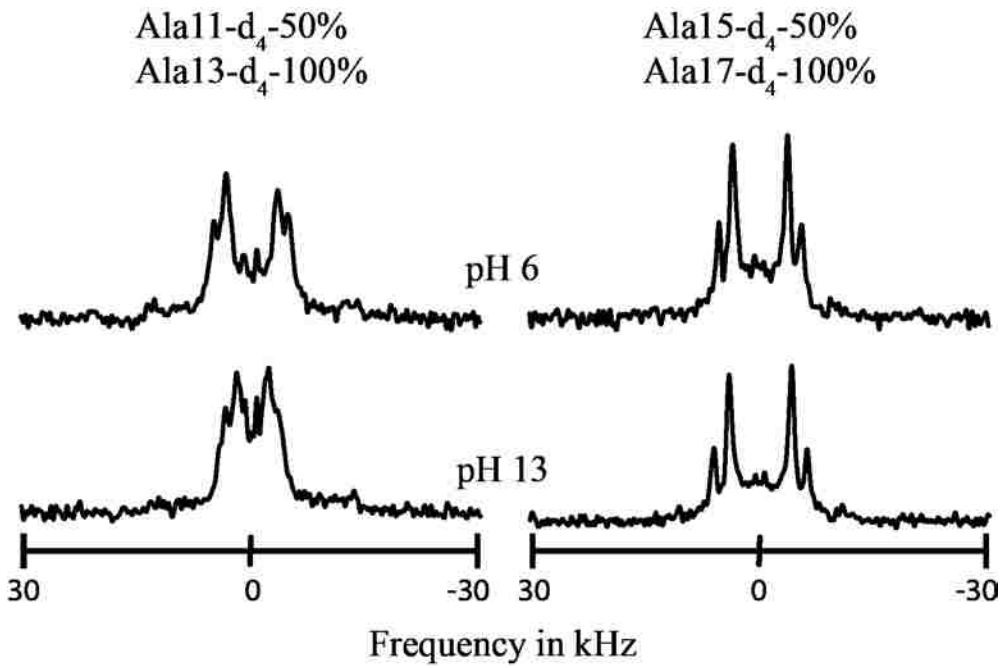

Figure S6. Deuterium NMR spectra for labeled alanine residues in GWALP23-E16 in DLPC ether bilayers, hydrated with 10 mM buffer at pH 6 (upper) or pH 13 (lower), showing $\beta = 90°$ sample orientation. The peptide:lipid ratio is 1:60 at a temperature of 50 °C.

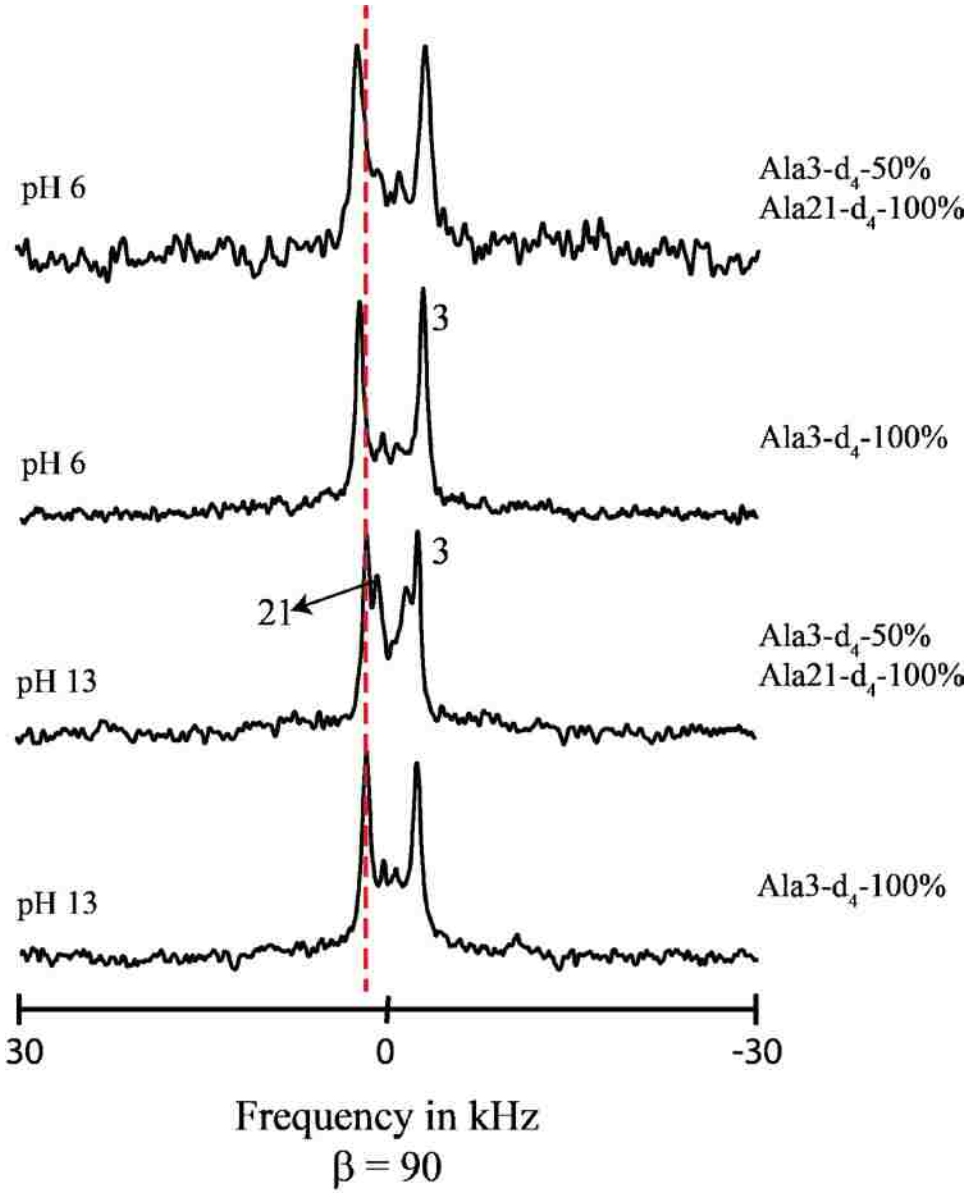

Figure S7. Assignment of resonances for deuterated methyl groups of A3 and A21 of GWALP23-E16 using a singly labeled peptide. At pH 6, the resonances of A3 and A21 overlap. At pH 13, the ^{2}H quadrupolar splitting magnitude is smaller for A21 than for A3. The peptide/lipid ratio is 1:60 at a temperature of 50 °C; $\beta = 90°$ sample orientation.

Figure S8. Deuterium NMR spectra for six labeled alanine residues in GWALP23-E12 in DLPC ether bilayers, hydrated with 10 mM buffer at indicated pH, showing β=90° sample orientation. The peptide/lipid ratio is 1:60 at a temperature of 50 °C.

CHAPTER 4: Ionization Properties of Buried Aspartic Acid Residues in the Lipid Bilayer Environment, with Glutamine as a Control

4.1 Abstract

I address the ionization properties of aspartic acid side chains of membrane proteins, and compare with results for glutamic acid side chains (Chapter 3), when the side chains are exposed directly to lipid acyl chains within lipid bilayer membranes. To investigate the pH dependence, ionization behavior, and orientational constraints when potentially negatively charged aspartic acid side chains are present in lipid bilayer membranes, I have employed GWALP23 (acetyl-GGALW^{5}LALALALALALALW^{19}LAGA-amide) as favorable host peptide framework. I have substituted an Asp residue for a Leu residue at position 14 (L14D) and have incorporated specific ^{2}H-labeled alanine residues within the core helical sequence or outside of the core region, near the ends of the sequence. As a control, I also use the GWALP23 framework to incorporate the neutral yet polar carboxamide side chain of glutamine at position 14. Solid-state ^{2}H-NMR spectra of labeled core alanine residues in GWALP23-D14 reveal little change to the orientation of the transmembrane helix over a pH range of 4 to 13 in DOPC bilayer membranes, quite in contrast to its Glu counterpart. The D14 peptides display surprisingly smeared and indistinct ^{2}H NMR spectra in aligned DLPC bilayers, with individual resonances being obscured for the core labels. The behavior is in stark contrast to that of many other related peptides in DLPC including those having Lys/His incorporated into GWALP23 peptides at positon 14. The rather modest shifts in the core alanine ^{2}H quadrupolar splitting magnitudes suggest that the orientation of the GWALP23-D14 transmembrane helix actually may change rather little at high pH. The spectra for samples with deuterium labels near the helix ends on alanines 3 and 21 show modest pH-dependent changes in the unwinding of the helix terminals in both DLPC and DOPC

bilayers. The difference in the unwinding and core labels may suggest a possible titration of the D14 Asp residue, but the results are as yet inconclusive.

4.2 Introduction

The most commonly found structural elements in membrane proteins are hydrophobic α-helices. The core amino acid sequence of the helix determines its insertion, position and also its function (1,2). But despite the propensity to have a hydrophobic core, polar and ionizable residues also may be found in core helices and are believed to be important in the functioning of many proteins. In a lot of instances, these ionizable residues in the hydrophobic core of a protein are accompanied by pK_a shifts that allow the side chain to be neutral (3,4). Similarly, burying a polar residue in a hydrophobic interior of a lipid membrane can be somewhat unfavorable. It is important to compare neutral polar side chains with the titrable side chains of Asp, Glu, Arg, Lys, and His, which may encounter an environment dependent energy barrier that modulates their ability to pick up or lose a proton. In case of RXFP3 relaxin receptor, substitution of charged Asp128, that plays a critical role in binding and activation of the receptor, with the neutral Asn considerably affects the receptor function (5).

In this chapter I will examine the titration and ionization properties of Asp and Gln residues within lipid bilayer membranes. Following through on the previous chapter we use the GWALP23 host system for our study. The GWALP23 model system has been a successful host for measuring the side-chain pK_a in actual bilayer membranes. We focus on examining the pK_a values transitioning between neutral to negative charge of Asp side chain at position 14 in bilayer membranes with varying thickness, namely DLPC and DOPC. We find that the hydrophobic membrane environment favors a neutral protonated state for Asp. We also report a unique trend for Asp distinct to the behavior of Glu residues in DLPC and DOPC ether bilayers.

While GWALP23-D14 does not appear to titrate throughout the pH range as high as pH 13, we observe low intensity poorly resolved alanine methyl NMR spectra. In the DOPC ether bilayers, GWALP23-D14 shows well characterized tilted peptide orientation with well-defined alanine methyl quadrupolar splittings quite distinct to the case when Glu is positioned at a similar position (see Chapter 3).

Results with the neutral GWALP23-Q14, lacking the carboxyl side-chain in DLPC ether bilayers display sharp well resolved ^{2}H-Ala methyl NMR resonances that do not respond to pH, in agreement with expectations. However, despite the neutral amide on the side-chain, the Q14 peptide displays a surprisingly broad smear of NMR signals in DOPC ether bilayers. The behavior of neutral polar residues at position 14 in GWALP23 remains puzzling.

Understanding the ionization properties of polar residues like Glu or Asp is significant for discerning their role in structural and functional properties of membrane proteins. A comparison between Asp and Glu, with Gln as a control residue, would also shed light on the propensity for either negatively charged residue to be conserved within membrane proteins.

4.3 Materials and Methods

Solid Phase Synthesis of ^{2}H-Labeled Peptides

Commercial L-alanine-d_4 from Cambridge Isotope Laboratories (Andover, MA) was modified with an Fmoc group, as described previously (14), and recrystallized from ethyl acetate:hexane, 80:20. NMR spectra (^{1}H) were used to confirm successful Fmoc-Ala-d_4 synthesis. Other protected amino acids and acid-labile "Rink" amide resin were purchased from NovaBiochem (San Diego, CA). All peptides were synthesized on a 0.1 mmol scale using "FastMoc™" methods and a model 433A synthesizer from Applied Biosystems by Life Technologies (Foster

City, CA). Typically, two deuterated alanines of differing isotope abundances were incorporated into each synthesized peptide. Selected precursors for deuterated residues therefore contained either 100% Fmoc-L-Ala-d_4 or 50% Fmoc-L-Ala-d_4 with 50% non-deuterated Fmoc-L-Ala. The final residue on each peptide was acetyl-Gly to yield a blocked, neutral N-terminal.

A peptide cleavage solution was prepared containing 85% trifluoroacetic acid (TFA) and 5% each (v/v or w/v) of triisopropylsilane, water, and phenol. TFA cleavage from "Rink" resin in 2 mL volume (2-3 h at 22 °C) leads to a neutral, amidated C-terminal. Peptides were precipitated by adding the TFA solution to 25 volumes of cold 50/50 MtBE/hexane. Peptides were collected by centrifugation, washed multiple times with MtBE/hexane and lyophilized from (1:1) acetonitrile/water. After lyophilization, crude peptide dissolved in TFE was purified via HPLC on a Zorbax Rx-C8 9.4 mm x 25 cm column packed with 5 μm octyl-silica (Agilent Technologies, Santa Clara, CA) with a typical gradient of 92-96% methanol/water (0.1% TFA) and a 1.7 mL/min. flow rate. Collected product is lyophilized multiple times to remove residual TFA. MALDI-TOF mass spectrometry was used to confirm peptide identity by molecular mass (Figure S1 in Supporting Information). Peptide purity was examined by reversed-phase HPLC (Figure S2) with 280 nm detection, using a 4.6 x 50 mm Zorbax SB-C8 column packed with 3.5 μm octyl-silica (Agilent Technologies, Santa Clara, CA), operated at 1 mL/min using a methanol/water gradient from 85% to 99% methanol (with 0.1% TFA) over five min. Peptide quantity was calculated by means of UV absorbance at 280 nm, using molar extinction coefficients of 5,600 M^{-1} cm^{-1} for each Trp and 1,490 M^{-1} cm^{-1} for each Tyr residue in the peptide (15).

^{2}H NMR Spectroscopy using Oriented Bilayer samples

Mechanically aligned samples for solid-state NMR spectroscopy (1/60, peptide/lipid) were prepared using DOPC or DLPC lipids from Avanti Polar Lipids (Alabaster, AL), and deuterium-depleted water (Cambridge; 45% w/w hydration), as described previously (Thomas et al. 2009). Bilayer alignment within each sample was confirmed using ^{31}P NMR at 50 ˚C on a Bruker Avance 300 spectrometer (Billerica, MA) at both $\beta = 0^{\circ}$ (bilayer normal parallel to magnetic field) and $\beta = 90^{\circ}$ macroscopic sample orientations (Figure S3). Deuterium NMR spectra were recorded at both sample orientations on a Bruker Avance 300 spectrometer, utilizing a quadrupolar echo pulse sequence (16) with 90 ms recycle delay, 3.2 μs pulse length and 115 μs echo delay. Between 0.5 and 1.5 million scans were accumulated during each ^{2}H NMR experiment. An exponential weighting function with 100 Hz line broadening was applied prior to Fourier transformation. Buffers for oriented samples were prepared at room temperature using vacuum-dried reagents and prepared in deuterium-depleted water. Buffers include: pH 4 Acetate buffer 50 mM (sodium acetate and acetic acid, Sigma, St. Louis, MO); pH 6 Citrate buffers 10 mM (EMD, Gibbstown, NJ); pH 8.5, and 9 Tris buffers 50 mM (Trizma® hydrochloride and Trizma® base, St. Louis, MO), pH 11.5 and 12 CABS buffer (Sigma Aldrich, St. Louis, MO), and pH 13 Phosphate buffers (Sigma Aldrich, St. Louis, MO).

CD Spectroscopy

Small lipid vesicles incorporating 125 nM peptide and 7.5 μM lipid (1/60) were prepared by sonication in unbuffered water. An average of ten scans was recorded on a Jasco (Easton, MD) J710 CD spectropolarimeter, using a 1 mm cell path length, 1.0 nm bandwidth, 0.1 nm slit and a scan speed of 20 nm/min.

4.4 Results

We investigate the ionization properties and influence of Asp carboxyl side chain on transmembrane peptide in lipid bilayers by incorporating single Asp residues into GWALP23 model peptide sequence at position 14. Based on previous results with Glu, we decided to pursue Asp, with a more polar but shorter side chain to determine how it would influence the membrane-peptide interaction. GWALP23 is an ideal model system for studying the ionization properties of charged residues as have been carried out in recent years with Arg, Lys, His and Glu residues (6-8) (Chapter 3). CD spectroscopy helped to confirm the retention of α-helical secondary structure with the introduction of the single Asp residue (Figure S4 of supporting information) showing pronounced double minima near 208 nm and 222 nm which is indicative of α-helical secondary structure.

We examined the helix orientation and dynamics with the help of ^{2}H-NMR spectra of deuterated alanine residues included in the core sequence as well as ends of GWALP23-D14 and GWALP23-Q14 peptides in aligned DLPC and DOPC ether linked bilayers. The samples were hydrated with 10 mM buffer at a variety of pH conditions.

GWALP23-D14.

The ^{2}H NMR spectra for aligned samples of GWALP23-D14 reveal poorly resolved low intensity signals for the ^{2}H-Ala methyl groups in DLPC ether bilayers (Figure 1). When hydrated with pH 6 buffer, the spectra exhibit low intensity poor resolution multiple peaks for each of the six core alanine residues. These are suggestive of multiple states in slow exchange on the NMR timescale. We find a progressive decline in the ^{2}H-Ala methyl NMR signals as for the labeled alanines from the N- to the C-terminal (Figure 1). This behavior of –D14 peptide is quite distinct in comparison to GWALP23-E14 which responded with well-defined spectra in DLPC ether bilayers. The GWALP23-D14 exhibits remarkably no change in the NMR observables at higher

pH with no observable changes between pH 6.0-13.0 (Figure 2). Based on the lack of response to the high pH we can deduce a pK_a possibly higher than 13.

To examine the possibility of change in helix fraying (9), we labeled alanines 3 and 21 of GWALP23-D14 with deuterium. Despite the lack of change in NMR signal for the core labels, surprisingly, the ^2H spectra for A3 and A21 suggest a change in unwinding of the C-terminal of GWALP23-D14 between pH 6 and 13 in DLPC ether bilayers (Figure 3). The end labels furthermore show somewhat better resolved spectra in DLPC as compared to the core labels. The deuterium quadrupolar splitting for A3 remains fixed in position between pH 6 and 13, while A21 shows significant changes.

Due to the large degree of uncertainty in measuring quadrupolar splittings for GWALP23-D14 ^2H-Ala labels in DLPC ether bilayers we were not able to determine helix integrity and dynamics. We however were able to assign tentative quadrupolar splittings (Table 1) for the core and helix terminal Ala ^2H-methyl groups in DLPC ether bilayers.

In the DOPC ether bilayers, GWALP23-D14 exhibits remarkably well defined spectra for ^2H-Ala methyl groups quite distinct in behavior to GWALP23-E14 which behaves very poorly in DOPC bilayers irrespective of pH. At a near-neutral pH of 6.0, the spectra exhibit well-defined ^2H-NMR signals for each of the six alanines indicative of a tilted conformation (Figure 4). In comparison to –D14 peptide in DLPC ether bilayers, we see a steady improvement in the resolution of the spectra for labels from the N- to the C-terminal.

The helix of GWALP23-D14 however does not respond to high pH even as high as pH 13 as observed by the lack of change in the NMR observables (Figure 5A). The indifferent response of the ^2H-Ala methyl quadrupolar splittings suggests the pK_a to be higher than 13.

We examined the possibility of helix fraying (9) by labeling alanines 3 and 21 of GWALP23-D14 with deuterium. The ^{2}H spectra for A3 and A21 although does exhibit unwinding of the helix ends, no change is observed in the fraying between pH 6 to pH 13 (Figure 5B).

The combined quadrupolar splittings (Table 1) reveal a well-defined transmembrane orientation with fraying near residues 3 and 21 in DOPC ether bilayers (Figure 6). The neutral -D14, in comparison to GWALP23-H^{0}14, reveals distinct changes in the helix tilt $\Delta\tau$ and azimuthal rotation $\Delta\rho$ (Table 2) (about 4.3°and 85°) when Asp is replaced with His at position 14 (8). We observe similar differences in helix orientation when we compare –D14 to GWALP23-K^{0}14 ($\Delta\tau = 6°$ and $\Delta\rho = 91°$) (7) and the parent L14 helix of GWALP23 (($\Delta\tau = 9°$ and $\Delta\rho = 12°$) (13). It is of further interest that the terminal unwinding of the –D14 peptide in DOPC, while present, shows no inclination to change with pH much like the case of –E14 in DOPC ether bilayers (Chapter 3).

GWALP23-Q14.

The incorporation of the neutral Gln residue in GWALP23-Q14 leads to sharp, well defined alanine methyl ^{2}H-quadrupolar splittings for samples in DLPC ether bilayers, indicative of a tilted transmembrane helix orientation (Figure 7A). We observe well defined, sharp ^{2}H-Ala methyl signals for GWALP23-Q14 indicative of a well-defined orientation. The NMR signals are more defined than for GWALP23-E14 or GWALP23-D14, suggesting that the neutral functional group behaves better in the hydrophobic lipid bilayer environment. Due to the absence of a titrable side chain group, the GWALP23-Q14 peptide does not show any changes in the quadrupolar splittings over the pH range of 6-13 (Figure 7A). Surprisingly, despite the neutral side chain chemistry, we still observe broad, poorly resolved alanine methyl ^{2}H quadrupolar splittings in DOPC ether bilayers (Figure 7B).

4.5 Discussion

We have investigated the ionization properties of lipid-facing Asp residues in a model transmembrane helix at position 14 and the influence on peptide orientation, dynamics and helix integrity. Our findings in DLPC ether bilayers include rather poorly resolved low intensity multi-state ^{2}H-NMR resonances for the buried Asp with very high pK_a values in lipids including some local helix-end unwinding. We will discuss the distinct behavior of D14 in DOPC bilayers and the lack of response of the buried D14 residue in both DLPC and DOPC bilayers. We will also be comparing the experimental results of D14 with predicted differences in titration behavior when Asp is incorporated in lipid-bilayer membrane.

We have consistently observed smeared, low intensity, poorly resolved alanine ^{2}H-methyl NMR signals for the GWALP23-D^{0}14 in DLPC bilayers. This is indicative of slow motion or perhaps multi-state like behavior which is distinct from the behavior of -E^{0}14 peptide in DLPC bilayers (Chapter 3) and GWALP23-H^{0}14 in DLPC bilayers (8). The ^{2}H-alanine methyl NMR resonances for –D14 are however independent of pH, even at high pH up to 13. Despite the multi-state NMR spectra, we find a small population to adopt a tilted conformation for the neutral polar –D^{0}14 which caused a change in rotation by about 160°. This is a very distinct behavior for a polar residue at position 14 as seen in previous studies with His (8), Lys (7), and Glu (Chapter 3) all of which effects a 40-50° change in rotation.

We also observe no changes in the unwinding of the helix terminals over the pH range of 6-13. One of the possibilities that the Asp remains neutral even at high pH could be that the short side chain being buried in the bilayer is not able to snorkel up to the interface to satisfy its hydration. We are however still puzzled as to why the GWALP23-E14 helices respond to pH but GWALP23-D14 does not.

The Asp incorporated GWALP23 peptides exhibit surprisingly well defined alanine ^{2}H-methyl NMR spectra indicative of tilted conformation in DOPC bilayers. This is in stark contrast to the behavior of GWALP23-E14 in DOPC bilayers which exhibit smeared, low intensity multi-state like behavior (Chapter 3). The GWALP23-D14 behavior is independent of pH between pH 6-13, similar to its behavior in DLPC bilayer.

The incorporation of Gln residue allowed us to have a control with a neutral, yet polar side chain instead of a potentially charged polar Glu side chain. Indeed, GWALP23-Q14 peptide behaved much better in ether linked DLPC bilayers compared to -E14 peptides. This suggests that the polar but uncharged carboxamide behaves much better in the hydrophobic lipid environment than the carboxyl group. However, we observe poorly resolved deuterated Ala-methyl NMR observables in the ether linked DOPC bilayers despite having a neutral functional group. This suggests that the polar side chain has a big influence on the behavior of the peptide in the lipid bilayer.

Similar experiments with model proteins containing Asp residues near the center to assess the topography of the peptides upon ionization of Asp (10). Under neutral conditions where the Asp residue is protonated, the peptides were observed to predominantly form normal transmembrane helix. At their ionization pK_a around 8.7, the topography results in the formation of truncated or shifted non-transmembrane structure. The formation of a truncated transmembrane structure depends on the position of Asp such that there is a residual segment of 12 or longer consecutive hydrophobic residues which would aid in forming a transmembrane segment. Despite the lower pK_a observed for the aspartic acid in these peptides, the drastic changes observed upon ionization of Asp suggests that the bilayer system would elevate the pK_a to keep it protonated.

The charge dependence of ionizable residues upon their depth in the bilayer has implications in the study of membrane electrostatics. The pK_a values for Asp are observed over a large range in transmembrane domains. Asp85 serves as a receptor for the Schiff base proton in the M-photolysis induced product of bacteriorhodopsin (11). Recent experiments with infrared measurements suggests a large increase in the pK_a of Asp85 receptor to above 11 units. The vibrational frequency of the Asp85 carboxyl group indicates a transient drop in the effective dielectric constant around the aspartate to ~2 which corresponds to the increased pK_a. Aspartic acid residues are highly conserved and critical for membrane protein function. We have aimed to elucidate further the Asp carboxyl side chain ionization properties in lipid bilayer membranes. The GWALP23 transmembrane helix with a specific Asp residue buried in DOPC bilayer membranes exhibits a stark contrast in its behavior to its Glu counterpart. When positioned slightly off center, D14 does not respond to pH (up to pH 13) but we observe changes in unwinding with pH which suggest that Asp might be titrating close to pH 13 but the core helix does not respond to the titration. These results are of interest and importance for further experimental as well as calculation based studies that address the properties of membrane proteins.

4.6 Acknowledgement

I thank Vitaly Vostrikov for software for semi-static GALA and modified Gaussian methods for analysis of helix integrity and dynamics. I would also like to thank Ashley Martfeld for helpful discussions.

4.7 References

1. Gratkowski, H., Lear, J. D., and DeGrado, W. F. (2001) Polar side chains drive the association of model transmembrane peptides. Proc. Natl. Acad. Sci. U. S. A. 98, 880-885

2. Caputo, G. A., and London, E. (2003) Cumulative effects of amino acid substitutions and hydrophobic mismatch upon the transmembrane stability and conformation of hydrophobic alpha-helices. Biochemistry 42, 3275-3285

3. Takayama, Y., Castaneda, C. A., Chimenti, M., Garcia-Moreno, B., and Iwahara, J. (2008) Direct evidence for deprotonation of a lysine side chain buried in the hydrophobic core of a protein. Journal of the American Chemical Society 130, 6714-+

4. Karp, D. A., Stahley, M. R., and Garcia-Moreno, E. B. (2010) Conformational Consequences of Ionization of Lys, Asp, and Glu Buried at Position 66 in Staphylococcal Nuclease. Biochemistry 49, 4138-4146

5. Liu, Y., Zhang, L., Shao, X. X., Hu, M. J., Liu, Y. L., Xu, Z. G., and Guo, Z. Y. (2016) A negatively charged transmembrane aspartate residue controls activation of the relaxin-3 receptor RXFP3. Archives of biochemistry and biophysics 604, 113-120

6. Vostrikov, V. V., Hall, B. A., Greathouse, D. V., Koeppe, R. E., and Sansom, M. S. P. (2010) Changes in Transmembrane Helix Alignment by Arginine Residues Revealed by Solid-State NMR Experiments and Coarse-Grained MD Simulations. Journal of the American Chemical Society 132, 5803-5811

7. Gleason, N. J., Vostrikov, V. V., Greathouse, D. V., and Koeppe, R. E. (2013) Buried lysine, but not arginine, titrates and alters transmembrane helix tilt. Proc. Natl. Acad. Sci. U. S. A. 110, 1692-1695

8. Martfeld, A. N., Greathouse, D. V., and Koeppe, R. E. (2016) Ionization Properties of Histidine Residues in the Lipid-Bilayer Membrane Environment. J. Biol. Chem.

9. Mortazavi, A., Rajagopalan, V., Sparks, K. A., Greathouse, D. V., and Koeppe, R. E., 2nd. (2016) Juxta-terminal Helix Unwinding as a Stabilizing Factor to Modulate the Dynamics of Transmembrane Helices. Chembiochem: A European Journal Of Chemical Biology 17, 462-465

10. Caputo, G. A., and London, E. (2004) Position and ionization state of Asp in the core of membrane-inserted alpha helices control both the equilibrium between transmembrane and nontransmembrane helix topography and transmembrane helix positioning. Biochemistry 43, 8794-8806

11. Braiman, M. S., Dioumaev, A. K., and Lewis, J. R. (1996) A large photolysis-induced pK(a) increase of the chromophore counterion in bacteriorhodopsin: Implications for ion transport mechanisms of retinal proteins. Biophys. J. 70, 939-947

12. Gleason, N. J., Vostrikov, V. V., Greathouse, D. V., Grant, C. V., Opella, S. J., and Koeppe, R. E., II. (2012) Tyrosine Replacing Tryptophan as an Anchor in GWALP Peptides. Biochemistry 51, 2044-2053

13. Sparks, K. A., Gleason, N. J., Gist, R., Langston, R., Greathouse, D. V., and Koeppe, R. E. (2014) Comparisons of Interfacial Phe, Tyr, and Trp Residues as Determinants of Orientation and Dynamics for GWALP Transmembrane Peptides. Biochemistry 53, 3637-3645

14. Thomas, R., Vostrikov, V. V., Greathouse, D. V., and Koeppe, R. E. (2009) Influence of Proline upon the Folding and Geometry of the WALP19 Transmembrane Peptide. *Biochemistry* **48**, 11883-11891

15. Pace, C. N., Vajdos, F., Fee, L., Grimsley, G., and Gray, T. (1995) How to Measure and Predict the Molar Absorption Coefficient of a Protein. *Protein Sci.* **4**, 2411-2423

16. Davis, J. H., Jeffrey, K. R., Bloom, M., Valic, M. I., and Higgs, T. P. (1976) Quadrupolar echo deuteron magnetic resonance spectroscopy in ordered hydrocarbon chains. *Chemical Physics Letters* **42**, 390-394

4.8 Tables

Table 1. Observed Ala-methyl ^2H quadrupolar splitting magnitudes ($|\Delta\nu_q|$)[a] for GWALP23-D14 in DLPC and DOPC ether lipid bilayers.

	Quadrupolar Splittings (kHz)			
	GWALP23-D14			
Lipid Bilayer	DLPC Ether		DOPC Ether	
Ala-d_4 position	pH 6	pH 13	pH 6	pH 13
Core helix				
7	28.4	24.8	22.0	19.4
9	31.2	31.6	14.4	12.2
11	22.6	27.2	27.2	27.4
13	27.6	18.0	18.0	18.2
15	4.0	6.4	27.2	20.7
17	2.0	2.2	8.0	8.0
Terminals				
3	30.6	30.4	24.1	25.0
21	30.6	23.2	39.0	20.0

[a] Quadrupolar splittings are reported in kHz for the $\beta = 0°$ sample orientation for at pH 6 and 13. Each value is an average of (the magnitude observed when $\beta = 0°$) and (twice the magnitude observed when $\beta = 90°$).

Table 2. Calculated Orientation and Dynamics of peptides in DOPC Lipid [a].

[a] The parent GWALP23 sequence is acetyl-GGALWLALALAL^{12}AL^{14}AL^{16}ALWLAGA-amide.

Peptide	pH	GALA Fit Results				Modified Gaussian Results				Reference
		τ_0	ρ_0	S_{zz}	RMSD (kHz)	τ_0	ρ_0	$\sigma\rho$	RMSD (kHz)	
GWALP23-D14	6.0	15°	335°	0.85	0.52	17°	334°	30°	0.59	This work
GWALP23-D14	13.0	14.7°	339°	0.83	0.83	20°	337°	45°	0.91	This work
GWALP23-$H^0$14	6.0	10.3°	250°	0.83	0.82	11°	249°	18°	0.67	(8)
GWALP23-H^+14	2.0	16.7°	248°	0.83	1.14	19°	247°	24°	1.28	(8)
GWALP23-$K^0$14	8.2	9.0°	244°	0.86	0.31	10°	243°	18°	0.36	(7)
GWALP23-K^+14	5.2	15.3°	228°	0.88	1.20	17°	227°	21°	1.28	(7)
GWALP23	-	21°	305°	0.71	0..7	9°	321°	48°	0.7	(12,13)

[b] The modified Gaussian analysis followed Sparks et al. (13), with $\sigma\tau$ assigned a fixed finite value of 10°.

4.9 Figures

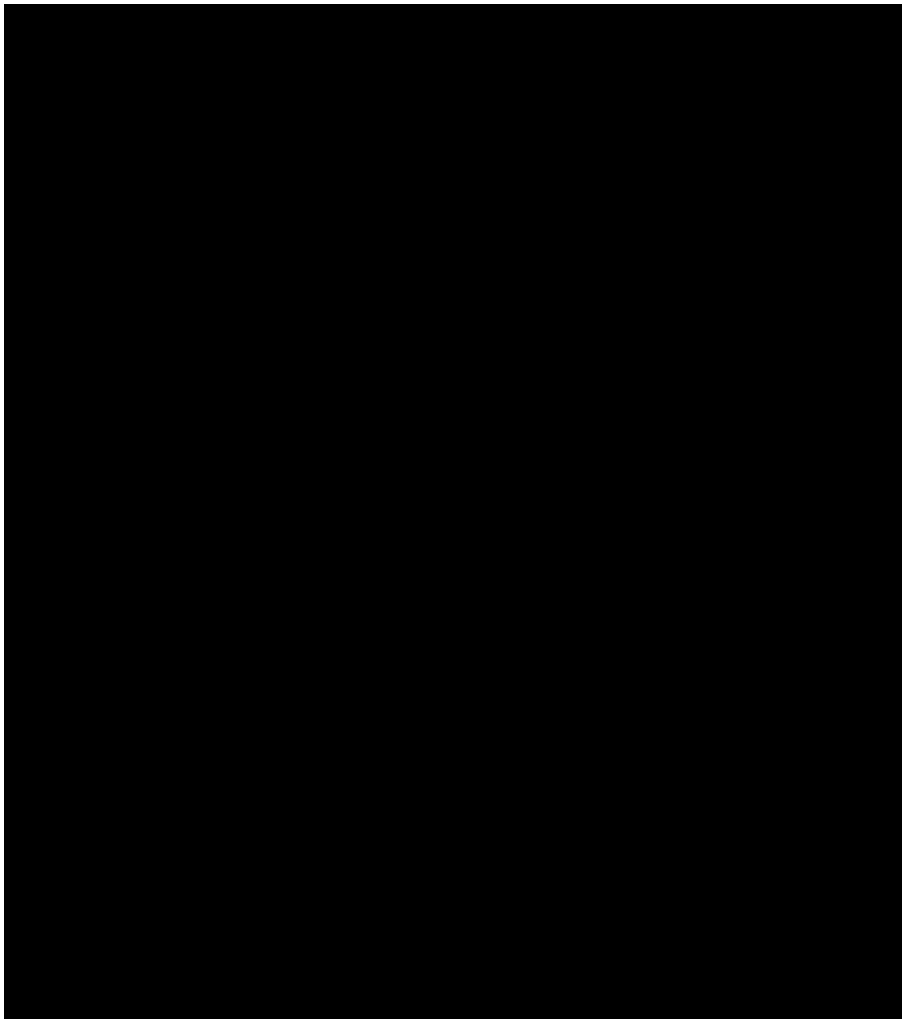

Figure 1: ^{2}H-NMR spectra of GWALP23-D14 with deuterium labeled alanines at positions 7, 9, 11, 13, 15 and 17, incorporated in DLPC ether bilayers hydrated with 10 mM buffer at pH 6. The poorly resolved spectra are suggestive of multi-state behavior and makes it difficult to assign the appropriate alanine labels. Spectra were recorded at $\beta = 90°$ sample orientation at 50°C

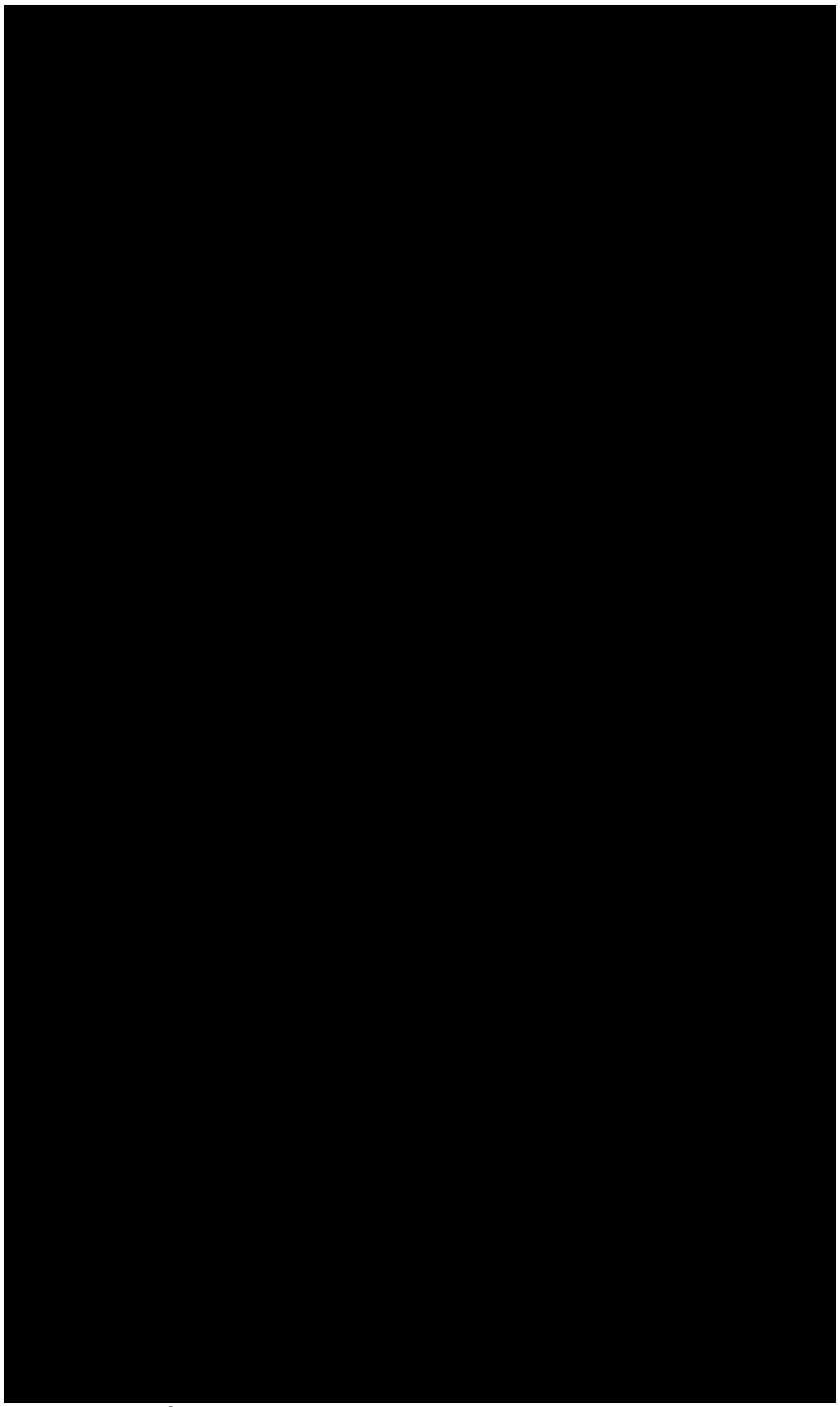

Figure 2: ^{2}H-NMR spectra of GWALP23-D14 peptide with deuterium labeled alanines at position 7 and 9 incorporated in DLPC ether bilayers hydrated with 10 mM buffer at indicated pH. The negligible difference in spectra in DLPC ether bilayers between pH 4 to 13 indicates that Asp residues does not respond to change in pH. Spectra was recorded at $\beta = 90°$ sample orientation. * - indicates samples incorporated in DLPC ester linked lipid bilayers.

Figure 3: ^{2}H-NMR spectra of GWALP23-D14 peptide with deuterium labeled alanines at position 3 and 21 incorporated in DLPC ether bilayers hydrated with 10 mM buffer at indicated pH. The difference in spectra in DLPC ether bilayers between pH 6 to 13 indicates that the helix terminals respond to a change in pH and a possible titration of the Asp 14 residue. Spectra were recorded at $\beta = 90°$ sample orientation at 50°C.

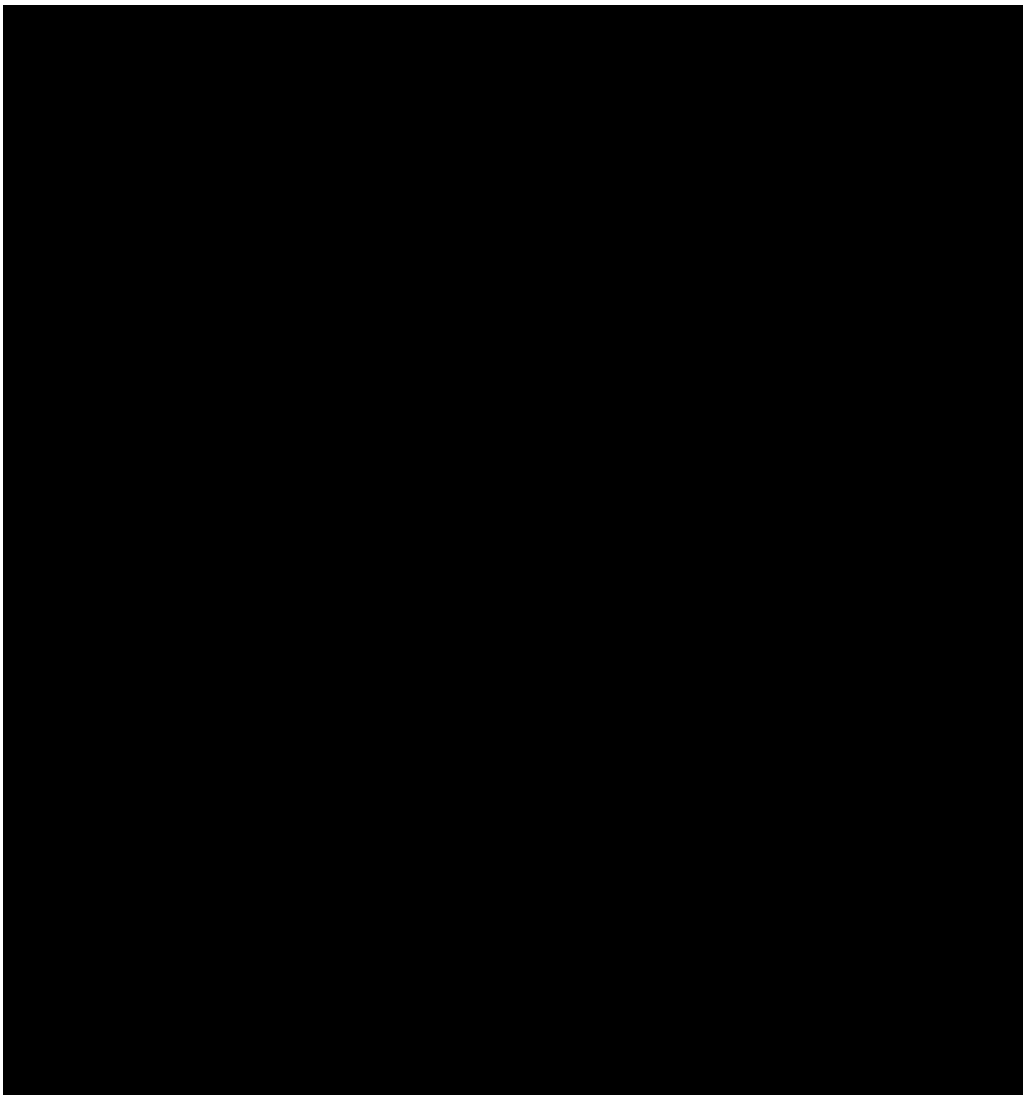

Figure 4: ^{2}H-NMR spectra of GWALP23-D14 with deuterium labeled alanines at positions 7, 9, 11, 13, 15 and 17, incorporated in DOPC ether bilayers hydrated with 10 mM buffer at the indicated pH. The resolved deuterium NMR signals indicate a single well defined orientation of the peptide in DOPC ether bilayers. Spectra were recorded at $\beta = 90°$ sample orientation at 50°C.

Figure 5: ^{2}H-NMR spectra of GWALP23-D14 peptides with deuterium labeled alanines at position 15, 17 (**A**) and 3, 21 (**B**) incorporated in DOPC ether bilayers hydrated with 10 mM buffer at indicated pH. The spectra show changes with pH for both set of labels, particularly for labels 15 and 21 suggesting a pK_a between 12.5-13. Spectra were recorded at $\beta = 90°$ sample orientation at 50°C.

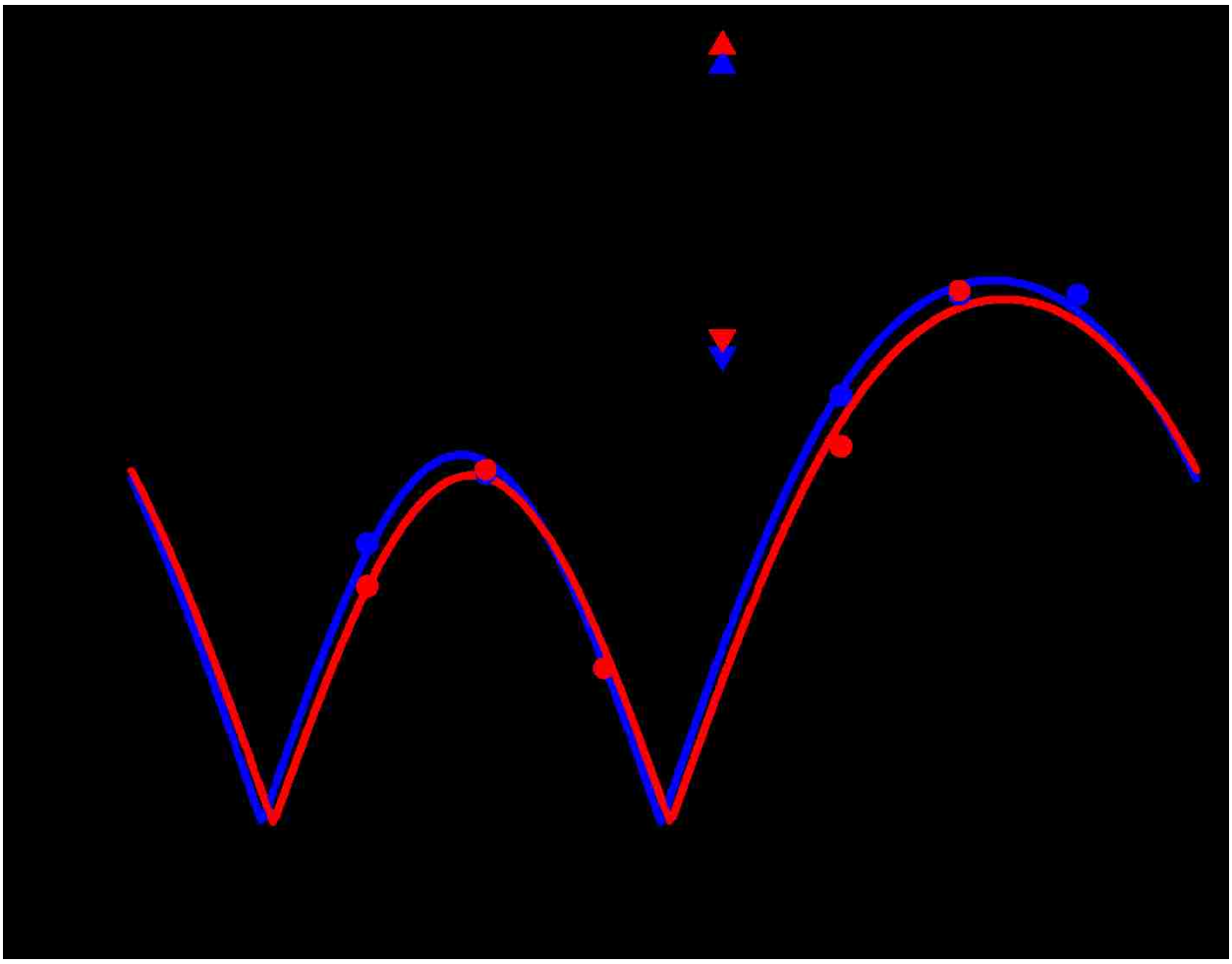

Figure 6: GALA quadrupolar wave plots of tilted membrane peptides in DOPC ether bilayers. GWALP23-D14 (blue; tilt $\tau = 15°$, rotation $\rho = 335°$, pH 6) has a distinct tilt and rotation which shows no significant change from the potentially charged GWALP23-D14 (red; tilt $\tau = 14.7°$, rotation $\rho = 339°$, pH 13). The wave plot for the parent GWALP23 is shown as black dash.

Figure 7: ^{2}H-NMR spectra of GWALP23-Q14 peptides with deuterium labeled alanines at position 7 and 9 incorporated in DLPC (**A)** and (**B**) DOPC ether bilayers hydrated with 10 mM buffer at indicated pH. As expected, the spectra show no response to changes with pH. Spectra were recorded at $\beta = 90°$ sample orientation at 50°C.

4.10 Supporting Information

Figure S1: MALDI mass spectrum of synthesized peptides GWALP23-D14 (top) and GWALP23-Q14 (bottom) with labeled ^{2}H-Ala residues. The expected monoisotopic mass for GWALP23-D14 is 2262.69 Daltons; adding 23 for Na^{+} and one ^{13}C atom is 2290 with 4 deuterons or 2294 with 8 deuterons present. The expected monoisotopic mass for GWALP23-Q14 is 2275.75 Daltons; adding 23 for Na^{+} and one ^{13}C atom is 2303 with 4 deuterons or 2307 with 8 deuterons present. Successive m/z peaks differ by ± one ^{13}C atom (present at ~1.1% natural abundance).

Figure S2: Analytical HPLC chromatogram of purified GWALP23-D14 (left) and GWALP23-Q14 (right).

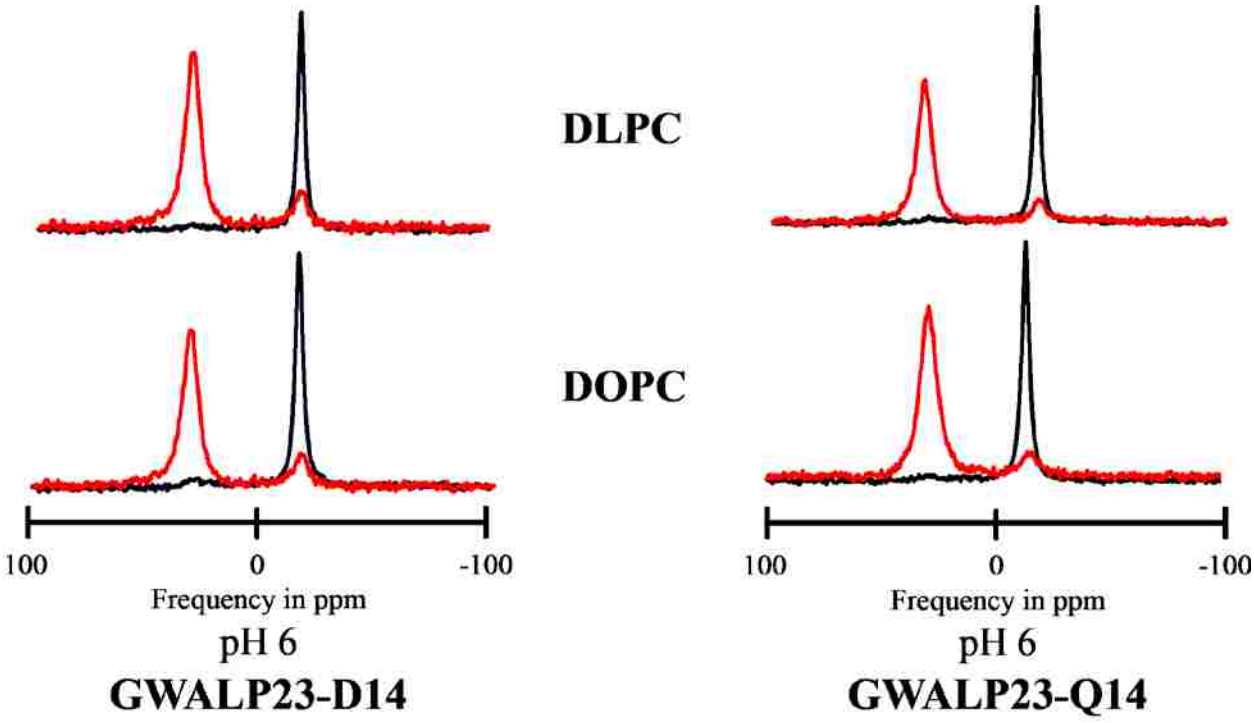

Figure S3: Examples of ^{31}P NMR spectra for oriented bilayers of DLPC and DOPC ether containing GWALP23-D14 and GWALP23-Q14. Samples were hydrated with 10 mM buffer at pH 6 and recorded with orientations parallel ($\beta = 0°$, red) or perpendicular ($\beta = 90°$, black) to the magnetic field.

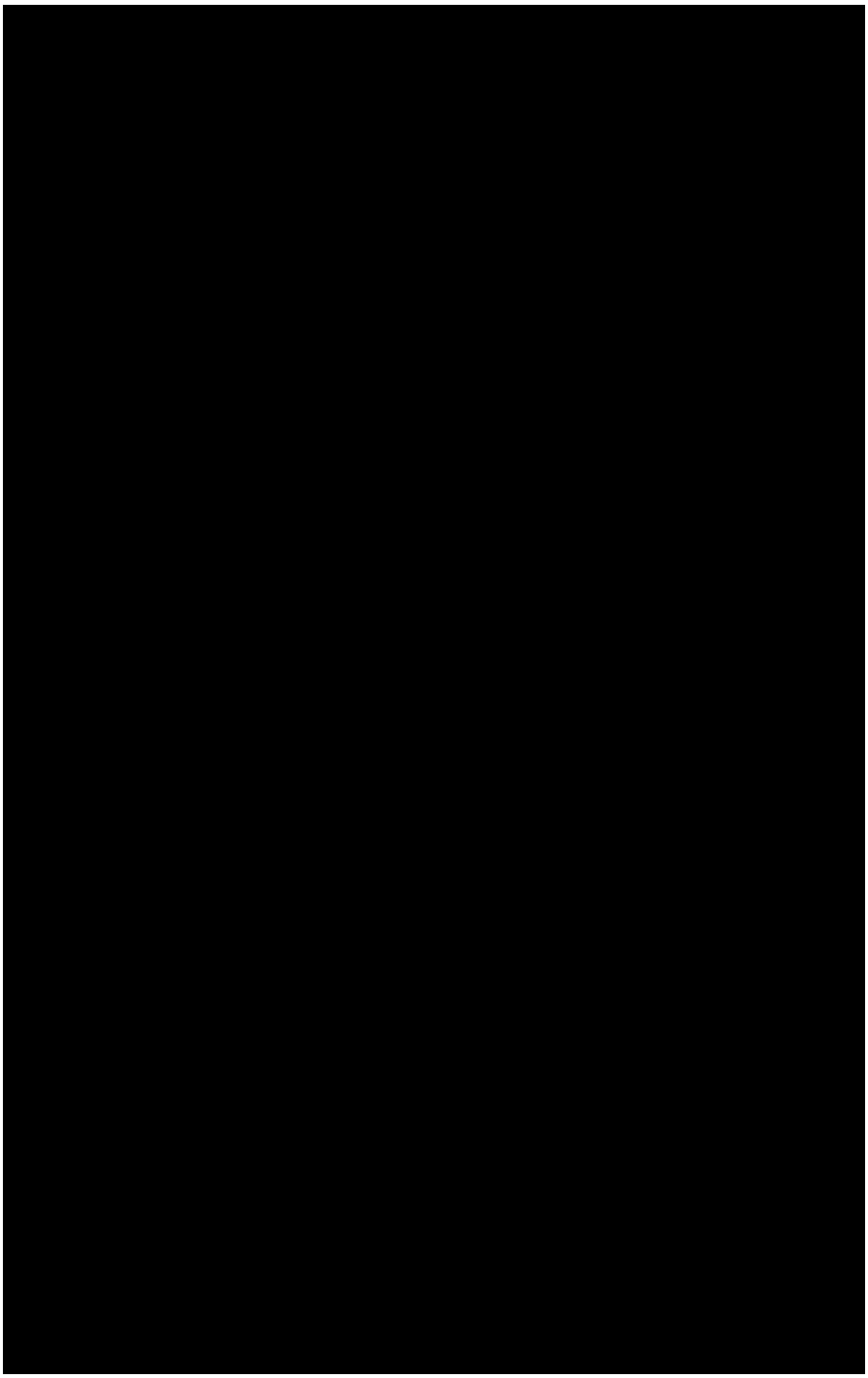

Figure S4: Circular dichroism spectra of GWALP23-D14 in DLPC (top) and DOPC (bottom) vesicles. Peptide to lipid ratio is 1:60.

CHAPTER 5: Conclusion

This dissertation addressed the key questions of how pH and side chain charges influence the behavior of model peptides in lipid bilayer.

The use of model peptides has proven to be useful in seeking experimental validation of fundamental principles that undergird lipid-protein interactions. We have employed the peptide framework of GWALP23 (acetyl-GGALW$(LA)_6$LWLAGA-amide) to investigate molecular orientation, conformation stability and dynamics, and charged residue interactions with lipids. The Y^5GWALP23 peptide, a modification of the GWALP23 that incorporates a single tyrosine (Y^5) at one end, displays reduced dynamics and greater sensitivity to lipid-peptide hydrophobic mismatch than the traditional WALP peptides. We observe the tyrosine residue in Y^5GWALP23 to titrate with a pK_a of about 10.5 in lipid bilayers membranes. (The peptide contains no other candidate groups that titrate.) The titration of Y5, however, affects only slightly the peptide helix integrity, orientation or dynamics within the membrane. These results corroborate with more recent calculations of Tyr residues along the membrane normal (Granseth, E. et.al. 2005; Teixeira, V.H., et.al. 2016) and emphasizes on the importance of properly modeling the protonation equilibrium in peptides interacting with membranes using MD simulations.

Negatively charged residues like glutamic acid and aspartic acid in the core of transmembrane proteins are highly conserved and play an important role in the stability and functioning of membrane proteins. This work has focused on elucidating the Glu and Asp carboxyl side chain ionization properties in lipid bilayer membranes. The GWALP23 transmembrane helix with a Glu side chain exhibits a position specific titration behavior in DLPC lipid bilayer membranes. When located at the center of the helix sequence, E12 does not respond to pH (up to pH 13). The slightly off-center E14 and the four-residue offset E16 display pK_a values around 12.5 in DLPC

bilayer membranes. The results are consistent with the high pK_a values calculated for model peptides and membrane proteins such as cytochrome c oxidase. We also observe the changes in helix fraying upon Glu titration to govern the transmembrane orientation. The results are also consistent with solvation structure predicted for Glu residues using MD simulations that strongly suggest that Glu aggressively holds on to the waters of hydration. The labeled Glu-containing GWALP23 peptides display broad ^2H NMR spectra in DOPC, suggesting slower helix dynamics and possibly indication peptide association or aggregation.

The model GWALP23 transmembrane helix with Asp residues incorporated in DOPC bilayer membranes exhibits a stark contrast in behavior to its Glu counterpart. The D14 peptide, positioned slightly off center, displays sharp NMR resonances for oriented samples in aligned DOPC bilayers. The spectra do not respond to pH (up to pH 13) but show minor changes in unwinding with pH, which suggest that the Asp residue might be titrating close to pH 13, but the core D14 helix does not respond to the titration.

Our results shed light on the influence of ionization behavior of charged residues on fundamental principles of lipid-protein interactions. These experiments are of interest and importance for further experimental studies to produce results that could improve the methods for computational prediction of structure and dynamics of key membrane proteins.